Electronic Supplementary Material (ESI) for Nanoscale Horizons.

Chiral Gold-PPA Nanocomposites with Tunable Helical Sense and Morphology

Julian Bergueiro[‡], Manuel Núñez-Martínez[‡], Sandra Arias, Emilio Quiñoá, Ricardo Riguera and Félix Freire*

Center for Research in Biological Chemistry and Molecular Materials (CIQUS) and Department of Organic Chemistry, University of Santiago de Compostela, E-15782 Santiago de Compostela, Spain

Email: felix.freire@usc.es

http://felixfreire.com

Electronic Supporting Information

CONTENTS

1. Materials and methods

Commercially available chemicals have been used as delivered. Solvents were purchased as reagent grade and distilled if necessary. Anhydrous solvents were either purchased as ultra-dry solvent from Acros Organics® or received from solvent purification system. For the coupling and polymerization reactions, dry THF was obtained from MBRAUN SPS 800 solvent purification system. Water was purified by Millipore water purification system.

Coupling reagents (2-(7-Aza-1H-benzotriazole-1-yl)-1,1,3,3-tetramethyluronium hexafluorophosphate) (HATU), 1-ethyl-3-(3-dimethylaminopropyl)carbodiimide hydrochloride (EDC.HCl), hydroxybenzotriazole (HOBt), 1-hydroxy-7-azabenzotriazole (HOAT), 4- ethynylbenzoic acid, and 4-ethynylaniline were purchased from AnaSpec Inc. (*L*)-Phenylglycine methyl ester hydrochloride ((*L*)-PGME), triphenylmethanethiol, 11-bromo-1-undecanol, methylsulfonyl chloride, 2,2-(ethylenedioxy)diethylamine, trifluoroacetic acid (TFA), triisopropylsilane, rhodium norbornadiene chloride dimer {$[Rh(nbd)Cl]_2$}, diisopropyltriethylamine (DIEA), triethylamine (TEA, 99%), tetraoctylamonium bromide (TOAB), dodecanethiol, sodium borohydride ($NaBH_4$) and tetrachloroauric acid ($HAuCl_4$) were purchased from Aldrich.

NMR experiments were carried out in a Varian Inova 250 (250 MHz resonance 1H).

Size exclusion chromatography studies were performed on Alliance 2695 HPLC System (Waters) liquid chromatography system equipped with a UV 2489 detector (Waters). The samples were eluted by three Phenogel columns connected to each other with stacionary phases of 10^3, 10^4 and 10^5 Amstrong and packed with a solid support of a cross-linked stiyrene and *p*-divinylbenzene copolymer.

CD measurements were done in a Jasco-720 spectropolarimeter.

UV spectra were registered in a Jasco-730 spectrophotometer.

FT-IR measurements were carried out on a Bruker IFS-66v while Raman measurements were carried out in a Renishaw confocal Raman spectrophotometer (Invia Reflex model), equipped with two lasers (diode laser 785 nm and Ar laser 514 nm).

DSC measurements were performed in a DSC Q200 Tzero Technology (TA Instruments, New Castle, UK) equipped with a refrigerated cooling system RCS90 (TA Instruments) using a Tzero low-mass aluminum pan.

TGA experiments were carried out in a Q5000SA instrument (TA Instruments, New Castle, UK) using a platinum pan.

DLS measurements were performed on a Nano-ZS 90 (Malvern) equipped with a He-Ne laser (l = 633 nm) under scattering angle of 173°. The samples were maintained at the designed temperature for 5 min before testing.

SEM samples were performed on a LEO-435VP electron microscope. A drop of polymer solution of 1 mg mL^{-1} in $CHCl_3$ (with 0.5 equivalents of a barium perchlorate solution for assembly experiments with Au-poly-($M\mathbf{1}_r$-*co*-$M\mathbf{2}_{1-r}$) (r = 0.95-0.99) was settled on a silicon wafer chip and allowed to dry at rt for 12 h.

TEM measurements were performed on a Phillips CM-12 electron microscope. A drop of a solution of 1 mg mL^{-1} in $CHCl_3$ (with 0.5 equivalents of a barium perchlorate solution for assembly experiments with Au-poly-($M\mathbf{1}_r$-*co*-$M\mathbf{2}_{1-r}$)) was settled on a carbon grid and allowed to dry at rt for 12 h.

2. Names and codes

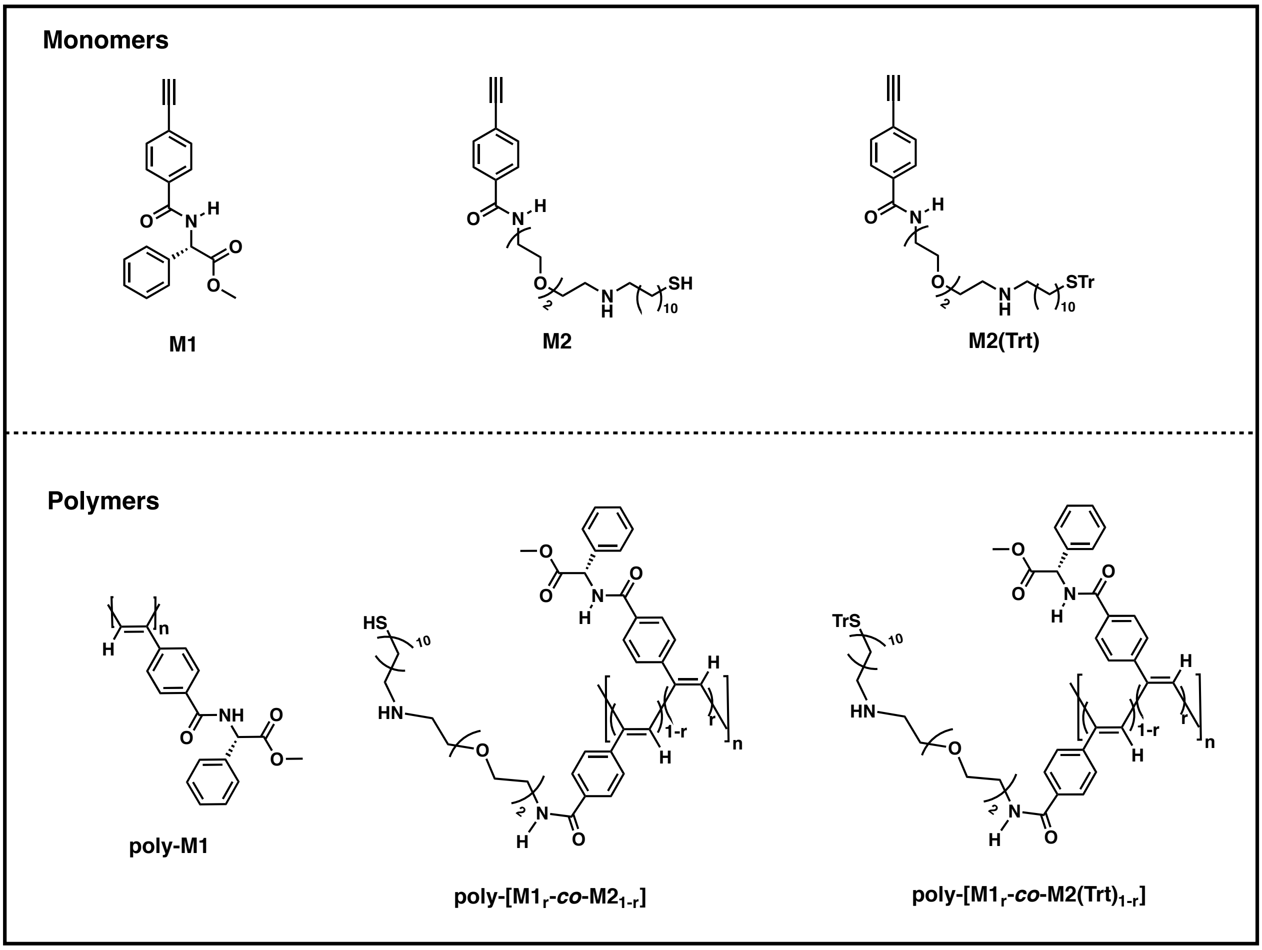

3. Synthesis of Monomers

Synthesis of M1:

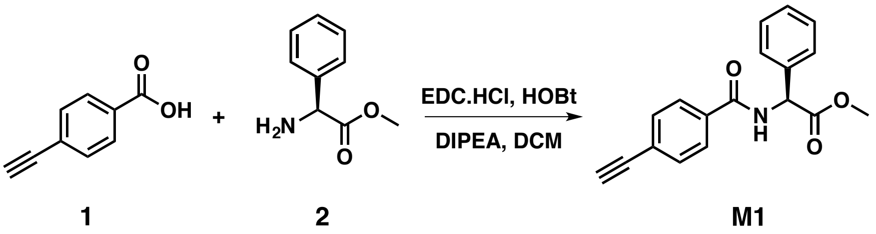

Monomer M**1** was prepared according to a previous work:[1] (*L*)-Phenylglycine methyl ester hydrochloride **2** (911 mg, 1.2 equiv.) was dissolved in water, basified with a saturated solution of $NaHCO_3$ and extracted with DCM. The aqueous layer was dried over anhydrous Na_2SO_4, filtrated and solvent was evaporated at reduced pressure. Then, the amino ester was dissolved in dried DCM (30 mL) and 1-ethyl-3-(3-dimethylaminopropyl)carbodiimide hydrochloride (EDC·HCl, 867 mg, 1.2 equiv.), 1-hydroxybenzotriazole (HOBt, 608 mg, 1.2 equiv.) and 4-ethynylbenzoic acid (**1**) were added (550 mg, 1.0 equiv.). The resulting suspension was stirred and monitored by TLC. When the reaction was judged as completed, the reaction mixture was washed with water, HCl (1M), water and a saturated solution of $NaHCO_3$. The combined organic layers were dried over anhydrous Na_2SO_4, filtered and the solvent was evaporated at reduced pressure. The crude product was chromatographed on silica gel (70-230 mesh) with hexane/ethyl acetate (4/1) as eluent to obtain 980 mg (89% yield) of pure product.

Spectroscopy data:

^1H NMR (250 MHz, $CDCl_3$) δ (ppm): 3.2 (s, 1H), 3.7 (s, 3H), 5.7 (d, 1H), 7.1 (d, 1H), 7.41 (m, 5H), 7.5 (d, 2H), 7.7 (d, 2H).

^{13}C NMR (62.5 MHz, $CDCl_3$) δ (ppm): 52.9, 56.8, 79.7, 82.6, 125.7, 127.1, 127.3, 128.6, 129.0, 132.2, 133.5, 136.5, 165,7, 171.4,

$[\alpha]_D$= +70 (15 mg mL^{-1}, $CHCl_3$).

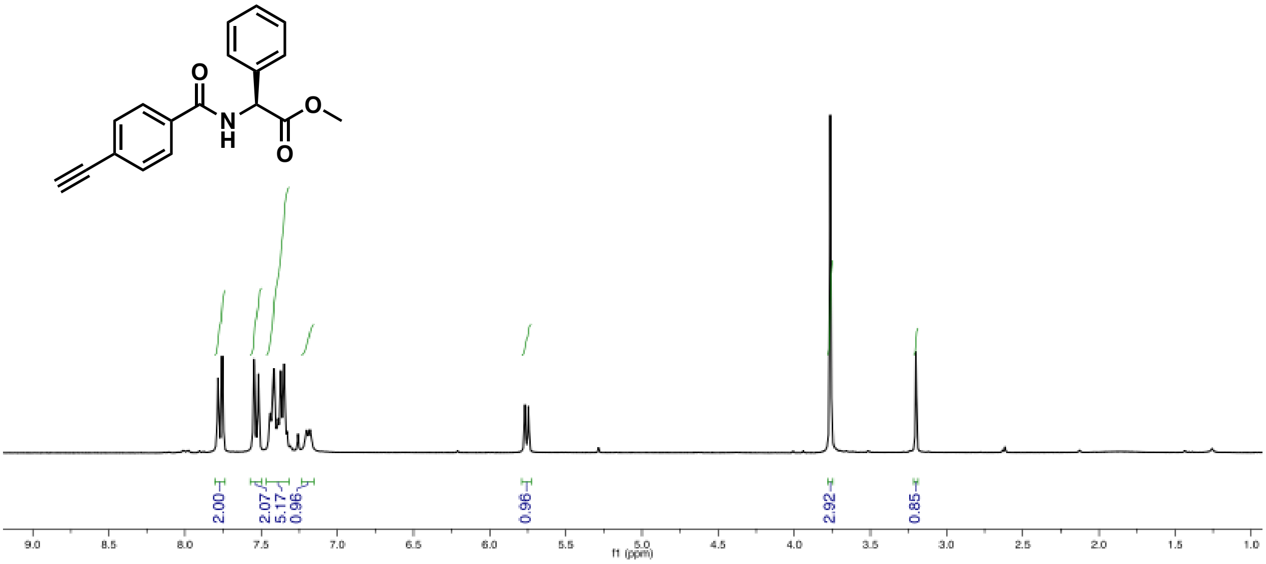

Figure S1: ^{1}H NMR for monomer M**1**.

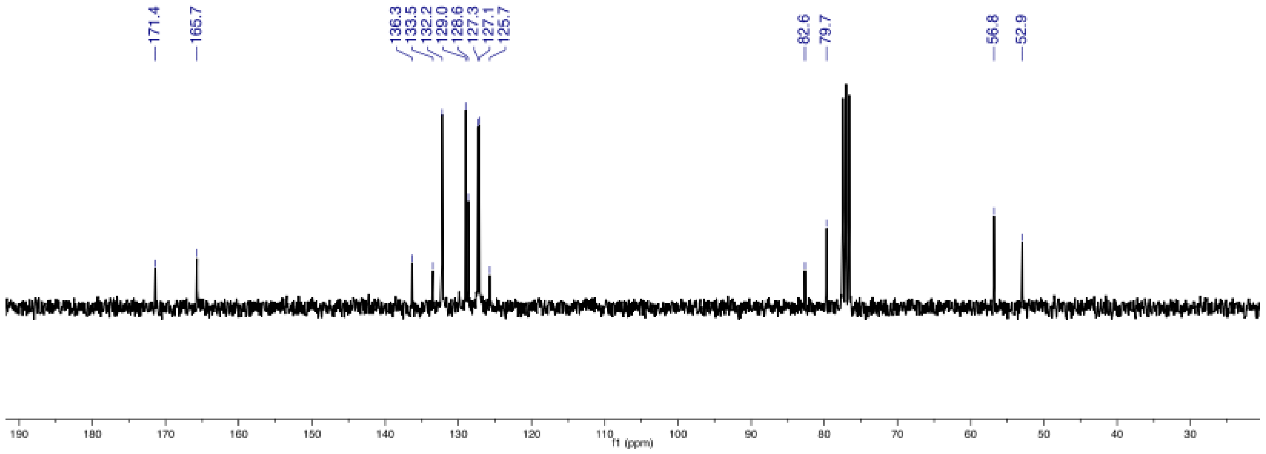

Figure S2: ^{13}C NMR for monomer M**1**.

Synthetic route for M2(Trt) and M2:

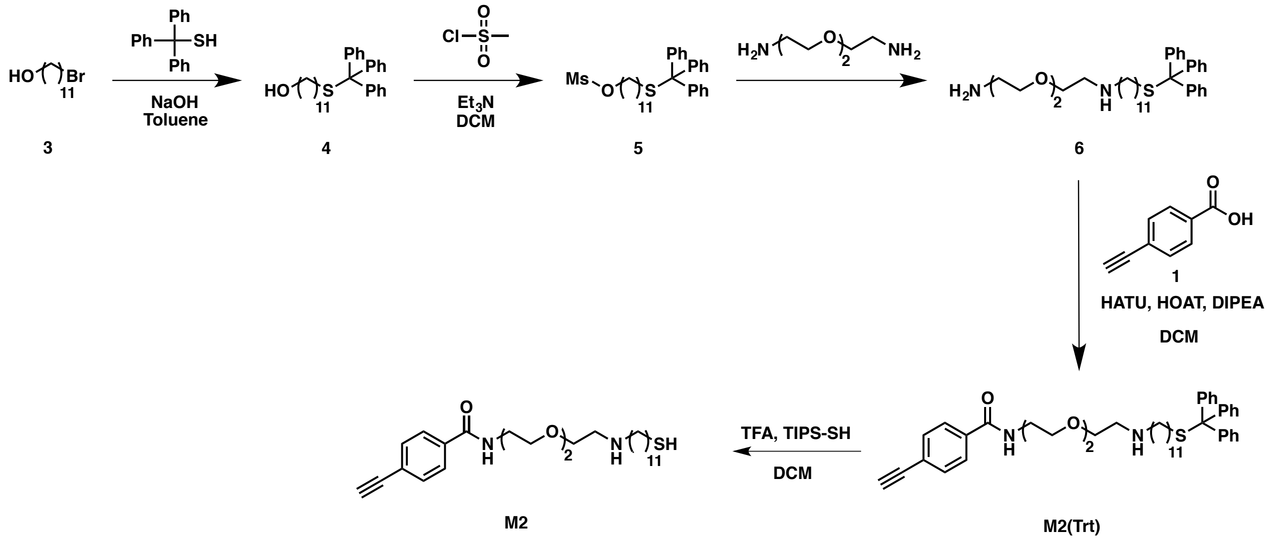

Scheme S1: Synthetic route for M**2(Trt)** and M**2**.

Synthesis of 4:

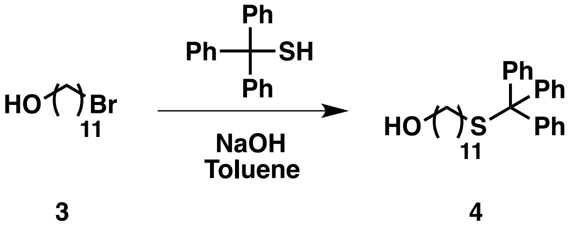

Triphenylmethanethiol (1.32 g, 4.37 mmol) was dissolved in a solution of ethanol/benzene (1:1, 4 mL) and NaOH (0.23 g, 5.97 mmol) in 3 mL of H_2O was added. Then 11-bromo-1-undecanol (**3**, 1.00 g, 3.98 mmol) was also dissolved in a solution of ethanol/benzene (1:1, 4 mL) and added to the triphenylmethanethiol mixture. The new reaction mixture was stirred overnight at room temperature. Once the reaction was completed (checked by TLC) all the mixture was poured into a saturated solution of $NaHCO_3$ and washed three times. The organic layer was separated and added into another solution saturated of NaCl and also washed for three times. Afterward the organic layer was separated, dried (Na_2SO_4) and concentrated. The crude product was purified by column chromatography over silica gel using hexane/ethyl acetate (9:1, 4:1 and 1:1, v/v) as an eluent. The solvent was removed in vacuum to obtain compound **4** as colorless oil (Yield 1.6 g, 95%).

Spectroscopy data:

^{1}H NMR (250 MHz, $CDCl_3$) δ (ppm): 1.0-2.0 (m, 18H), 2.1-2.2 (m, 2H), 3.5-3.7 (m, 2H), 7.0-7.5 (m, 15H).

^{13}C NMR (62.5 MHz, $CDCl_3$) δ (ppm): 25.8, 28.6, 29.0, 29.2, 29.4, 29.5, 29.6, 32.1, 32.8, 63.0, 66.4, 126.5, 127.5, 129.6, 130.1, 154.1.

HRMS (ESI) m/z calculated for $C_{30}H_{38}NO_2$ [M + Na$^+$]: 469.2536, found: 469.2535.

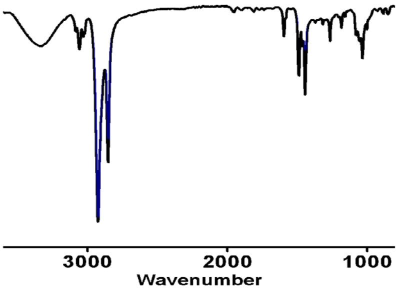

Figure S3: FT-IR spectrum for compound **4**.

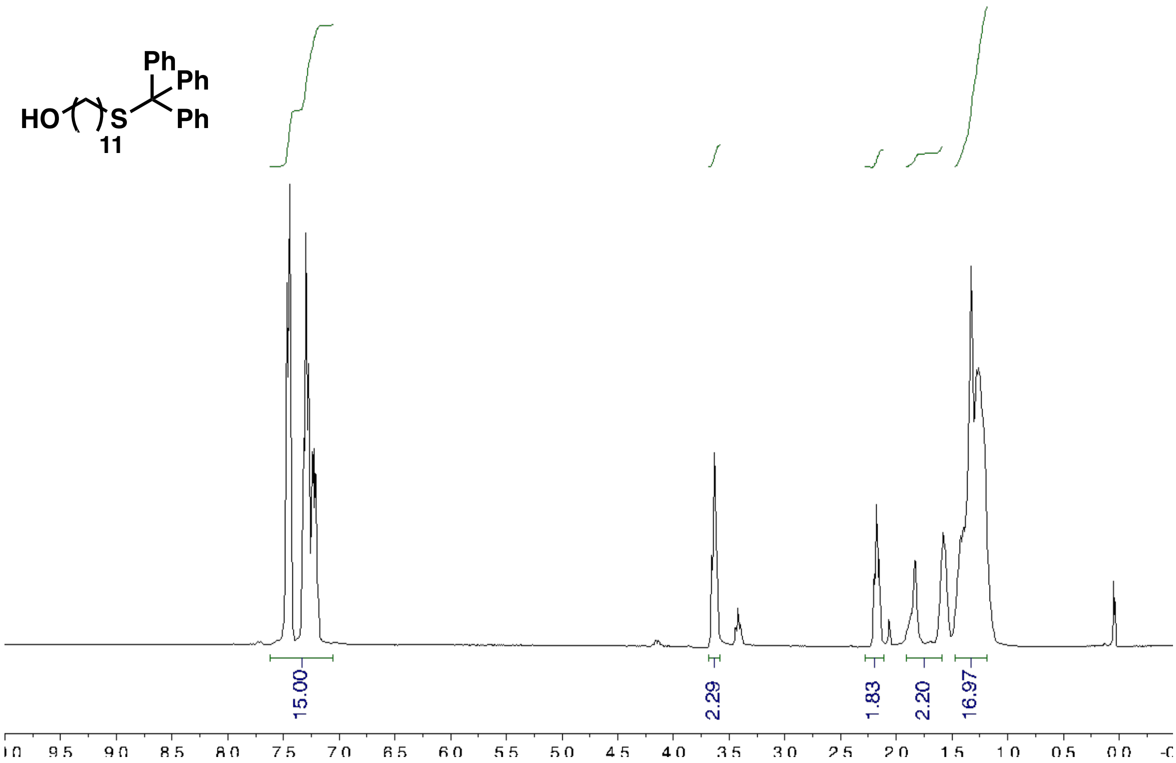

Figure S4: ^{1}H NMR spectrum for compound **4**.

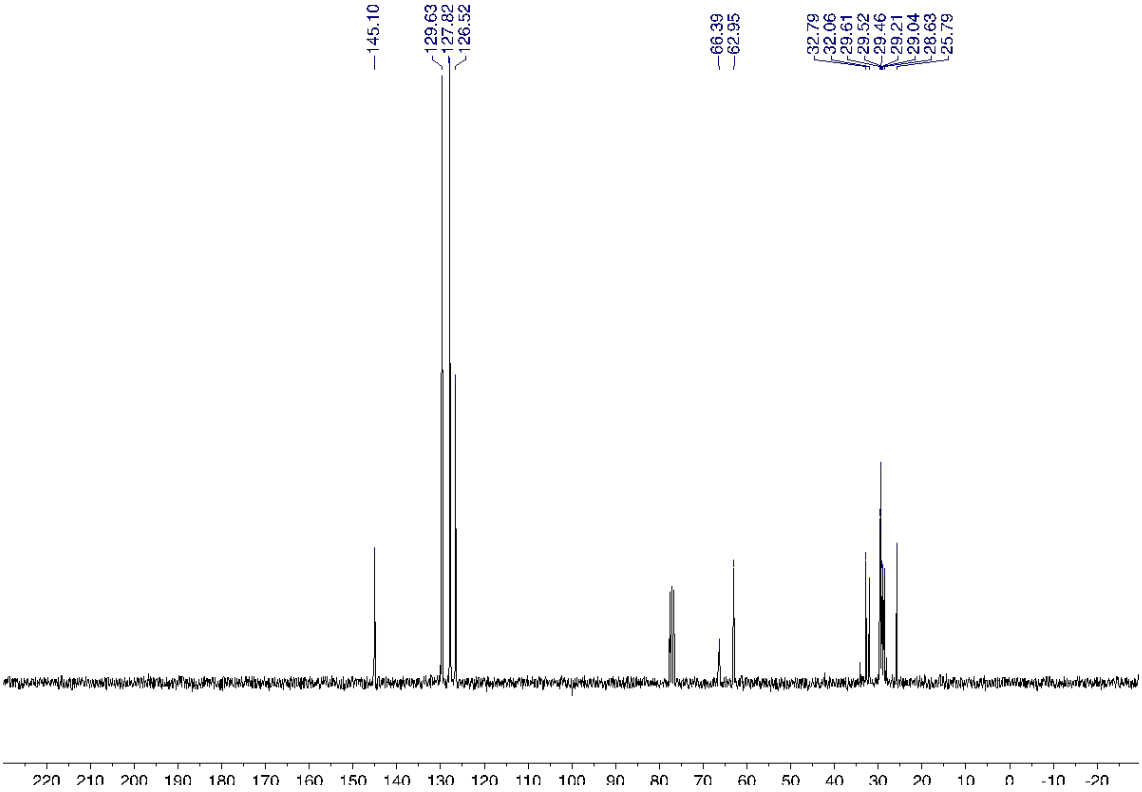

Figure S5: ^{13}C NMR spectrum for compound **4**.

Synthesis of 5:

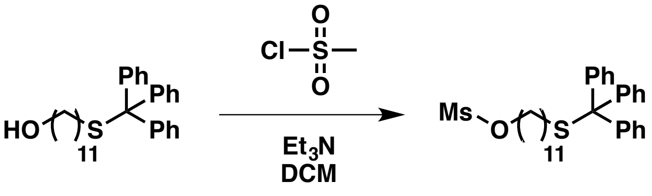

4 5

To a solution of compound **4** (1 g, 2.23 mmol) in dry DCM at 4° C, triethylamine (0.45 g, 4.47 mmol) was added. Methylsulfonyl chloride (0.38 g, 3.35 mmol) was injected drop by drop to the solution maintaining the temperature less than 5°C. After 30 minutes the reaction mixture was warmed up to room temperature and stirred for another 30 minutes. Once the reaction was completed (according to TLC), the DCM was evaporated at reduced pressure. The viscous compound was again diluted with DCM and poured into solution of HCl (1 M) and treated twice. Organic layer was poured into a saturated solution of $NaHCO_3$ and washed three times. The organic layer was separated and added into another solution saturated of NaCl and also treated three times. Afterward organic layer was separated, dried (Na_2SO_4) and concentrated at reduced pressure. The crude product was purified by column chromatography over silica gel using hexane/ethyl acetate (1:1, v/v) as an eluent. Solvent was removed in vacuum to afford compound **5** as colorless oil (Yield 1.09 g, 93%).

Spectroscopy data:

^{1}H NMR (250 MHz, $CDCl_3$) δ (ppm): 1.1-1.5 (m, 16H), 1.77 (t, 2H), 2.20 (t, 2H), 2.92 (s, 3H), 3.20 (t, 2H), 7.2-7.6 (m, 15H).

^{13}C NMR (62.5 MHz, $CDCl_3$) δ (ppm): 25.5, 28.6, 29.1, 29.4, 32.0, 32.8, 34.1, 37.3, 66.4, 70.3, 126.6, 127.9, 128.0, 129.6, 145.1.

HRMS (ESI) m/z calculated for $C_{31}H_{40}O_3S_2$ [M + Na$^+$]: 547.2312, found: 547.2311.

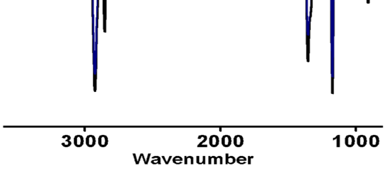

Figure S6: FT-IR spectrum for compound **5**.

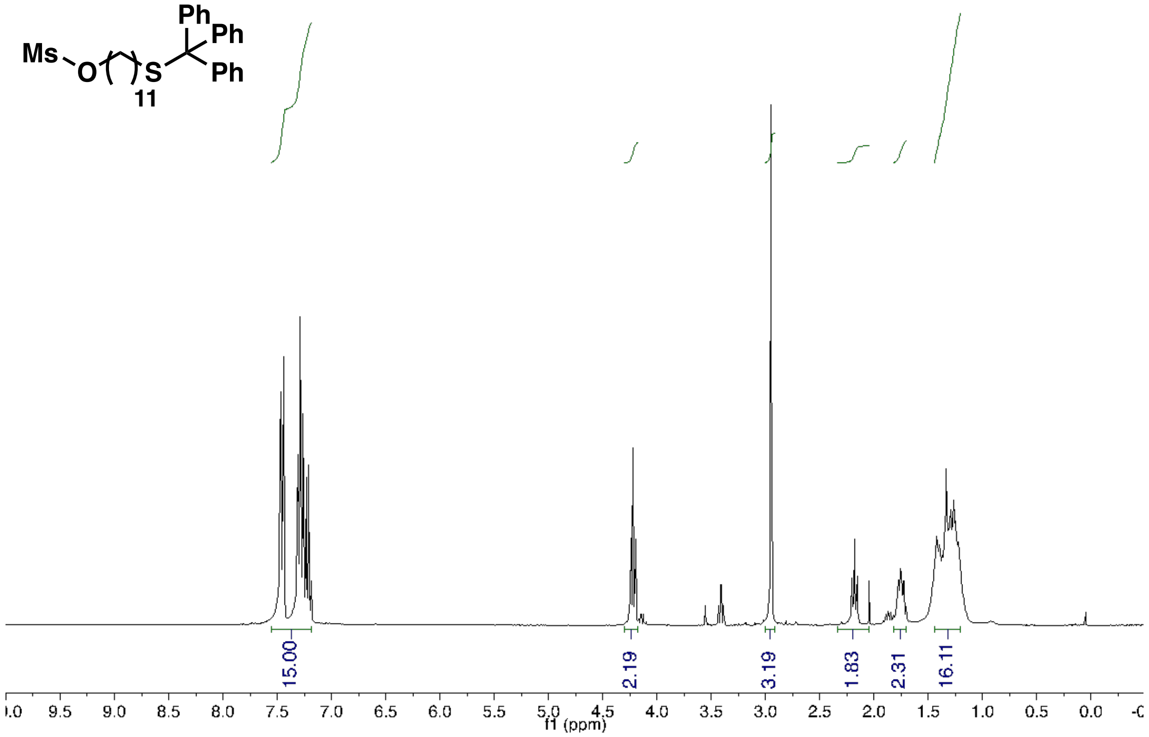

Figure S6: ^{1}H NMR spectrum for compound **5**.

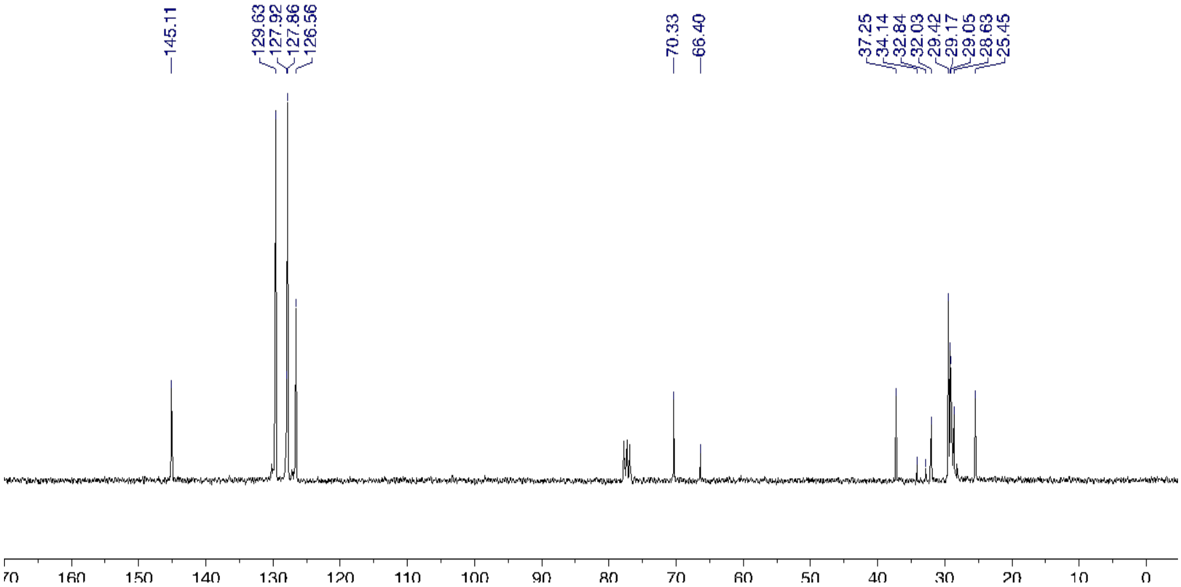

Figure S7: ^{13}C NMR Spectrum for compound **5**.

Synthesis of 6:

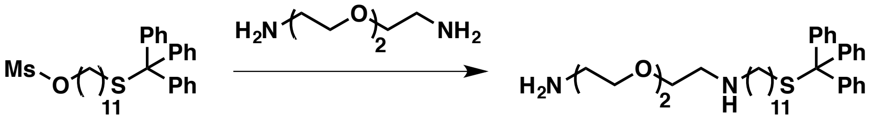

5 **6**

Compound **5** (0.9g, 1.71 mmol) was dissolved in a 2,2-(ethylenedioxy)diethylamine (2.54 g, 17.15 mmol). Once the reaction was completed after 4 hours (according to TLC). The compound was diluted with DCM and poured into a saturated solution of $NaHCO_3$ and washed two times. Afterward organic layer was separated, dried (Na_2SO_4) and concentrated at reduced pressure. Solvent was removed in vacuum to afford compound **6** (Yield 0.89 g, 92%).

Spectroscopy data:

^{1}H NMR (250 MHz, $CDCl_3$) δ (ppm): 1.0-1.6 (m, 22H), 2.15 (t, 2H), 2.62 (t, 2H), 2.75 (t, 2H), 2.82 (t, 2H), 3.51 (t, 2H), 3.63 (t, 2H), 7.0-7.5 (m, 15H).

^{13}C NMR (62.5 MHz, $CDCl_3$) δ (ppm): 27.4, 28.6, 29.0, 29.2, 29.4, 29.6, 30.2, 32.0, 41.8, 49.4, 50.1, 66.3, 70.3, 70.7, 73.4, 126.5, 127.8, 129.6, 145.1.

HRMS (ESI) m/z calculated for $C_{36}H_{52}N_2O_2S$ [M + H]: 577.37, found: 577.3832.

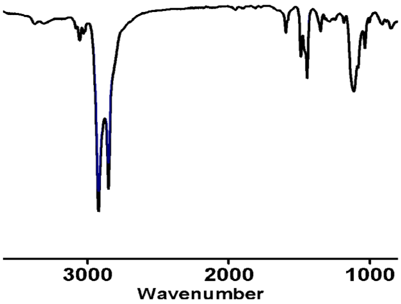

Figure S8: FT-IR spectrum for compound **6**.

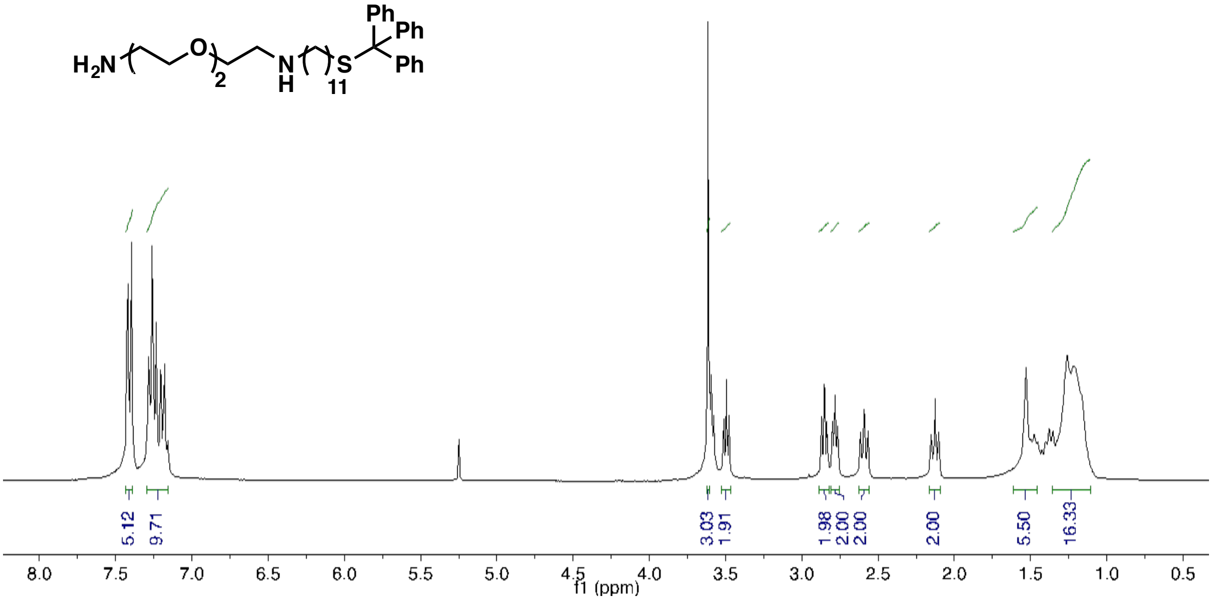

Figure S9: ^{1}H NMR spectrum for compound **6**.

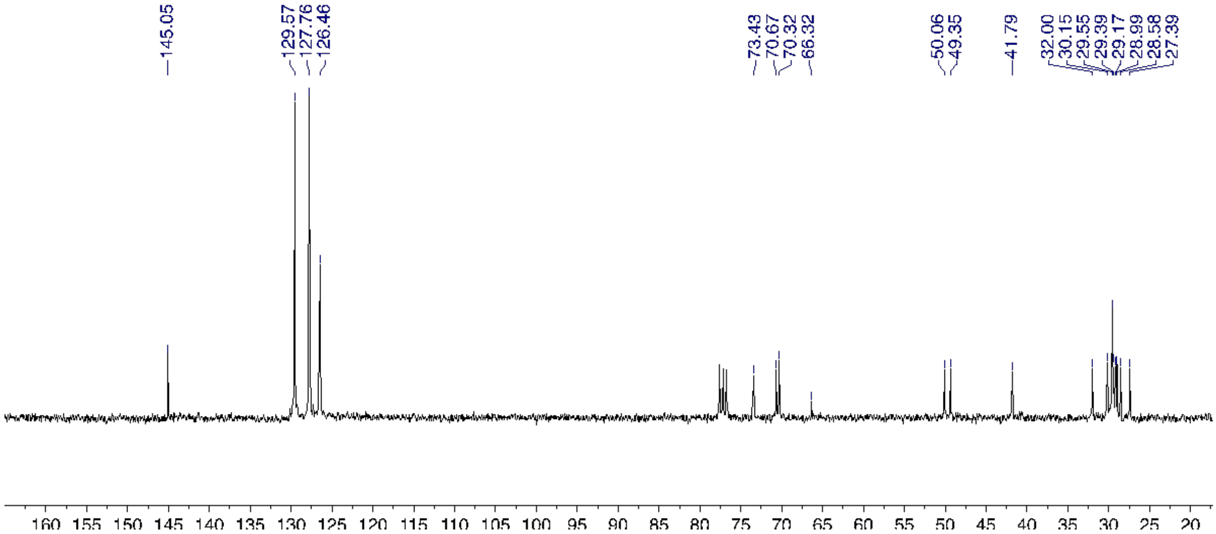

Figure S10: ^{13}C NMR spectrum for compound **6**.

Synthesis of M2(Trt):

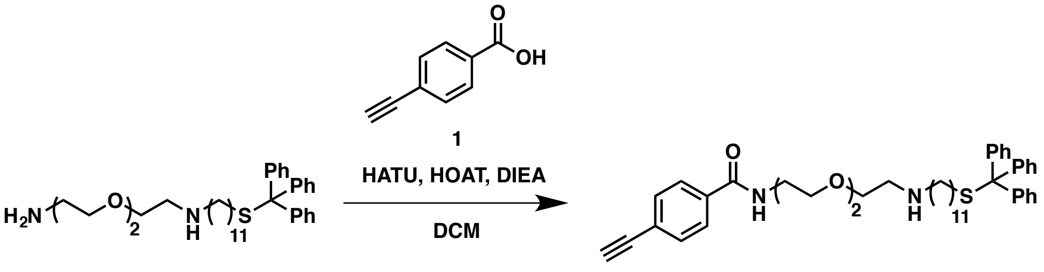

(2-(7-Aza-1H-benzotriazole-1-yl)-1,1,3,3-tetramethyluronium hexafluorophosphate) (HATU, 2.02 g, 5.31mmol) 1-hydroxy-7-azabenzotriazole (HOAt, 0.717, 5.31 mmol), 4-methylbenzoic acid (**1**, 0.78 g, 5.31 mmol) and diisopropyltriethylamine (DIPEA, 0.69 mL, 5.31 mmol) were dissolved in 35 mL of DCM, and the mixture was stirred for 15 min to activate the acid. Then, the compound **6** (2 g, 3.35 mmol) was added and the reaction mixture was stirred overnigth. The organic layer was washed with a saturated solution of $NaHCO_3$ three times. The combined organic layers were dried over anhydrous Na_2SO_4, filtered and the solvent was evaporated at reduced pressure. The crude product was chromatographed on silica gel (70-230 mesh) with hexane/ethyl acetate (1/1) as eluent obtaining compound M**2**(Trt) in a 90% yield (2.25 g).

Spectroscopy data:

^{1}H NMR (250 MHz, $CDCl_3$) δ (ppm): 1.0-1.6 (m, 22H), 2.15 (t, 2H), 3.15 (s, 1H), 3.2-3.6 (m, 17H), 7.1-7.8 (m, 19H).

^{13}C NMR (62.5 MHz, $CDCl_3$) δ (ppm): 25.0, 26.4, 28.6, 28.6, 29.0, 29.4, 31.0, 32.0, 32.0, 36.6, 38.6, 39.9, 66.3, 69.9, 70.5, 79.3, 82.8, 126.5, 127.1, 127.8, 129.6, 129.6, 132.1, 145.1.

HRMS (ESI) m/z calculated for $C_{45}H_{56}N_2O_3S$ [M + H]: 705.01, found: 705.0124.

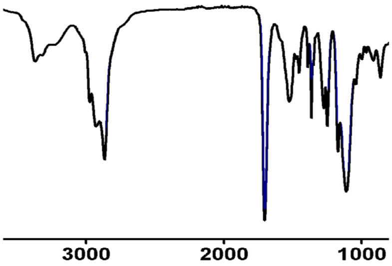

Figure S11: FT-IR spectrum for compound M**2**(Trt).

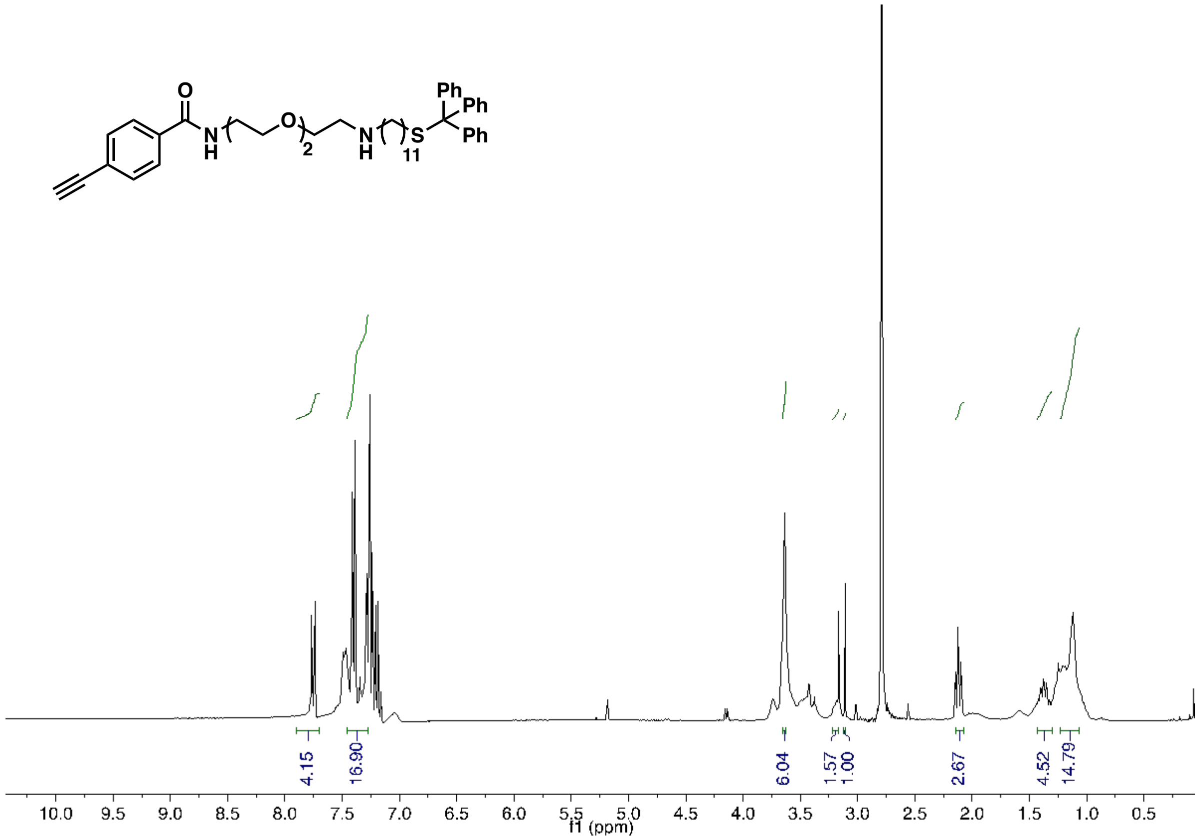

Figure S12: ^{1}H NMR spectrum for compound M**2**(Trt).

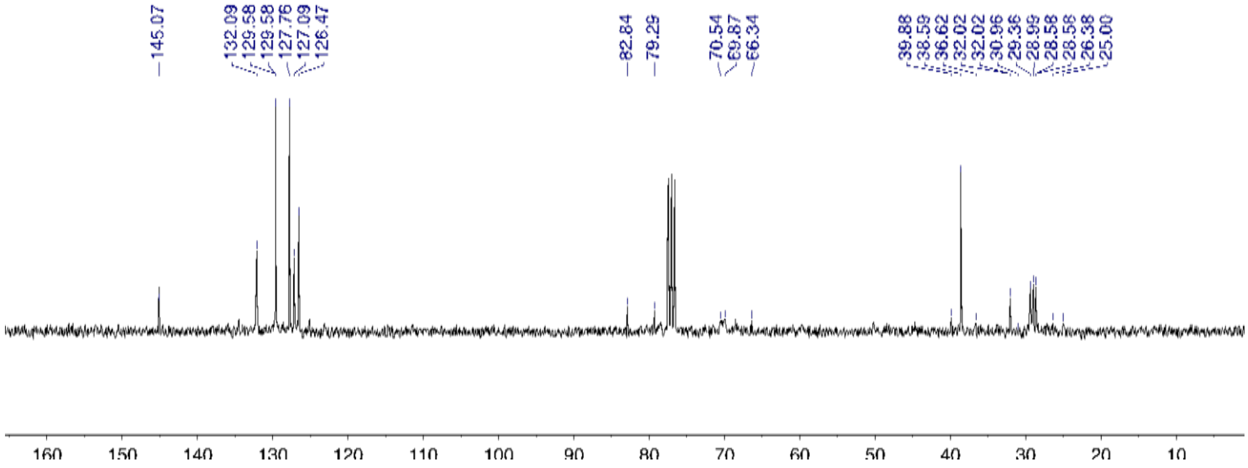

Figure S13: ^{13}C NMR spectrum for monomer M**2**(Trt).

Synthesis of M2:

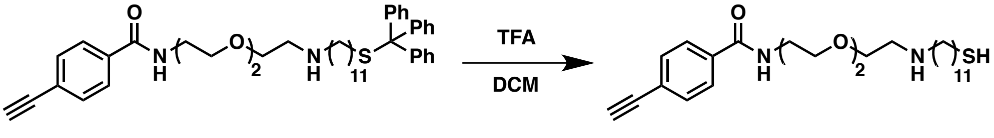

8

M2

Compound **7** (0.4 g, 0.567 mmol) was dissolved in a mixture of equal parts of trifluoroacetic acid, triisopropylsilane and DCM (1:1:1, 2.83 mL). After 2 hours the reaction was completed (according to TLC) and the solvent was evaporated at reduced pressure. The compound was again diluted with DCM and poured into hexane treated twice. Solvent was removed in vacuum to afford monomer M**2** (Yield 0.19 g, 72%).

Spectroscopy data:

^{1}H NMR (250 MHz, $CDCl_3$) δ (ppm): 1.1-1.4 (m, 16H), 1.5-1.8 (m, 10H), 2.30(t, 2H), 2.51 (q, 4H), 2.81 (t, 4H), 3.09 (s, 1H), 7.3-7.6 (m, 4H).

^{13}C NMR (62.5 MHz, $CDCl_3$) δ (ppm): 24.6, 25.5, 25.7, 28.3, 28.8, 29.0, 29.0, 29.3, 34.0, 37.8, 44.1, 83.4, 83.5, 117.4, 119.3, 132.9, 138.5, 171.6.

HRMS (ESI) m/z calculated for $C_{26}H_{42}N_2O_3S$ [M + H]: 462.69, found: 462.2878.

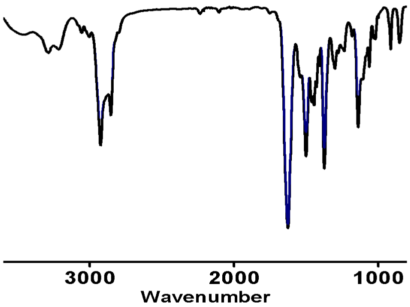

Figure S14: FT-IR spectrum for monomer M**2**.

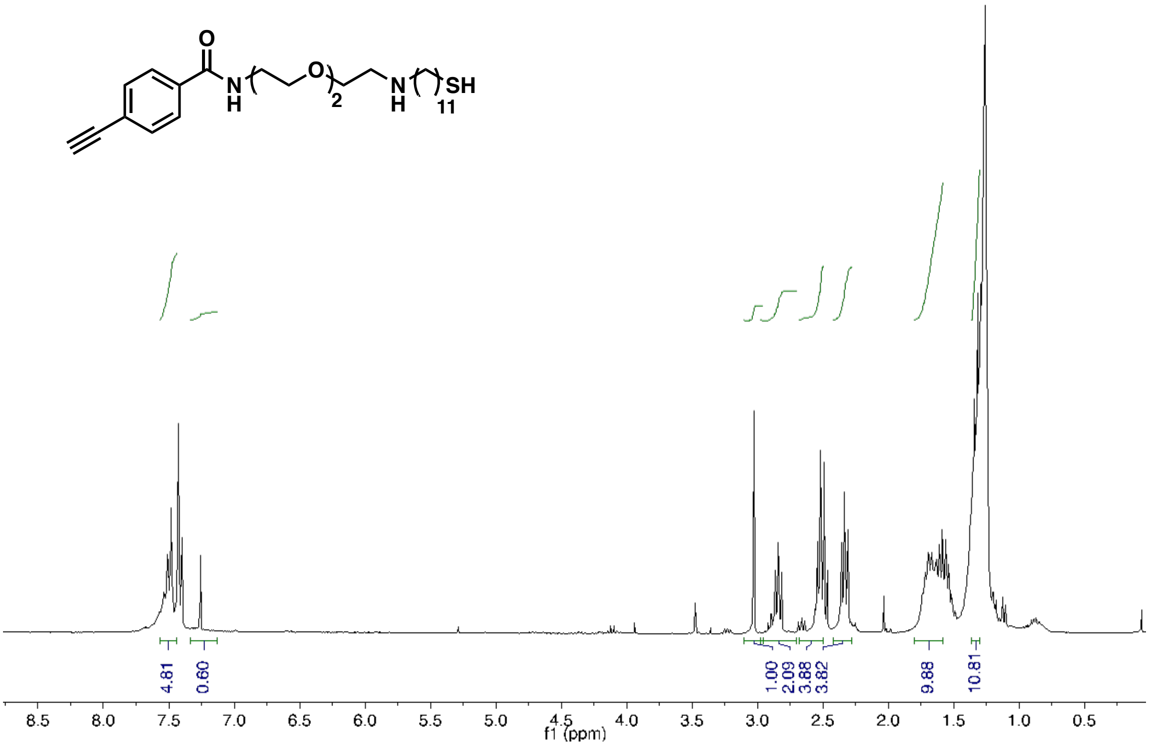

Figure S15: ^{1}H NMR spectrum for monomer M**2**.

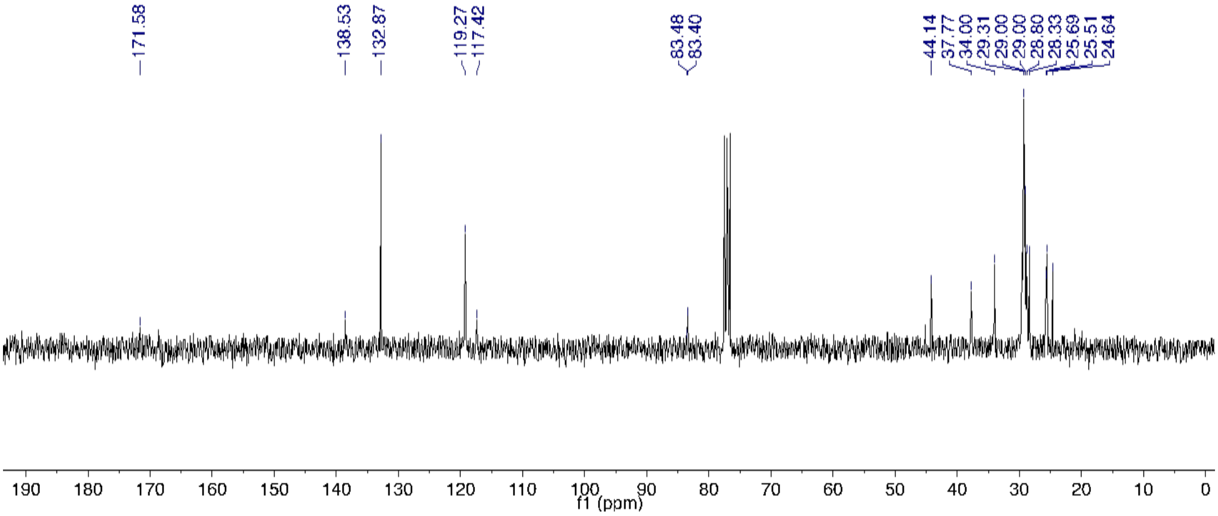

Figure S16: ^{13}C NMR spectrum for monomer M**2**.

4. Synthesis Homo- and Copolymers

General procedure for polymerization: The reaction flask (sealed ampoule) was dried under vacuum and argon flushed for three times before a monomer amount was added as a solid. Then, the flask was evacuated on a vacuum line and flushed with dry argon (three times). Dry THF was added with a syringe and then triethylamine dropwise. A solution of rhodium norbornadiene chloride dimer {$[Rh(nbd)Cl]_2$} in THF was added at 30 °C. The reaction mixture was stirred at 30 °C for 6 h. Then, the resulting polymer was diluted in DCM and it was precipitated in a large amount of methanol, centrifuged (2 times), reprecipitated in hexane and centrifuged again.

4.1 Synthesis of Poly-M1

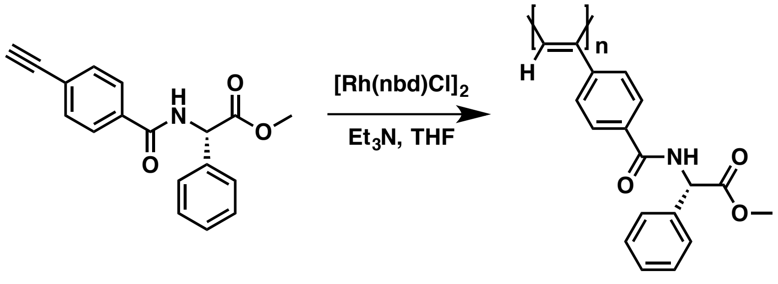

M1 **poly-M1**

Following the general procedure 73.3 mg (0.250 mmol) of M**1**, 7 µL of Et_3N and 0.576 mg of $[Rh(nbd)Cl]_2$ were employed in 0.75 mL of THF to obtain after purification 67.4 mg of poly-M**1** (Yield 92%).[1]

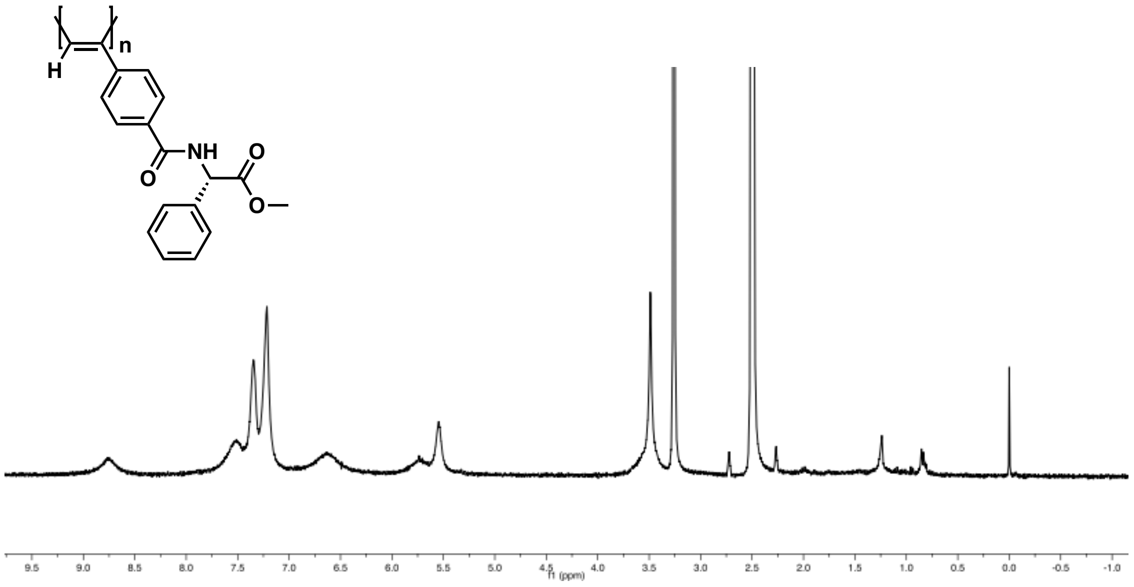

Figure S17: ^1H NMR for poly-M**1** in DMSO-d_6.

4.2 Synthesis of copolymers poly-(M1$_r$-*co*-M2(Trt)$_{1-r}$)

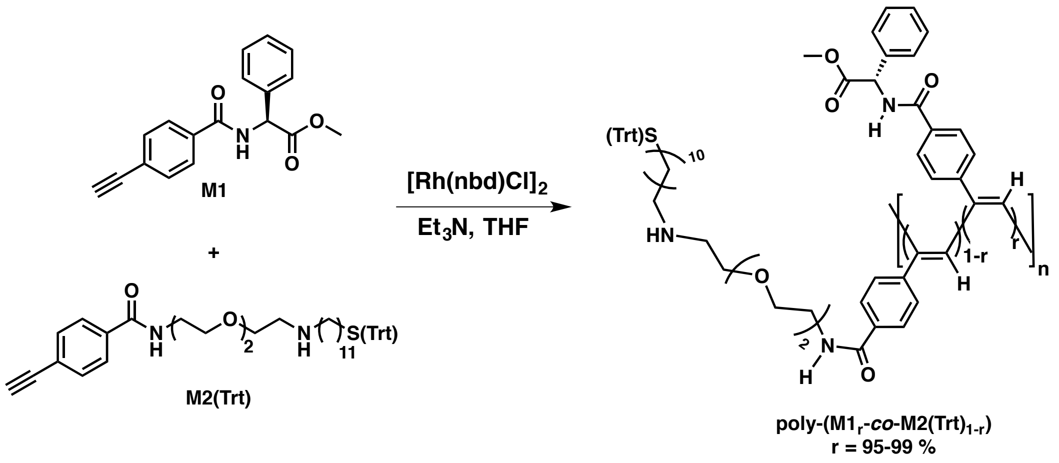

Following the general procedure quantities of M**1**, M**2**(Trt), Et$_3$N, [Rh(nbd)Cl]$_2$, and THF as shown in Table S1 were employed. Reaction yield is also indicated in the Table S1.

Table S1:

Copolymer	M1 mg	M1 (mmol	M2(Trt) (mg)	M2(Trt) (mmol)	Cat (mg)	THF (mL)	Et$_3$N (µL)	Poly (mg)	Yield (%)
Poly-(M1$_{0.99}$-*co*-M2(Trt)$_{0.01}$)	97.6	0.335	2.3	0.003	1.2	0.70	7	71	71
Poly-(M1$_{0.98}$-*co*-M2(Trt)$_{0.02}$)	95.1	0.327	4.6	0.006	1.2	0.70	7	65	65
Poly-(M1$_{0.97}$-*co*-M2(Trt)$_{0.03}$)	93.1	0.320	7.0	0.008	1.2	0.70	7	50	50
Poly-(M1$_{0.96}$-*co*-M2(Trt)$_{0.04}$)	90.5	0.311	9.1	0.005	1.2	0.70	7	75	76
Poly-(M1$_{0.95}$-*co*-M2(Trt)$_{0.05}$)	88.8	0.305	11.1	0.003	1.2	0.70	7	74	74

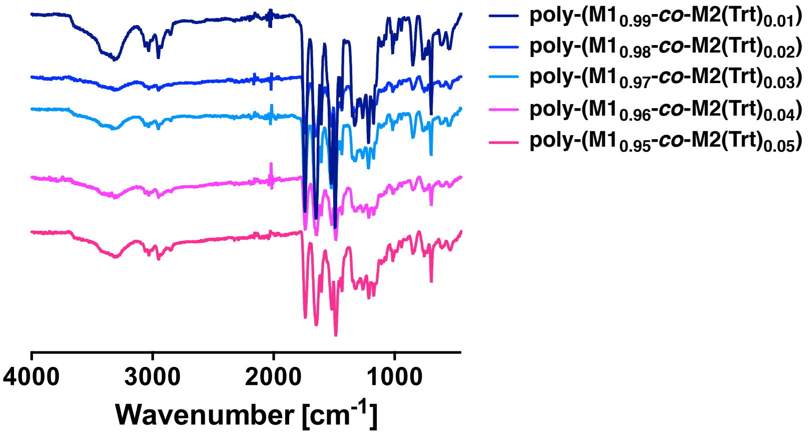

Figure S18: FT-IR spectra for copolymers poly-(M**1**$_r$-*co*-M**2**(Trt)$_{1-r}$) (r = 0.95-0.99).

GPC studies

Table S2: GPC data for copolymers poly-(M**1**$_r$-*co*-M**2**(Trt)$_{1-r}$).

Polymer	M$_n$	M$_w$	M$_p$	M$_z$	PDI
Poly-M1	26252	47057	35345	102574	1.79
Poly-(M1$_{0.99}$-*co*-M2(Trt)$_{0.01}$)	14376	19378	18699	25269	1.34
Poly-(M1$_{0.98}$-*co*-M2(Trt)$_{0.02}$)	6799	16269	19383	24542	2.39
Poly-(M1$_{0.97}$-*co*-M2(Trt)$_{0.03}$)	16004	20473	28176	35683	1.33
Poly-(M1$_{0.96}$-*co*-M2(Trt)$_{0.04}$)	19493	36052	43918	57338	1.84
Poly-(M1$_{0.95}$-*co*-M2(Trt)$_{0.05}$)	13020	28433	33670	49560	2.18

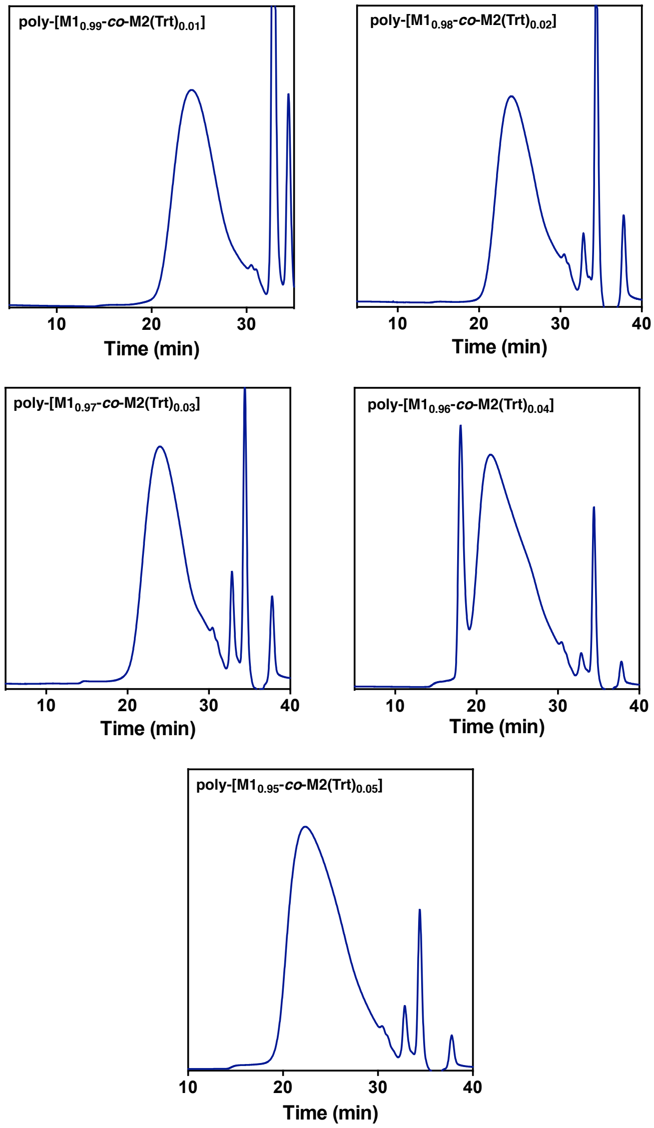

Figure S19: GPC chromatograms for poly-[M**1**$_r$-*co*-M**2**(Trt)$_{1-r}$] series.

The *cis* stereoregularity of the copolymers was determined by ^{1}H NMR spectroscopy where the vinyl proton resonates at 5.8 ppm, and Raman resonances. The peak at 1580 cm^{-1} is assigned to C=C bond stretching in the *cis* poly(acetylene) and overlaps with that of the phenyl ring. The peak at 1340 cm^{-1} is assigned to the *cis* C-C bond coupled with the single bond connecting the main chain and the phenyl ring. The peak at 1004 cm^{-1} is assigned to the C-H bond deformation of the *cis* form.

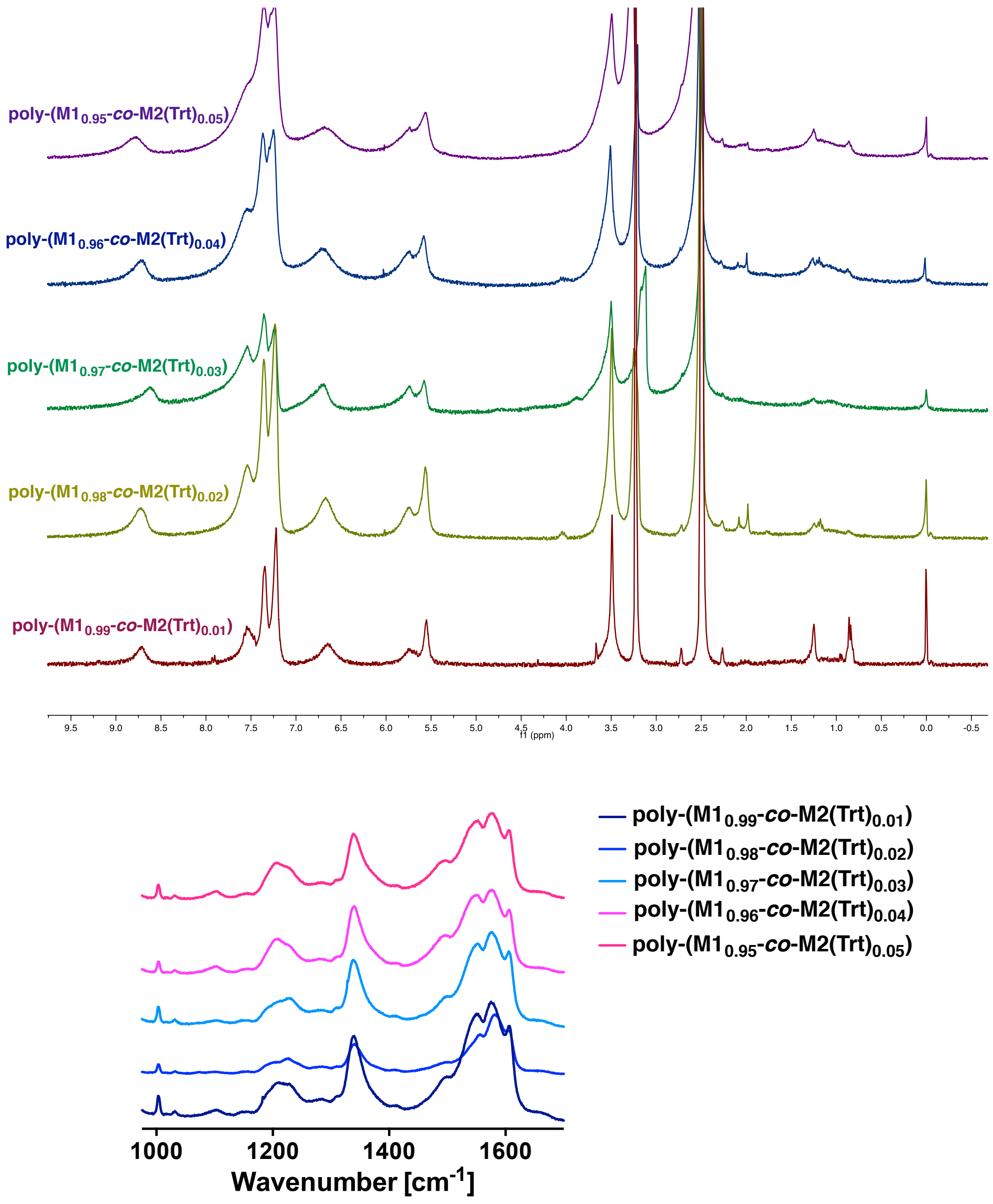

Figure S20: H NMR in DMSO-d$_6$ and Raman spectra for copolymers poly-(M**1**$_r$-*co*-M**2**(Trt)$_{1-r}$) (r = 0.95-0.99).

5. Thermal studies for copolymers poly-(M1$_r$-*co*-M2(Trt)$_{1-r}$)

5.1 DSC studies for poly-(M1$_r$-*co*-M2(Trt)$_{1-r}$)

DSC studies were carried out in order to determine de geometry of the polymer backbone. As a general protocol, a polymer sample was kept in an aluminum pan and heated from 40 °C to 350 °C with a heating rate of 10 °C/min.

The thermograms of the polymers show typical traces for a *cis-trans* backbone, where two exothermal peaks corresponding to the *c-t* to *c-c* and the *c-c* to *t-t* were observed.

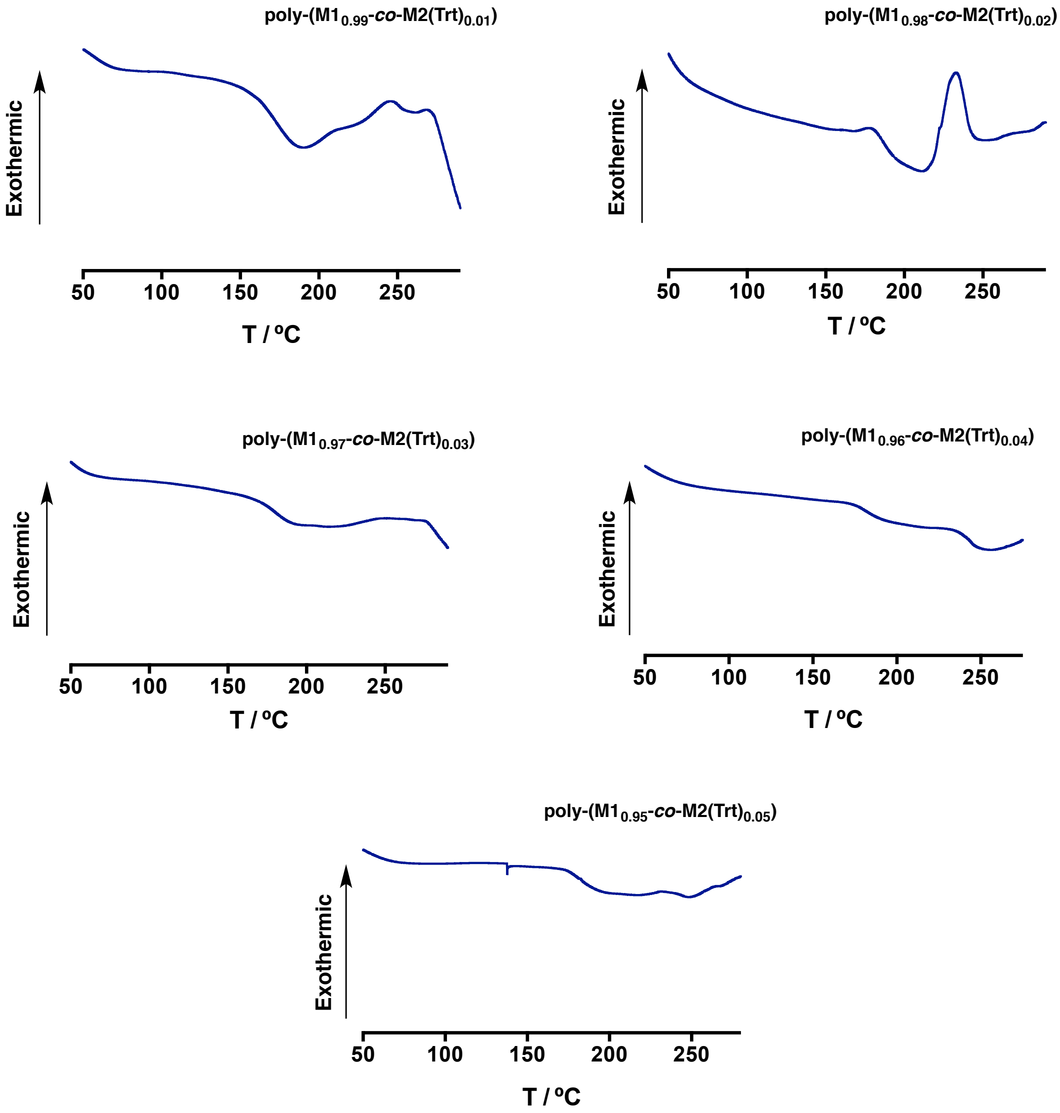

Figure S21: DSC thermograms for copolymers poly-(M**1**$_r$-*co*-M**2**(Trt)$_{1-r}$).

5.2 TGA studies for copolymers poly-(M1$_r$-*co*-M2(Trt)$_{1-r}$)

TGA Studies were carried out in order to determine the thermal stability of the copolymers. As a general protocol, a polymer sample was kept in a platinum pan and heated from 40 °C to 850 °C with a heating rate if 10 °C/min.

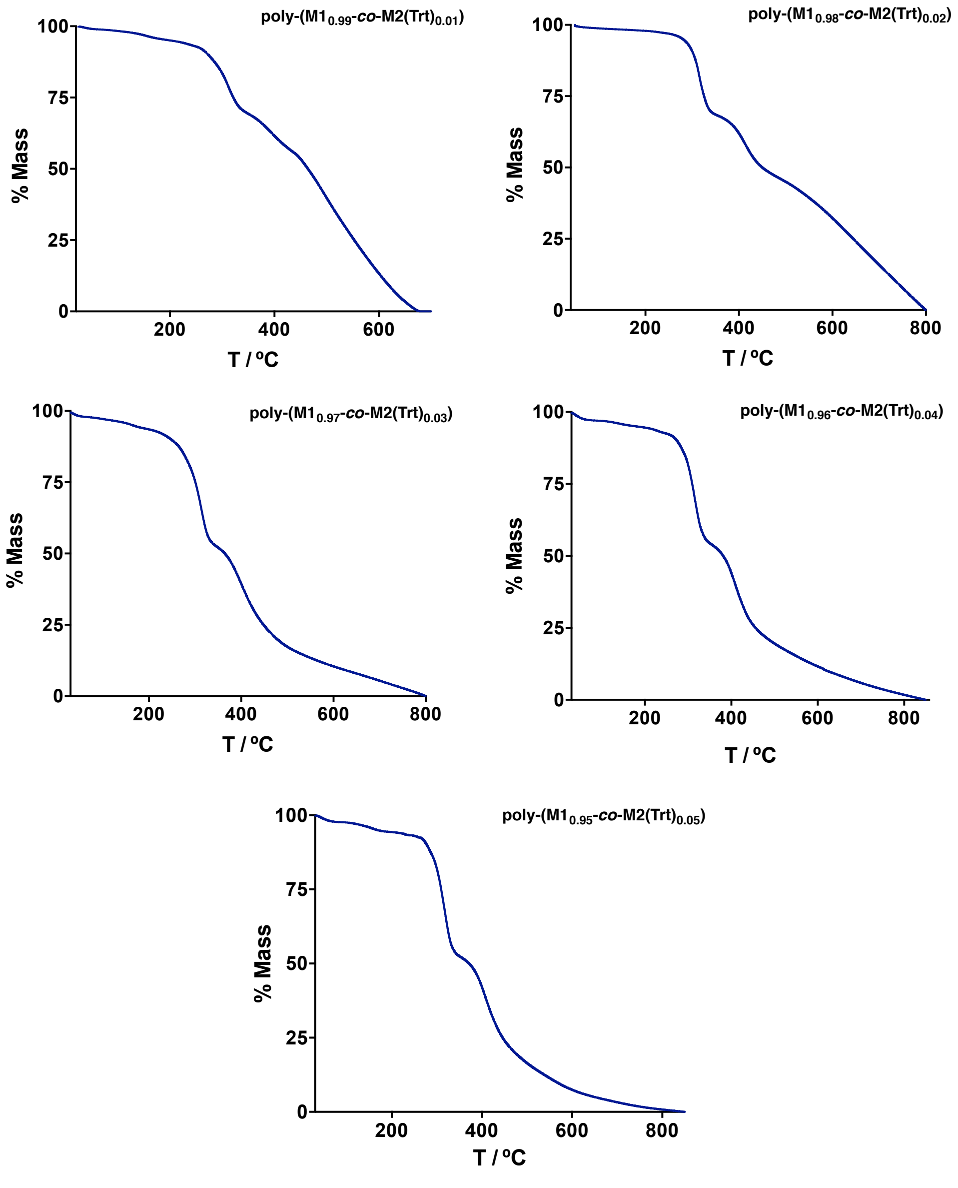

Figure S22: TGA thermograms for copolymers poly-(M**1**$_r$-*co*-M**2**(STrt)$_{1-r}$).

6. CD and UV-Vis studies for poly-(M1$_r$-*co*-M2(Trt)$_{1-r}$) in polar and low polar solvents

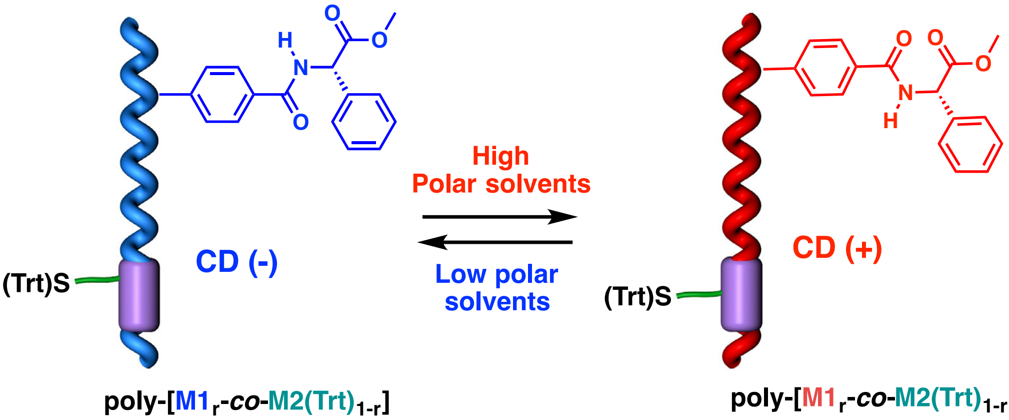

CD and UV-Vis studies were performed with a solution of poly-(M**1**$_r$-*co*-M**2**(Trt)$_{1-r}$) in different high polar (DMSO, DMF) and low polar ($CHCl_3$, THF) solvents which concentration was 0.3 mg mL^{-1}.

Poly-(M**1**$_r$-*co*-M**2**(Trt)$_{1-r}$) dissolved in low polar solvents ($CHCl_3$, THF) presents a negative Cotton effect (*M* helices) in the vinylic region corresponding to a *anti* conformation between carbonyl groups in the pendant group. On the other hand, poly-(M**1**$_r$-*co*-M**2**(Trt)$_{1-r}$) dissolved in high polar solvents (DMF, DMSO) presents a positive Cotton effect (*P* helices) corresponding to a *syn* between carbonyl groups in the pendant group.

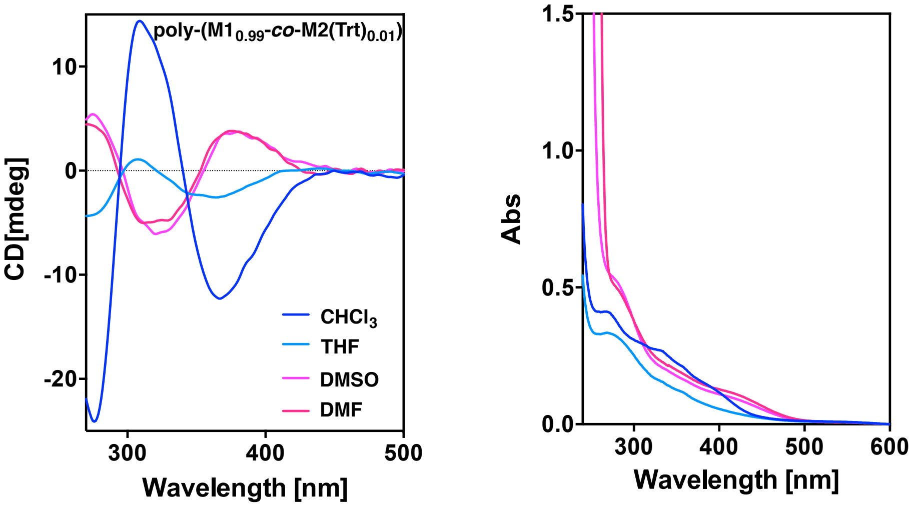

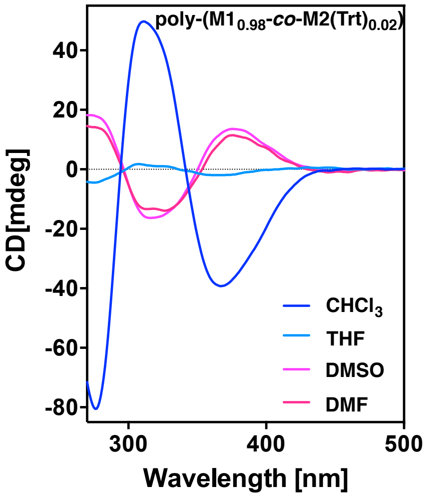
poly-(M1$_{0.98}$-*co*-M2(Trt)$_{0.02}$)
CD[mdeg]
40
20
0
-20
-40
-60
-80
300
400
500
Wavelength [nm]
CHCl$_3$
THF
DMSO
DMF

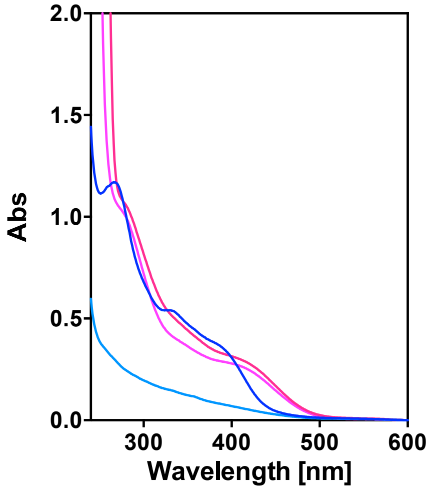
Abs
2.0
1.5
1.0
0.5
0.0
300
400
500
600
Wavelength [nm]

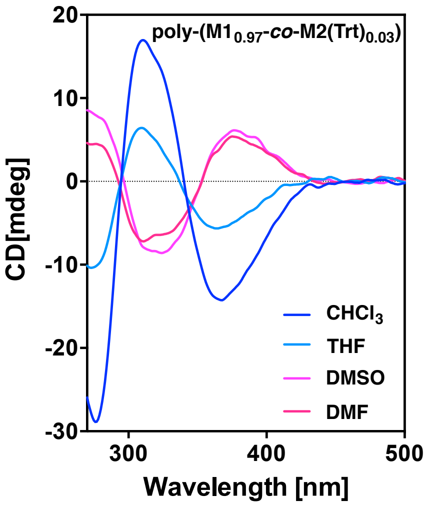
poly-(M1$_{0.97}$-*co*-M2(Trt)$_{0.03}$)
CD[mdeg]
20
10
0
-10
-20
-30
300
400
500
Wavelength [nm]
CHCl$_3$
THF
DMSO
DMF

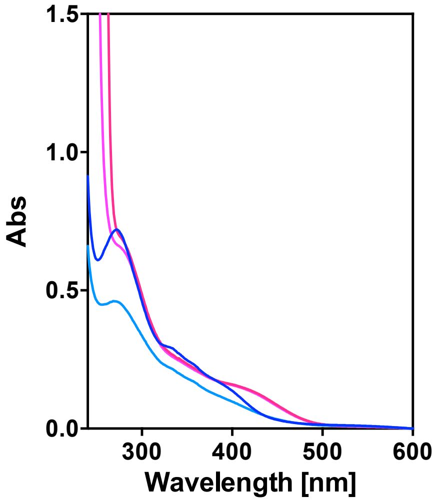
Abs
1.5
1.0
0.5
0.0
300
400
500
600
Wavelength [nm]

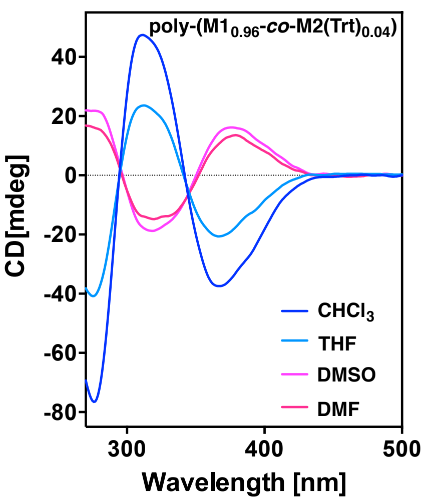
poly-(M1$_{0.96}$-*co*-M2(Trt)$_{0.04}$)
CD[mdeg]
40
20
0
-20
-40
-60
-80
300
400
500
Wavelength [nm]
CHCl$_3$
THF
DMSO
DMF

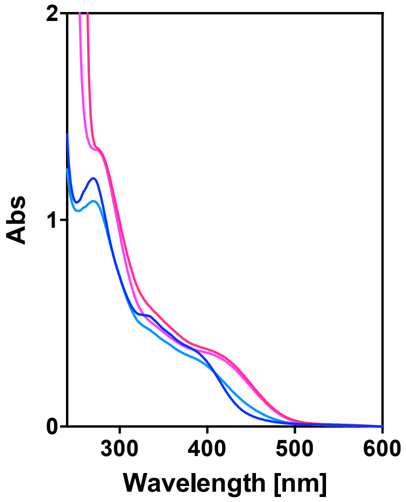
Abs
2
1
0
300
400
500
600
Wavelength [nm]

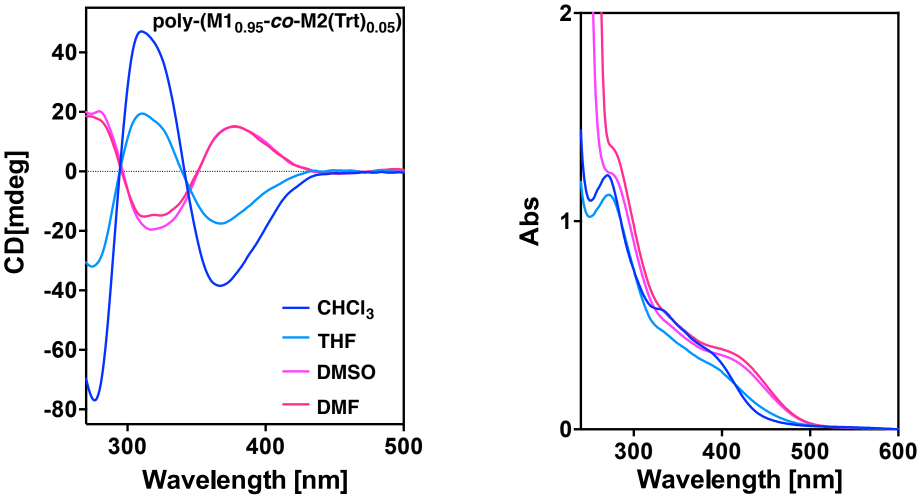

Figure S23: CD and UV-Vis spectra for copolymers poly-(M**1**$_r$-*co*-M**2**(Trt)$_{1-r}$) in polar (DMF, DMSO) and non-polar solvents (CHCl$_3$, THF) at 0.3 mg mL^{-1} of concentration.

7. CD and UV-Vis studies of poly-(M1$_r$-*co*-M2(Trt)$_{1-r}$) in presence of LiClO$_4$

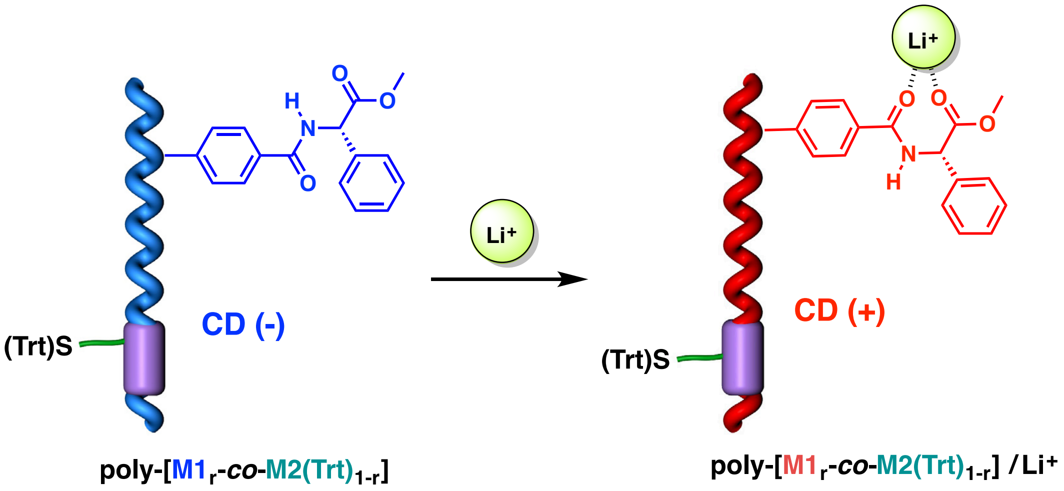

CD and UV-Vis studies were performed with a solution of poly-(M**1**$_r$-*co*-M**2**(Trt)$_{1-r}$) in CHCl$_3$ (0.3 mg mL^{-1}) using LiClO$_4$ dissolved in MeOH which concentration was 10.0 mg mL^{-1}.

Thus, poly-(M**1**$_r$-*co*-M**2**(Trt)$_{1-r}$) dissolved in CHCl$_3$ shows a negative Cotton effect (*M* helices) in the vinylic region corresponding to a *anti* conformation between carbonyl groups. On the other hand, the addition of Li$^+$ ions promotes a *syn* between carbonyl groups lead to a positive Cotton Effect in the vinylic region (*P* helices).

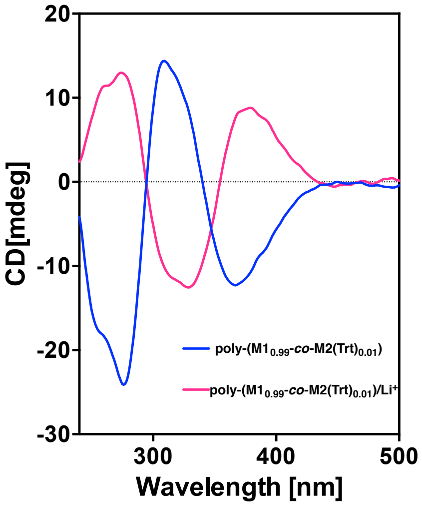
20
10
0
-10
-20
-30
CD[mdeg]
300
400
500
Wavelength [nm]
poly-(M1$_{0.99}$-*co*-M2(Trt)$_{0.01}$)
poly-(M1$_{0.99}$-*co*-M2(Trt)$_{0.01}$)/Li^{+}

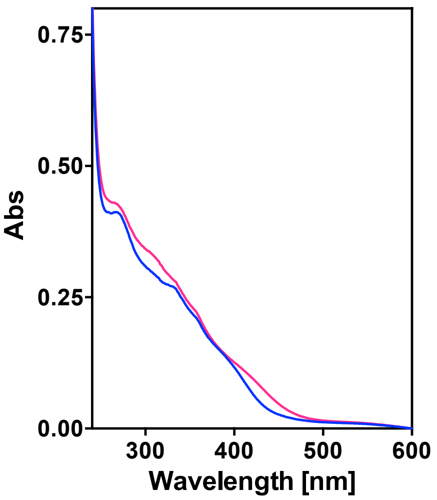
0.75
0.50
0.25
0.00
Abs
300
400
500
600
Wavelength [nm]

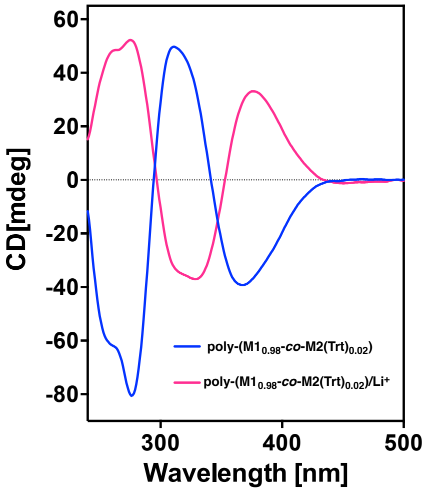
60
40
20
0
-20
-40
-60
-80
CD[mdeg]
300
400
500
Wavelength [nm]
poly-(M1$_{0.98}$-*co*-M2(Trt)$_{0.02}$)
poly-(M1$_{0.98}$-*co*-M2(Trt)$_{0.02}$)/Li^{+}

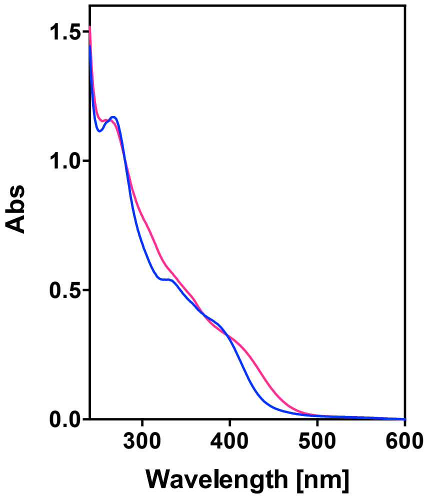
1.5
1.0
0.5
0.0
Abs
300
400
500
600
Wavelength [nm]

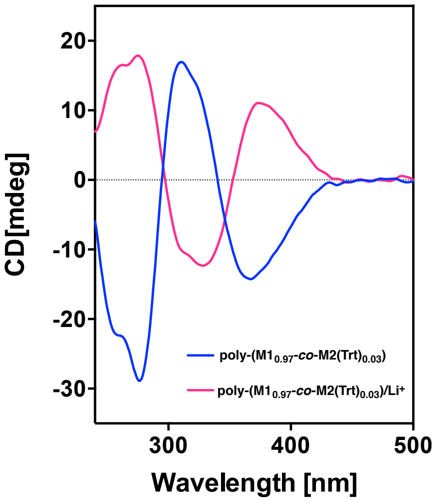
20
10
0
-10
-20
-30
CD[mdeg]
300
400
500
Wavelength [nm]
poly-(M1$_{0.97}$-*co*-M2(Trt)$_{0.03}$)
poly-(M1$_{0.97}$-*co*-M2(Trt)$_{0.03}$)/Li^{+}

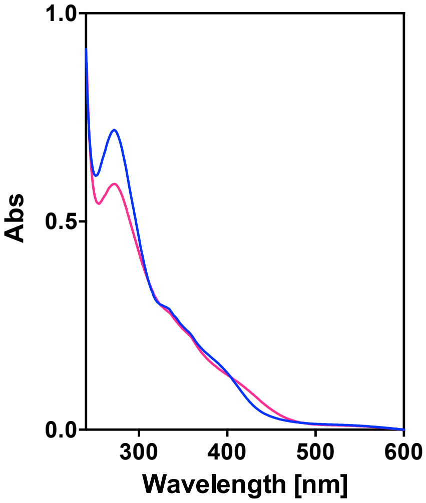
1.0
0.5
0.0
Abs
300
400
500
600
Wavelength [nm]

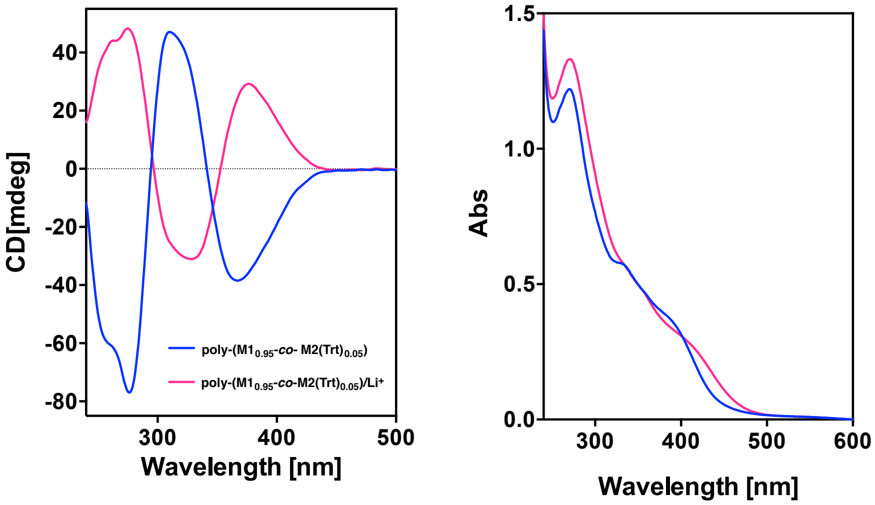

Figure S24: CD and UV-Vis studies for poly-(M**1**$_r$-*co*-M**2**(Trt)$_{1-r}$) in $CHCl_3$ (0.3 mg mL^{-1}) in presence of Li^+ ions.

8. Deprotection of copolymers poly-(M1$_r$-*co*-M2(Trt)$_{1-r}$)

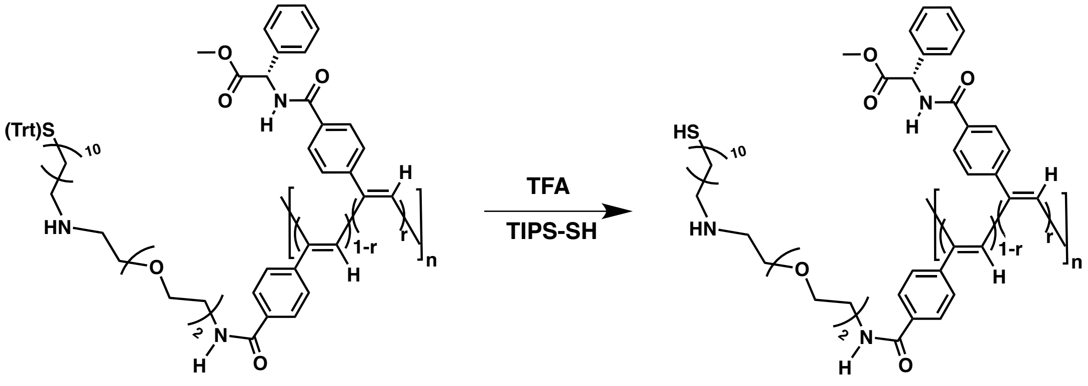

poly-(M1$_r$-*co*-M2(Trt)$_{1-r}$)
r = 95-99 %

poly-(M1$_r$-*co*-M2(Trt)$_{1-r}$)/TFA
r = 95-99 %

To a solution of copolymers poly-(M**1**$_r$-*co*-M**2**(Trt)$_{1-r}$ (3 mg mL^{-1}, $CHCl_3$) was added a mixture of TFA/TIPS-SH (1% v/v). After 1 hour, the copolymers were precipitated in MeOH and redisolved in a mixture of $CHCl_3$/MeCN. Finally, the solvent was evaporated at reduced pressure and the resulting copolymers were characterized by NMR, CD and UV-Vis.

8.1 ^{1}H NMR for poly-(M1$_r$-*co*-M2$_{1-r}$) and poly-(M1$_r$-*co*-M2$_{1-r}$)/TFA

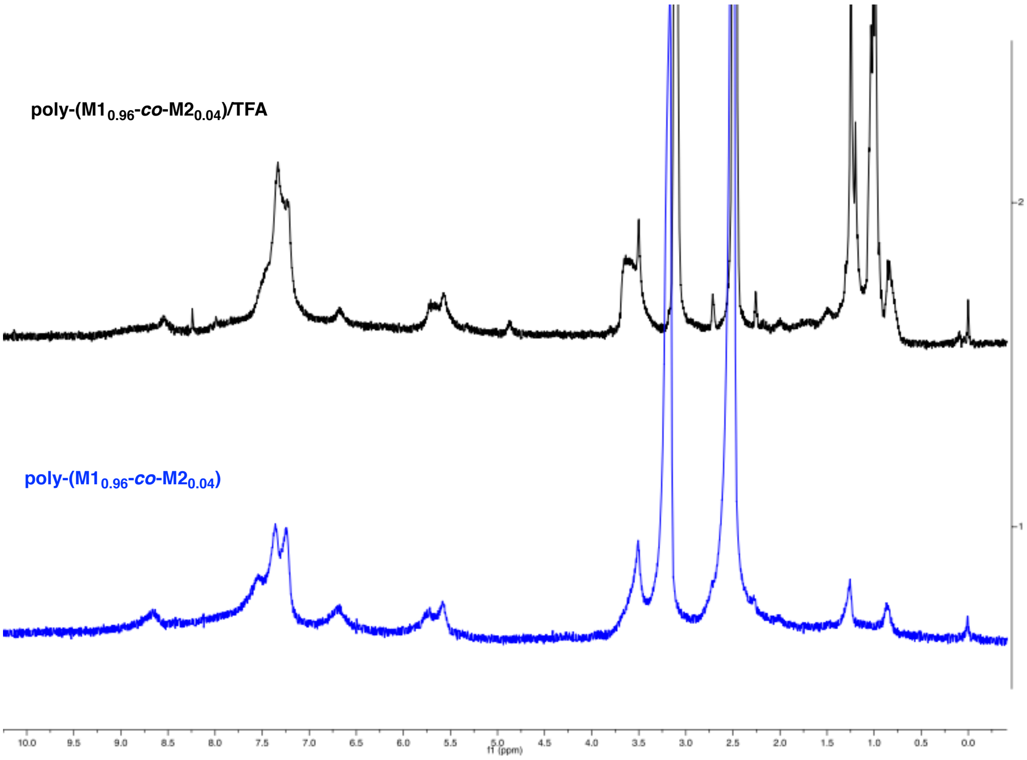

Figure S25: ^{1}H NMR Comparative spectra for copolymers poly-(M**1**$_{0.96}$-*co*-M**2**$_{0.04}$) and poly-(M**1**$_{0.96}$-*co*-M**2**$_{0.04}$) titrated with TFA.

8.2 CD studies for copolymers poly-(M1$_r$-*co*-M2$_{1-r}$) titrated with TFA

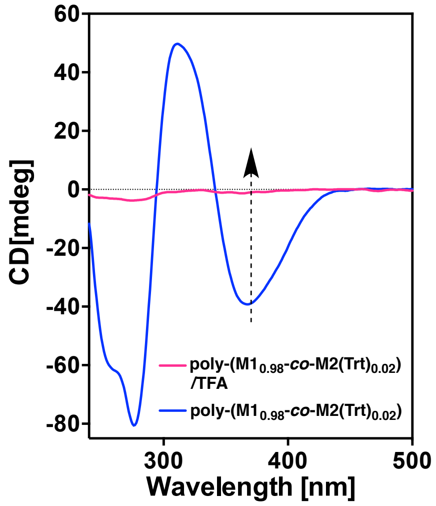

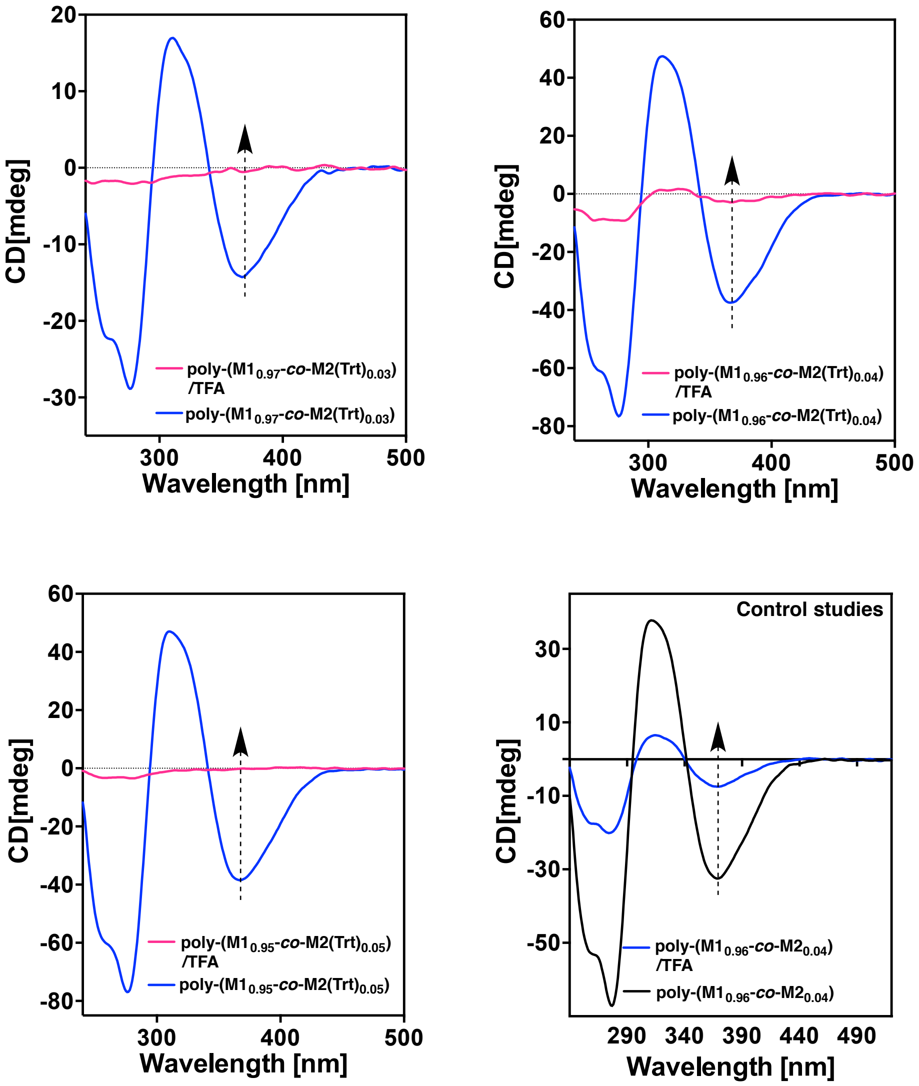

Figure S26: CD and UV-Vis studies for titration of copolymers poly-(M**1**$_r$-*co*-M**2**(Trt)$_{1-r}$) (0.3 mg mL^{-1}, CHCl$_3$) with TFA/TIPS-SH (1% v/v).

9. Synthesis for the co-polymer series poly-(M**1**$_r$-*co*-M**2**$_{1-r}$)

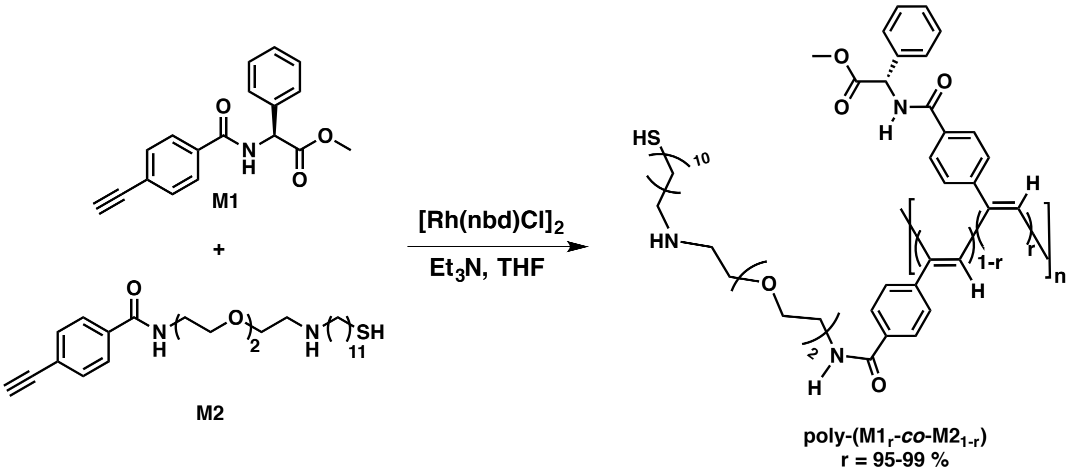

Following the general procedure quantities of M**1**, M**2**, Et$_3$N, [Rh(nbd)Cl]$_2$, and THF as shown in Table S3 were employed. Reaction yield is also indicated in the Table S3.

Table S3:

Copolymer	M1 (mg)	M1 (mmol)	M2 (mg)	M2 (mmol)	Cat (mg)	THF (mL)	Et$_3$N (µL)	poly (mg)	Yield (%)
poly-(M1$_{0.95}$-*co*-M2$_{0.05}$)	69.7	0.238	5.7	0.013	0.576	0.75	7	62.0	71
poly-(M1$_{0.96}$-*co*-M2$_{0.04}$)	70.3	0.240	4.6	0.010	0.576	0.75	7	54.7	73
poly-(M1$_{0.97}$-*co*-M2$_{0.03}$)	71.1	0.243	3.4	0.008	0.576	0.75	7	57.7	77
poly-(M1$_{0.98}$-*co*-M2$_{0.02}$)	71.8	0.245	2.3	0.005	0.576	0.75	7	60.7	81
poly-(M1$_{0.99}$-*co*-M2$_{0.01}$)	72.5	0.248	1.1	0.003	0.576	0.75	7	66.0	88

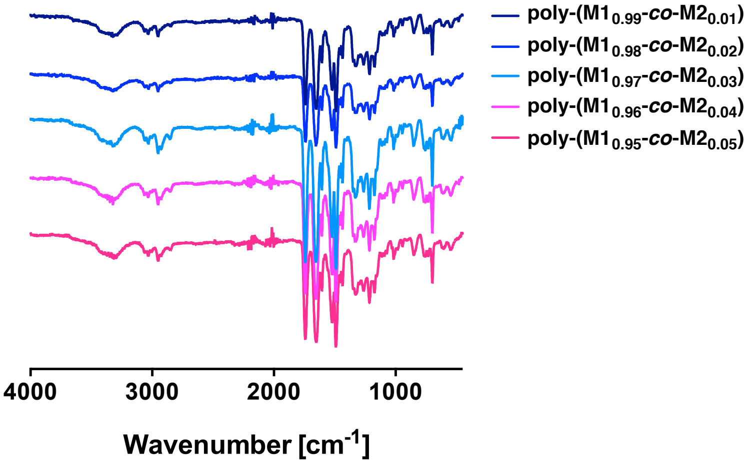

Figure S27: FT-IR spectra for the copolymers poly-(M**1**$_r$-*co*-M**2**$_{1-r}$).

Table S4: GPC data for poly-M**1** and poly-(M**1**$_r$-*co*-M**2**$_{1-r}$).

Polymer	M_n	M_w	M_p	M_z	PDI
Poly-M**1**	26252	47057	35345	102574	1.79
poly-(M**1**$_{0.99}$-*co*-M**2**$_{0.01}$)	16024	65822	24020	39072	4.10
poly-(M**1**$_{0.98}$-*co*-M**2**$_{0.02}$)	15830	40045	25930	91247	2.53
poly-(M**1**$_{0.97}$-*co*-M**2**$_{0.03}$)	16195	38108	32056	78513	2.35
poly-(M**1**$_{0.96}$-*co*-M**2**$_{0.04}$)	13462	28799	18798	57885	2.13
poly-(M**1**$_{0.95}$-*co*-M**2**$_{0.05}$)	11774	23219	15450	46952	1.97

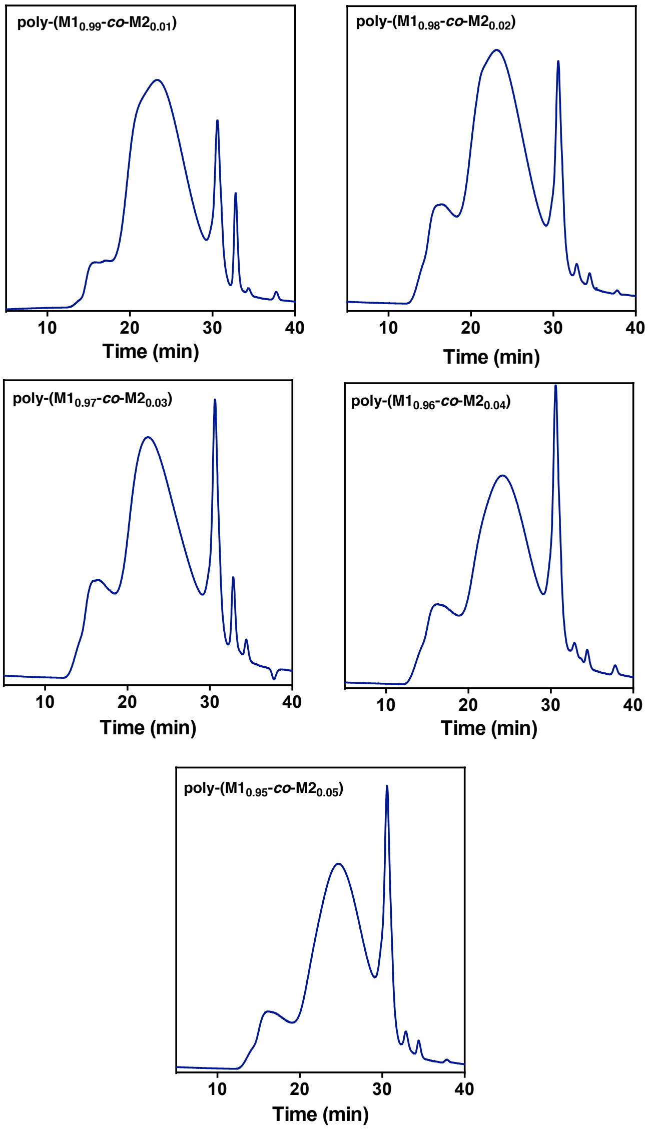

Figure S28: GPC chromatograms for poly-(M**1**$_r$-*co*-M**2**$_{1-r}$) series.

The *cis* stereoregularity of the copolymers was determined by ^{1}H NMR spectroscopy where the vinyl proton resonates at 5.8 ppm, and Raman resonances. The peak at 1585 cm^{-1} is assigned to C=C bond stretching in the *cis* poly(acetylene) and overlaps with that of the phenyl ring. The peak at 1342 cm^{-1} is assigned to the *cis* C-C bond coupled with the single bond connecting the main chain and the phenyl ring. The peak at 1006 cm^{-1} is assigned to the C-H bond deformation of the *cis* form.

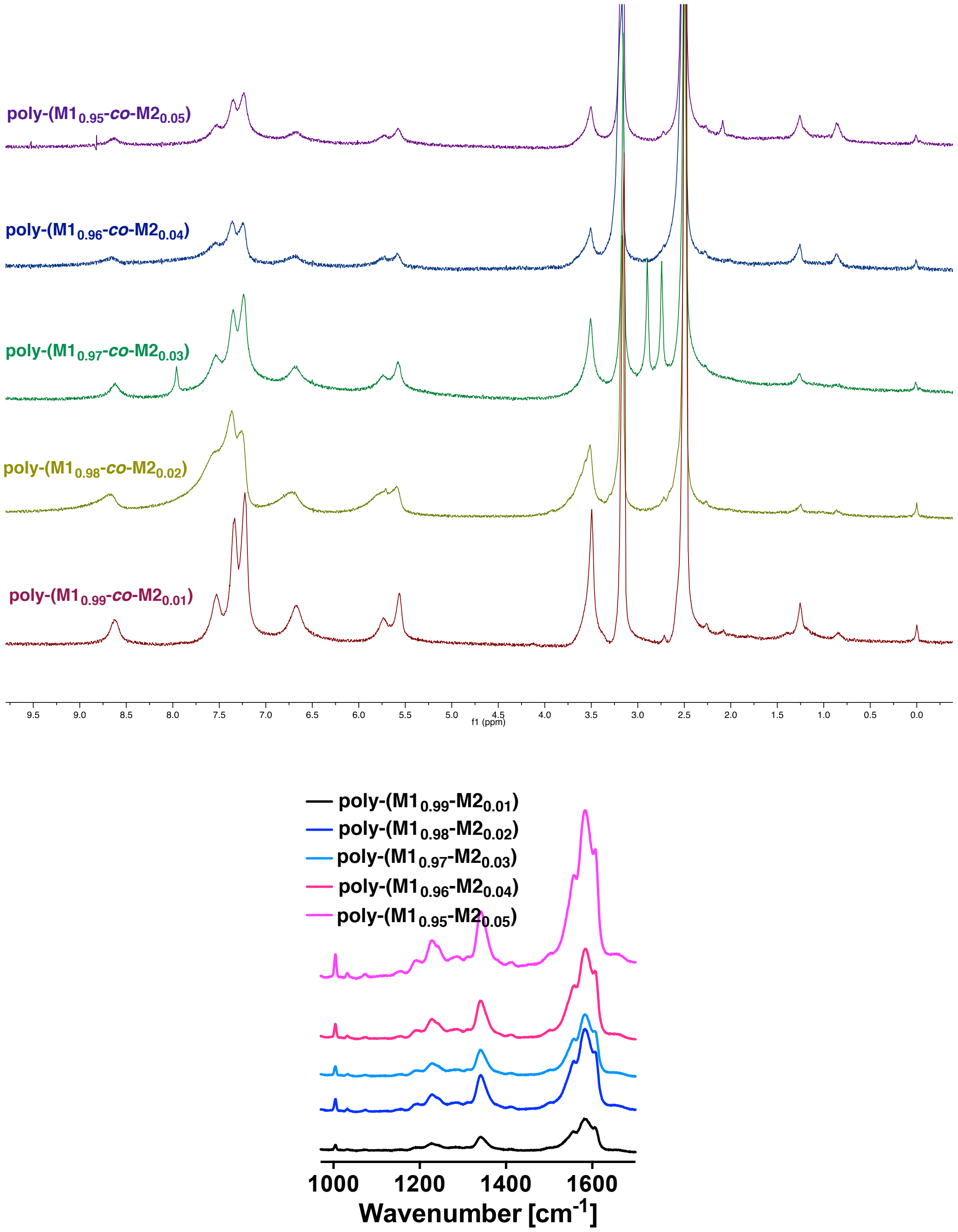

Figure S29: ^{1}H NMR in DMSO-d$_6$ and Raman spectra for copolymers poly-(M**1**$_r$-*co*-M**2**$_{1-r}$).

10. CD and UV-Vis studies for copolymers poly-(M1$_r$-*co*-M2$_{1-r}$) in high polar and low polar solvents

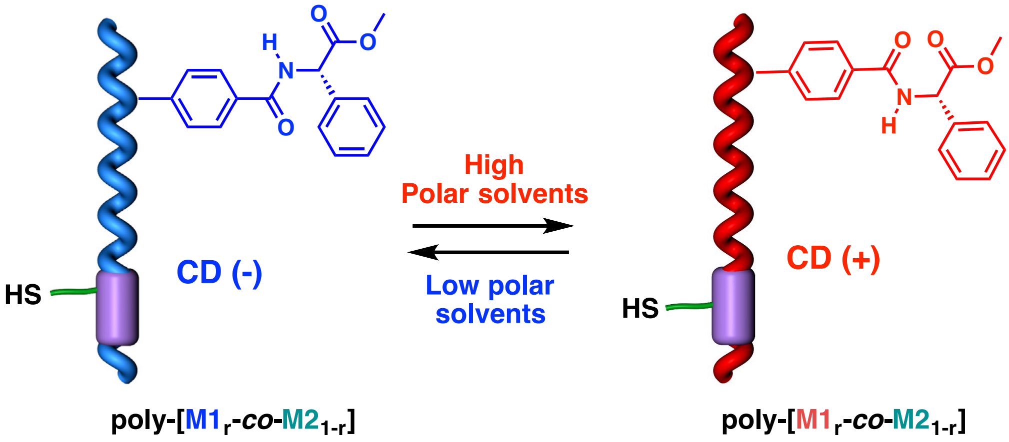

CD and UV-Vis studies were performed with a solution of poly-(M1$_r$-*co*-M2$_{1-r}$) in different high polar (DMSO, DMF) and low polar ($CHCl_3$, THF) solvents which concentration was 0.3 mg mL^{-1}.

Poly-(M**1**$_r$-*co*-M**2**$_{1-r}$) dissolved in low polar solvents ($CHCl_3$, THF) presents a negative Cotton effect in the vinylic region (*M* helices) corresponding to a *anti* conformation between carbonyl groups in the pendant group whereas poly-(M**1**$_r$-*co*-M**2**$_{1-r}$) dissolved in high polar solvents (DMF, DMSO) presents a positive Cotton effect (*P* helices) corresponding to a *syn* between carbonyl carbonyl groups in the pendant group.

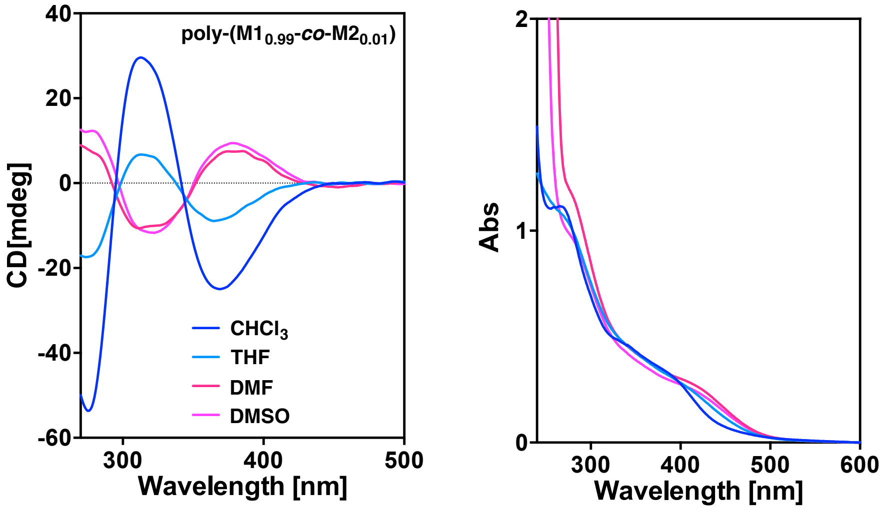

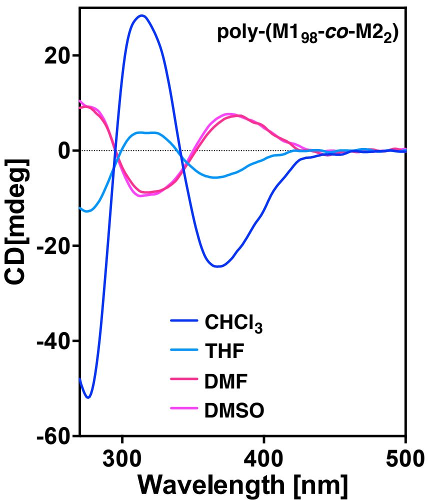
poly-(M1$_{98}$-*co*-M2$_{2}$)
CD[mdeg]
20
0
-20
-40
-60
300
400
500
Wavelength [nm]
CHCl$_3$
THF
DMF
DMSO

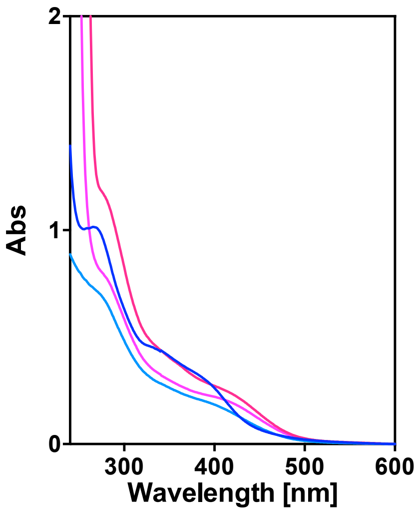
Abs
2
1
0
300
400
500
600
Wavelength [nm]

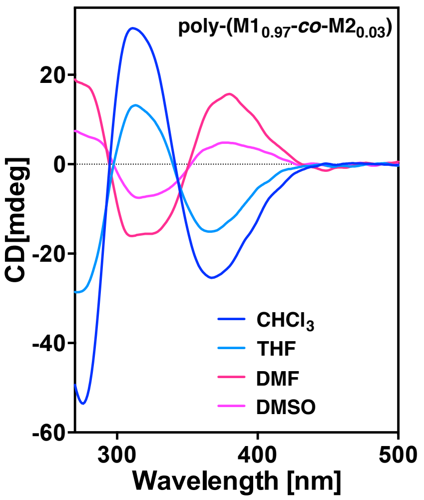
poly-(M1$_{0.97}$-*co*-M2$_{0.03}$)
CD[mdeg]
20
0
-20
-40
-60
300
400
500
Wavelength [nm]
CHCl$_3$
THF
DMF
DMSO

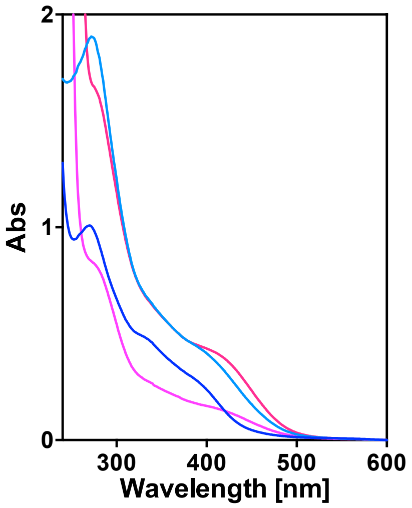
Abs
2
1
0
300
400
500
600
Wavelength [nm]

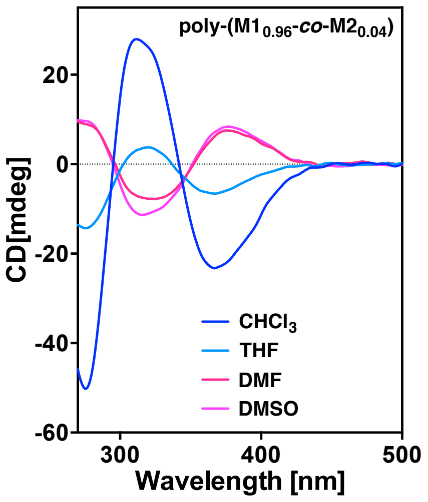
poly-(M1$_{0.96}$-*co*-M2$_{0.04}$)
CD[mdeg]
20
0
-20
-40
-60
300
400
500
Wavelength [nm]
CHCl$_3$
THF
DMF
DMSO

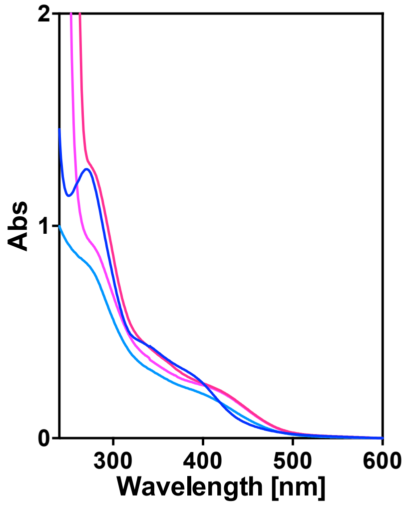
Abs
2
1
0
300
400
500
600
Wavelength [nm]

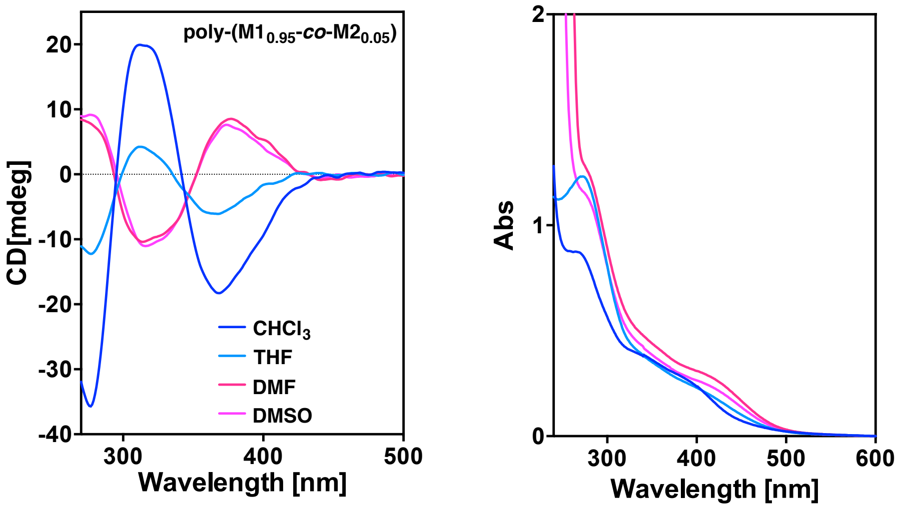

Figure S30: CD and UV-Vis studies for copolymers poly-(M**1**$_r$-*co*-M**2**$_{1-r}$) in polar (DMF, DMSO) and low polar solvents (THF, CHCl$_3$) at 0.3 mg mL^{-1} of concentration.

11. CD and UV-Vis studies for copolymers poly-(M1$_r$-*co*-M2$_{1-r}$) in presence of LiClO$_4$

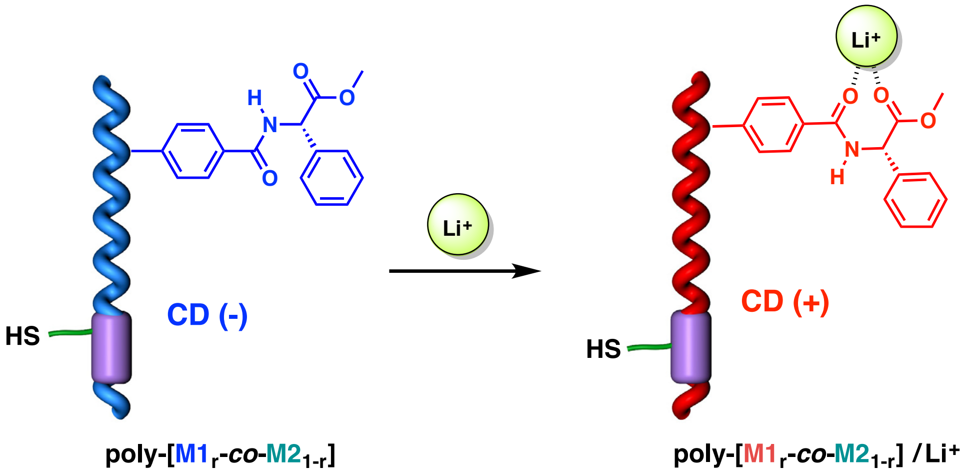

CD and UV-Vis studies were performed with a solution of poly-(M**1**$_r$-co-M**2**$_{1-r}$) in CHCl$_3$ (0.3 mg mL^{-1}) using LiClO$_4$ dissolved in MeOH which concentration was 10.0 mg mL^{-1}.

Thus, poly-(M**1**$_r$-co-M**2**$_{1-r}$) dissolved in CHCl$_3$ shows a negative Cotton effect in the vinylic region (*M* helices) corresponding to a *anti* conformation between carbonyl groups in the pendant group. The addition of Li$^+$ ions promotes a *syn* between carbonyl groups lead to a positive Cotton Effect in the vinylic region (*P* helices).

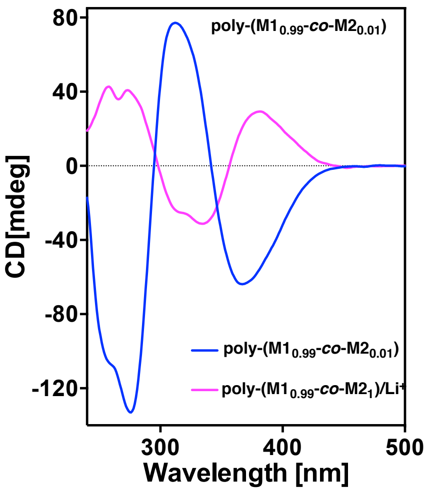
poly-(M1$_{0.99}$-*co*-M2$_{0.01}$)
80
40
0
-40
-80
-120
CD[mdeg]
300
400
500
Wavelength [nm]
poly-(M1$_{0.99}$-*co*-M2$_{0.01}$)
poly-(M1$_{0.99}$-*co*-M2$_{1}$)/Li+

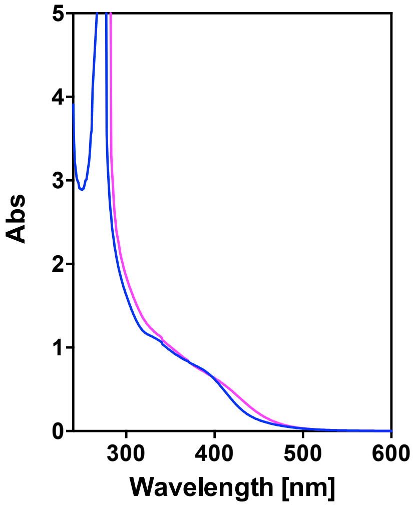
5
4
3
2
1
0
Abs
300
400
500
600
Wavelength [nm]

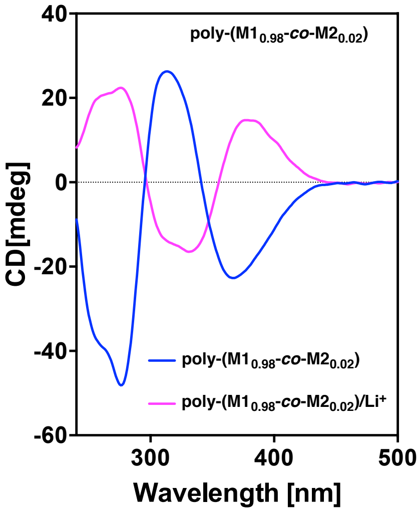
poly-(M1$_{0.98}$-*co*-M2$_{0.02}$)
40
20
0
-20
-40
-60
CD[mdeg]
300
400
500
Wavelength [nm]
poly-(M1$_{0.98}$-*co*-M2$_{0.02}$)
poly-(M1$_{0.98}$-*co*-M2$_{0.02}$)/Li+

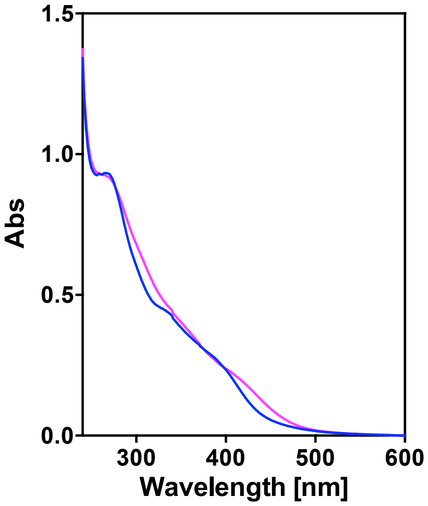
1.5
1.0
0.5
0.0
Abs
300
400
500
600
Wavelength [nm]

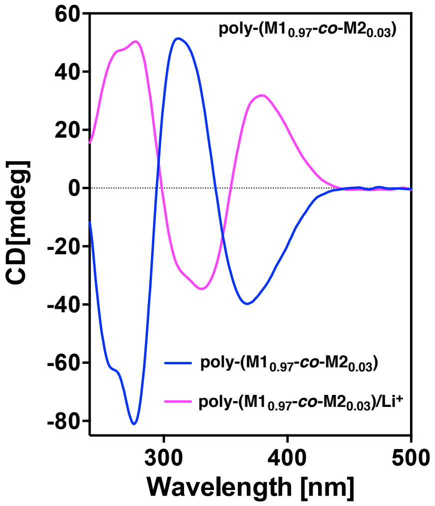
poly-(M1$_{0.97}$-*co*-M2$_{0.03}$)
60
40
20
0
-20
-40
-60
-80
CD[mdeg]
300
400
500
Wavelength [nm]
poly-(M1$_{0.97}$-*co*-M2$_{0.03}$)
poly-(M1$_{0.97}$-*co*-M2$_{0.03}$)/Li+

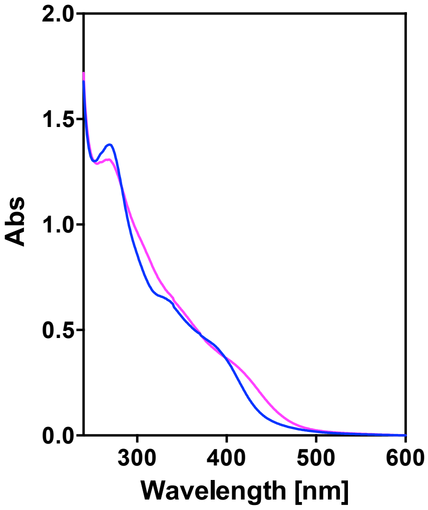
2.0
1.5
1.0
0.5
0.0
Abs
300
400
500
600
Wavelength [nm]

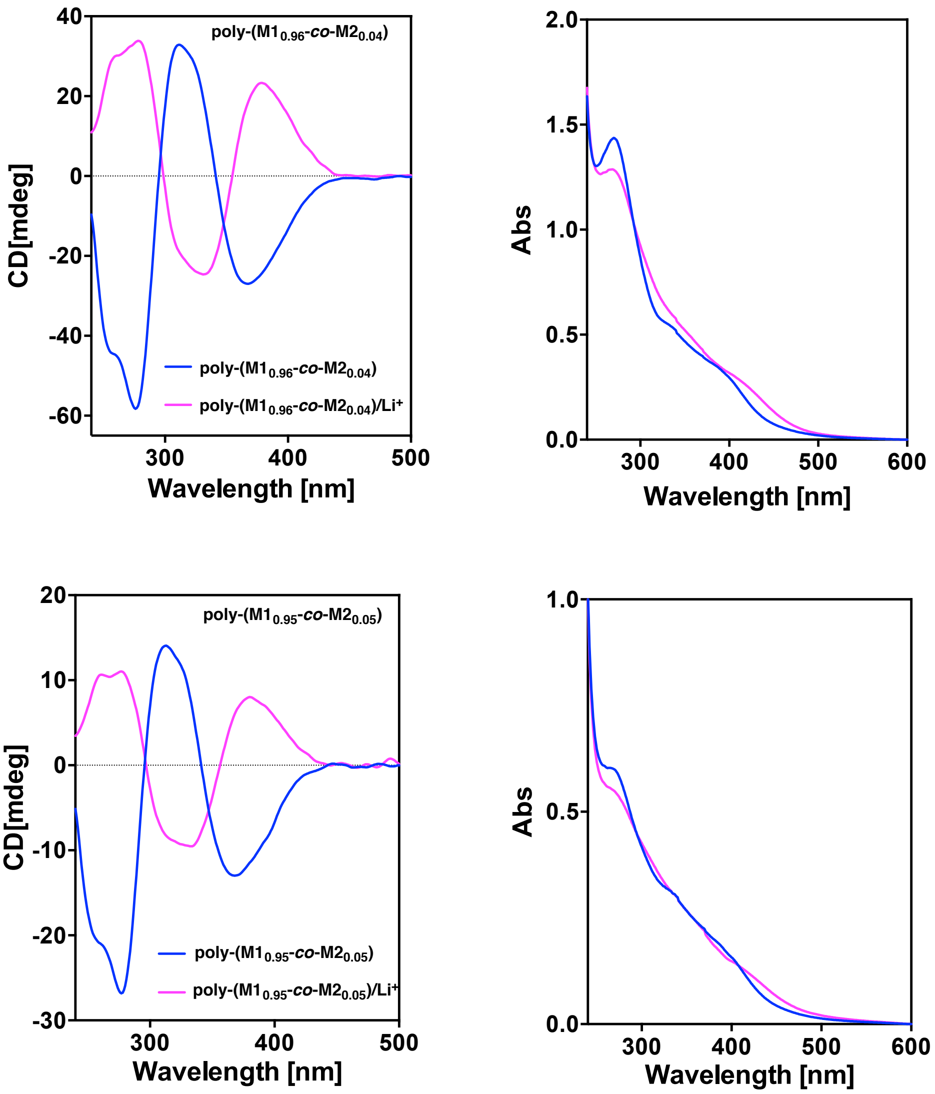

Figure S31: CD and UV-Vis studies for copolymers poly-(M**1**$_r$-*co*-M**2**$_{1-r}$) (r = 0.95-0.99) dissolved in CHCl$_3$ (0.3 mg mL^{-1}) in presence of LiClO$_4$ (10.0 mg mL^{-1}, MeOH).

Table S5: FT IR studies for poly-(M**1**$_r$-*co*-M**2**$_{1-r}$) and poly-(M**1**$_r$-*co*-M**2**$_{1-r}$)/Li$^+$

	C=O$_{(1)}$ (ester)/ (cm^{-1})	C=O$_{(2)}$ (amide)/ (cm^{-1})	OMe/ (cm^{-1})
poly-(M**1**$_r$-*co*-M**2**$_{1-r}$)	1741	1646	1090
poly-(M**1**$_r$-*co*-M**2**$_{1-r}$)/Li$^+$	1736	1642	1091

12. Thermal studies for copolymer series poly-(M1$_{r}$-*co*-M2$_{1-r}$)

12.1 DSC studies for poly-(M1$_{r}$-*co*-M2$_{1-r}$)

DSC studies were carried out in order to determine de geometry of the polymer backbone. As a general protocol, a polymer sample was kept in an aluminium pan and heated from 40 °C to 350 °C with a heating rate of 10 °C/min.

The thermograms of the polymers show typical traces for a *cis-trans* backbone, where two exothermal peaks corresponding to the *c-t* to *c-c* and the *c-c* to *t-t* were observed.

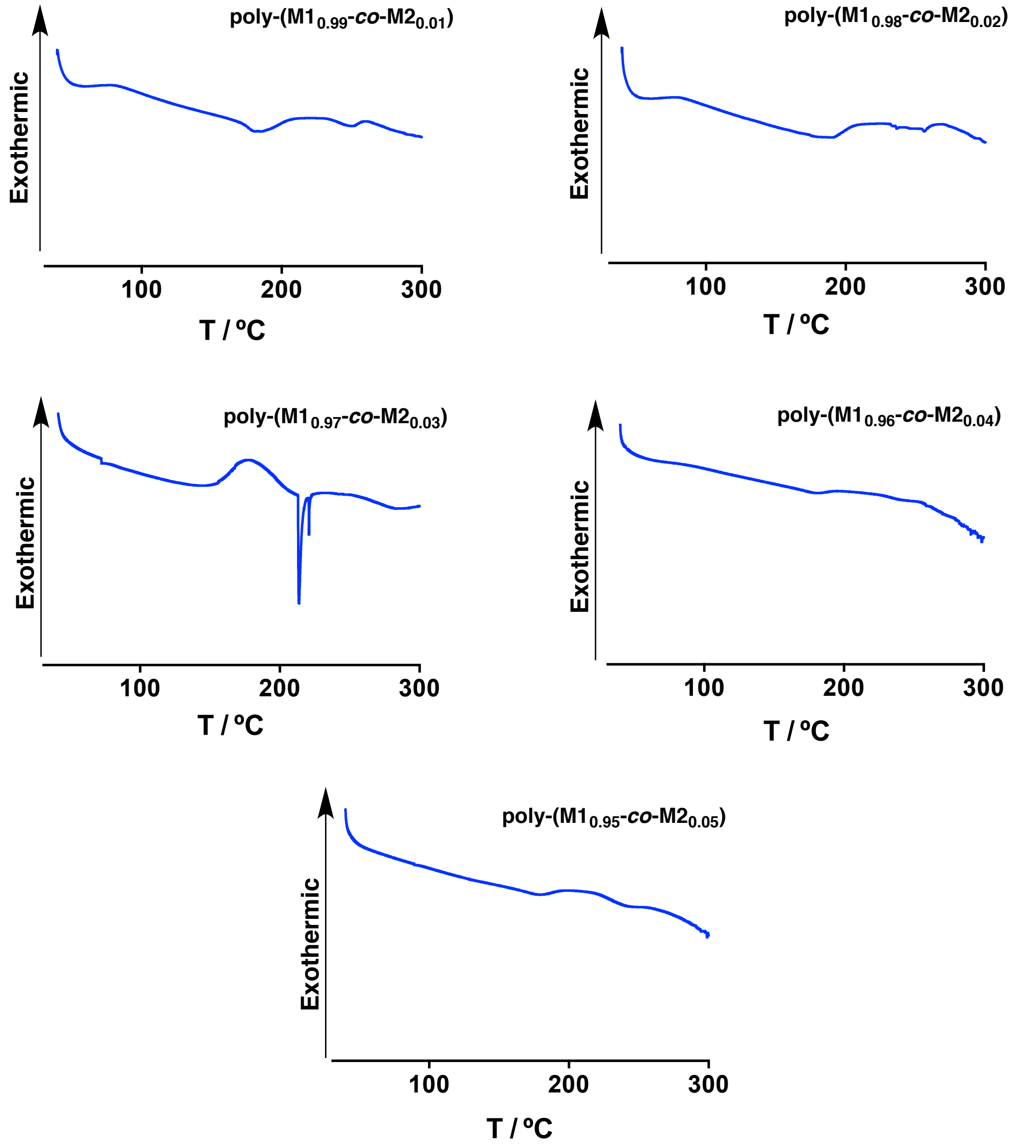

Figure S32: DSC thermograms for copolymers poly-(M**1**$_{r}$-*co*-M**2**$_{1-r}$) .

12.2 TGA studies for copolymers poly-(M1$_r$-*co*-M2$_{1-r}$)

TGA Studies were carried out in order to determine the thermal stability of the copolymers. As a general protocol, a polymer sample was kept in a platinum pan and heated from 40 °C to 850 °C with a heating rate if 10 °C/min.

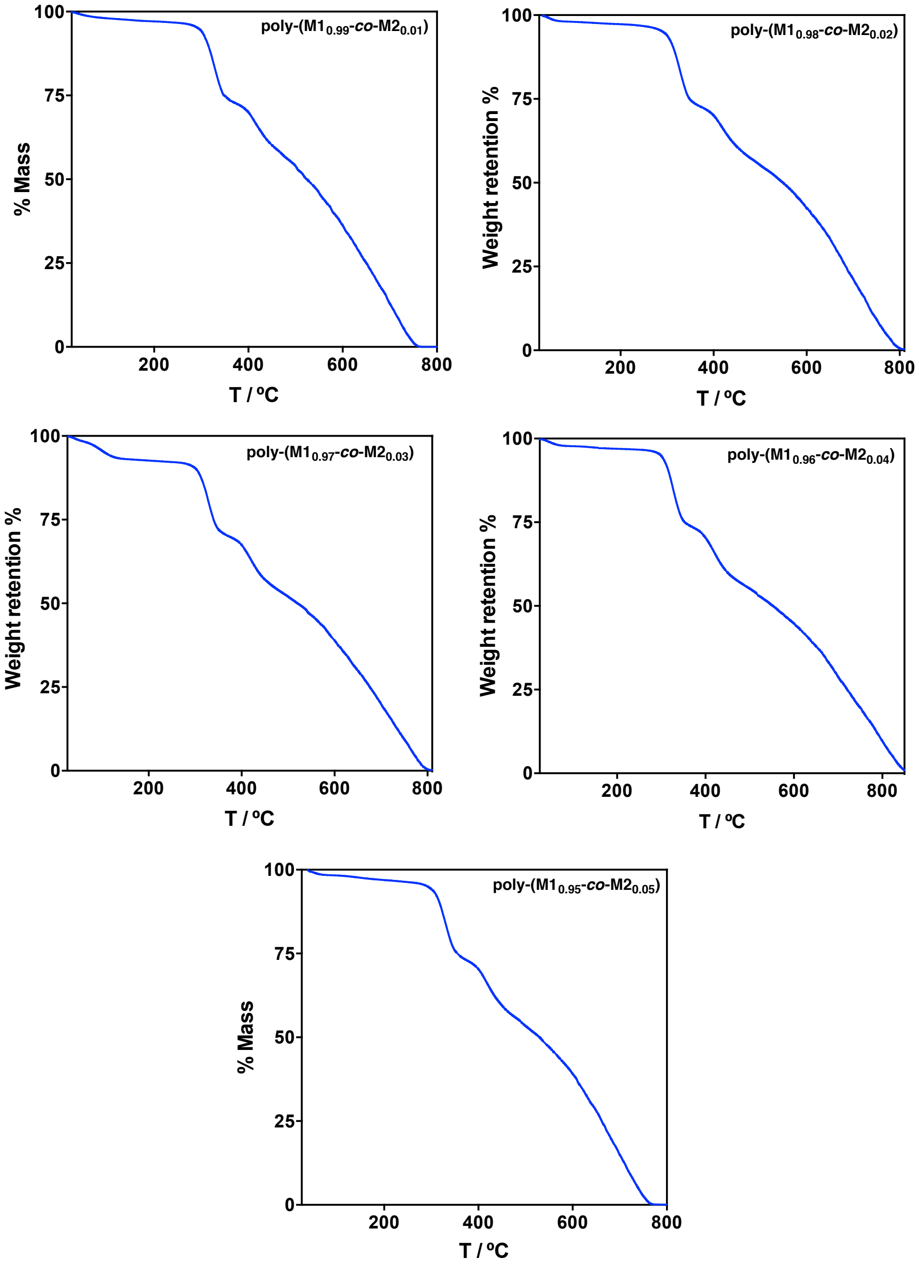

Figure S33: TGA thermograms for copolymers poly-(M**1**$_r$-*co*-M**2**$_{1-r}$) (r = 0.99-0.95).

13. Synthesis of Gold Nanoparticles (AuNPs)

13.1 Synthesis for AuNPs@dodecanethiol

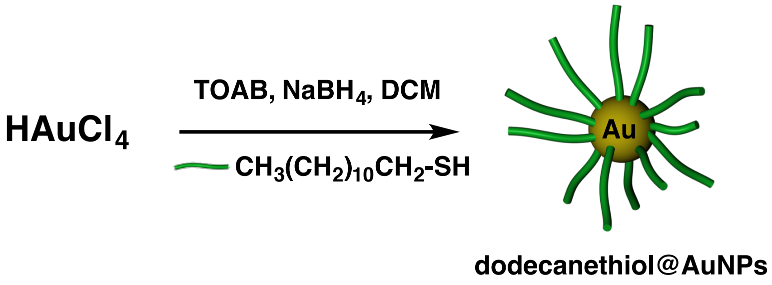

To a solution of tetraoctylamonium bromide (TOAB, 0.444 g, 0.812 mmol) into DCM (20mL) was added a solution of $HAuCl_4$ (0.080 g, 0.202 mmol) in distilled water (1.25 mL) and allowed to stir at rt. After some time, the mixture was washed with DCM (20 mL x 3). A solution of dodecanethiol (40 μL) in DCM (5 mL) were prepared, both solutions were added simultaneously to the reaction mixture and allowed to stir at -4°C for 30 min. After this time was added as a reducing agent, a solution of $NaBH_4$ (76 mg) in distilled water (2 mL). The reaction mixture turns a yellow-orange to brown – black. EtOH (HPLC grade, 50 mL) is added to the solution and left at -4 ° C for 18 h. After this time, the reaction mixture was filtered using a filter plate. The precipitate obtained was dissolved in $CHCl_3$ and a second process was conducted in toluene precipitation using centrifuge (1h, 11000 rpm) and obtaining AuNPs-dodecanethiol in a quantitative yield.

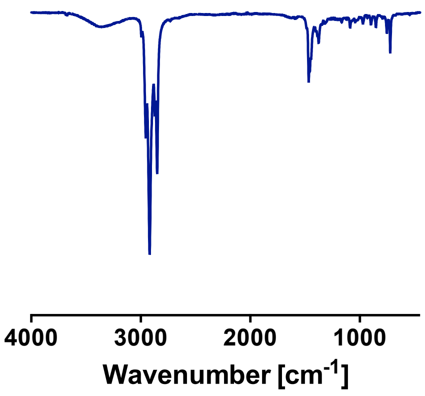

Figure S34: FT-IR spectrum for AuNP@dodecanethiol.

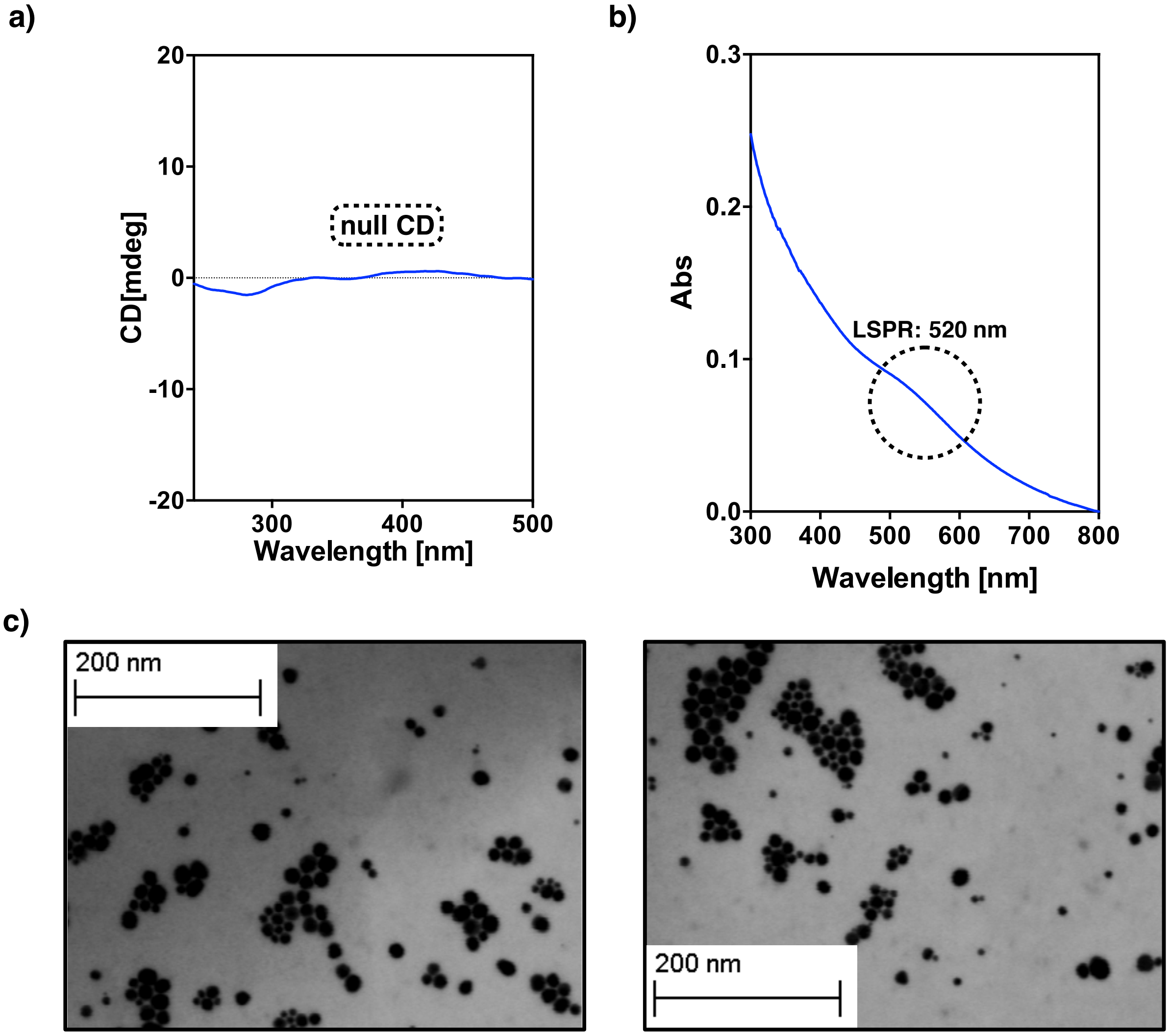

Figure S35: a) CD spectrum for Au@dodecanethiol in $CHCl_3$ at 1.0 mg mL^{-1} of concentration. b) UV-Vis spectrum for Au@dodecanethiol in $CHCl_3$ at 1.0 mg mL^{-1} of concentration. c) TEM images for Au@dodecanethiol (size: 13 nm, SD: 3 nm, scale bar: 200 nm, 255 nanoparticles).

13.2 Synthesis of Au-poly-($M1_r$-*co*-$M2_{1-r}$) nanocomposites

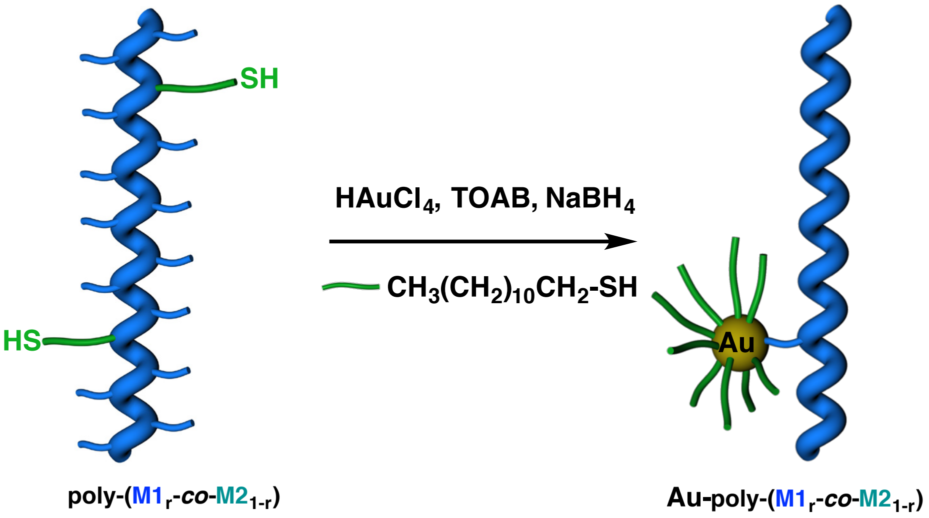

To a solution of tetraoctylamonium bromide (TOAB, 0.444g, 0.812 mmol) into DCM (20mL) was added a solution of $HAuCl_4$ (0.080 g, 0.202 mmol) in distilled water (1.25 mL) and allowed to stir at rt. After some time the mixture was washed with DCM (20 mL x 3). A copolymer (poly-M**1**$_r$-*co*-M**2**$_{1-r}$) solution (0.020 g) in DCM (5 mL) and another solution of dodecanethiol (40 uL) in DCM (5 mL) were prepared, both solutions were added simultaneously to the reaction mixture and allowed to stir at - 4°C for 30 min. After this time was added as a reducing agent, a solution of $NaBH_4$ (0.076 mg) in distilled water (2 mL). The reaction mixture turns a yellow-orange to brown – black. EtOH (HPLC grade, 50 mL) is added to the solution and left at -4 ° C for 18 h. After this time, the reaction mixture was filtered using a filter plate. The precipitate obtained was dissolved in $CHCl_3$ and a second process was conducted in toluene precipitation using centrifuge (1h, 11000 rpm) and obtaining poly-(M**1**$_r$-*co*-M**2**$_{1-r}$)-Au. Extra purification was required for the nanonanocomposites. The peak corresponding to poly-(M**1**$_r$-*co*-M**2**$_{1-r}$)-Au was collected and further analyzed by means of UV, CD and SEM.

13.3 GPC characterization for Au-poly-(M1$_r$-co-M2$_{1-r}$) nanocomposites

Size exclusion chromatography studies were performed on a Alliance 2695 HPLC System (Waters) liquid chromatography system equipped with a UV 2489 detector (Waters) using. The samples were eluted by two Phenogel columns connected to each other with stacionary phases of 10^3 and 10^5 Amstrong and packed with a solid support of a cross-linked stiyrene and *p*-divinylbenzene copolymer. To characterize the hybrid materials Au-poly-(M**1**$_r$-*co*-M**2**$_{1-r}$) GPC chromatograms were recorded at 380 (polymer absorption) and 540 nm (gold nanoparticles absorption).

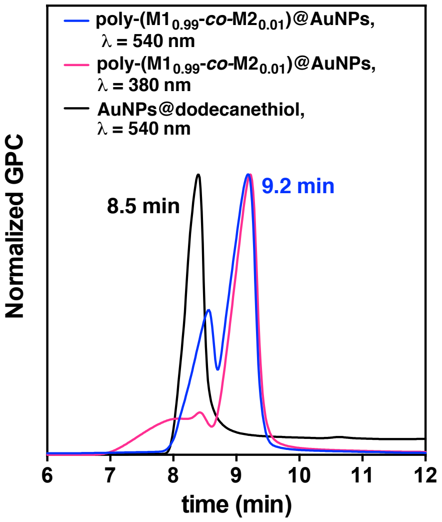

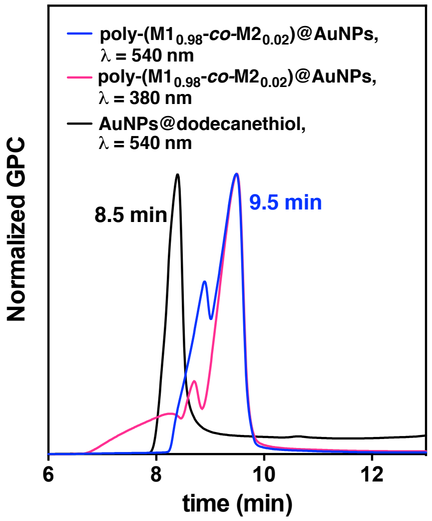

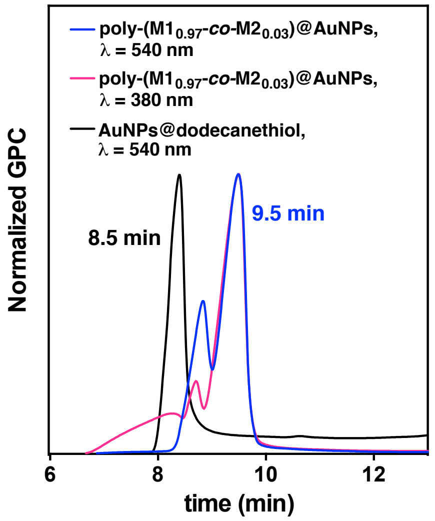

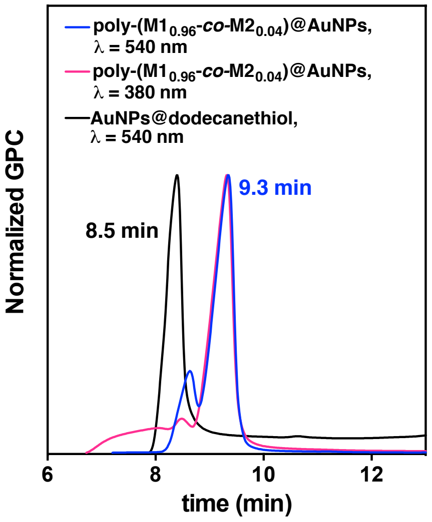

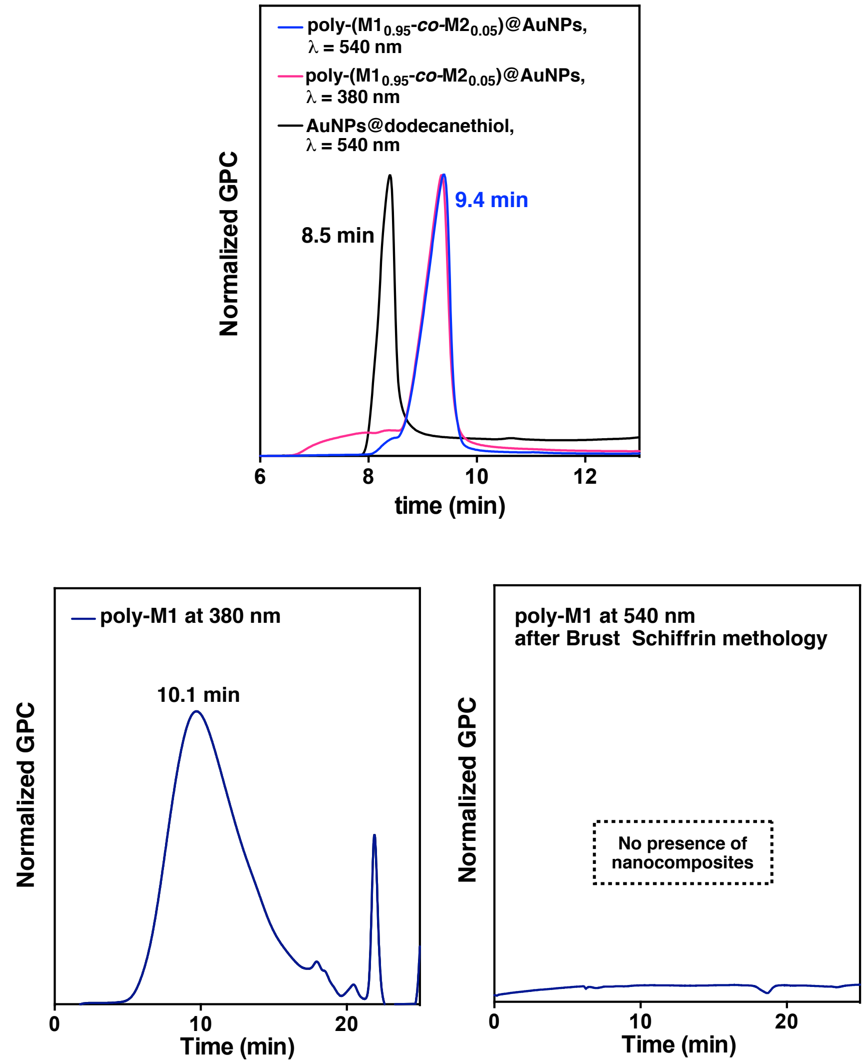

Figure S36: GPC chromatograms for Au-poly-(M**1**$_r$-*co*-M**2**$_{1-r}$) nanocomposites and control studies for poly-M**1.**

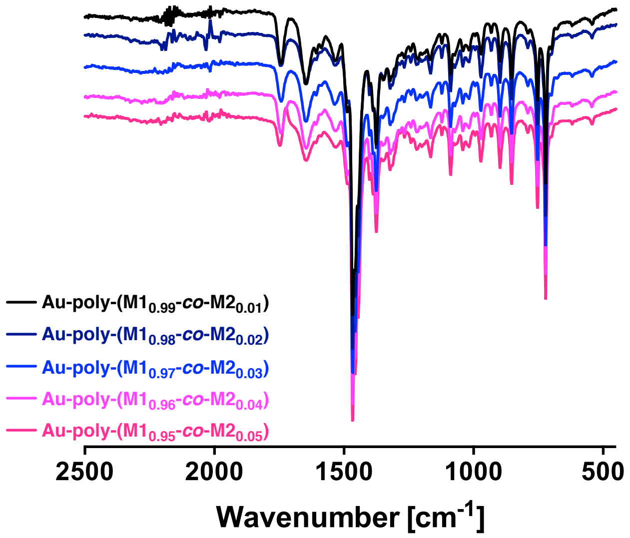

Figure S37: FT-IR spectra for Au-poly-(M**1**$_r$-*co*-M**2**$_{1-r}$) nanocomposites.

14. Thermal studies for Au-poly-($M1_r$-*co*-$M2_{1-r}$) nanocomposites

14.1 DSC studies for Au-poly-($M1_r$-*co*-$M2_{1-r}$) nanocomposites

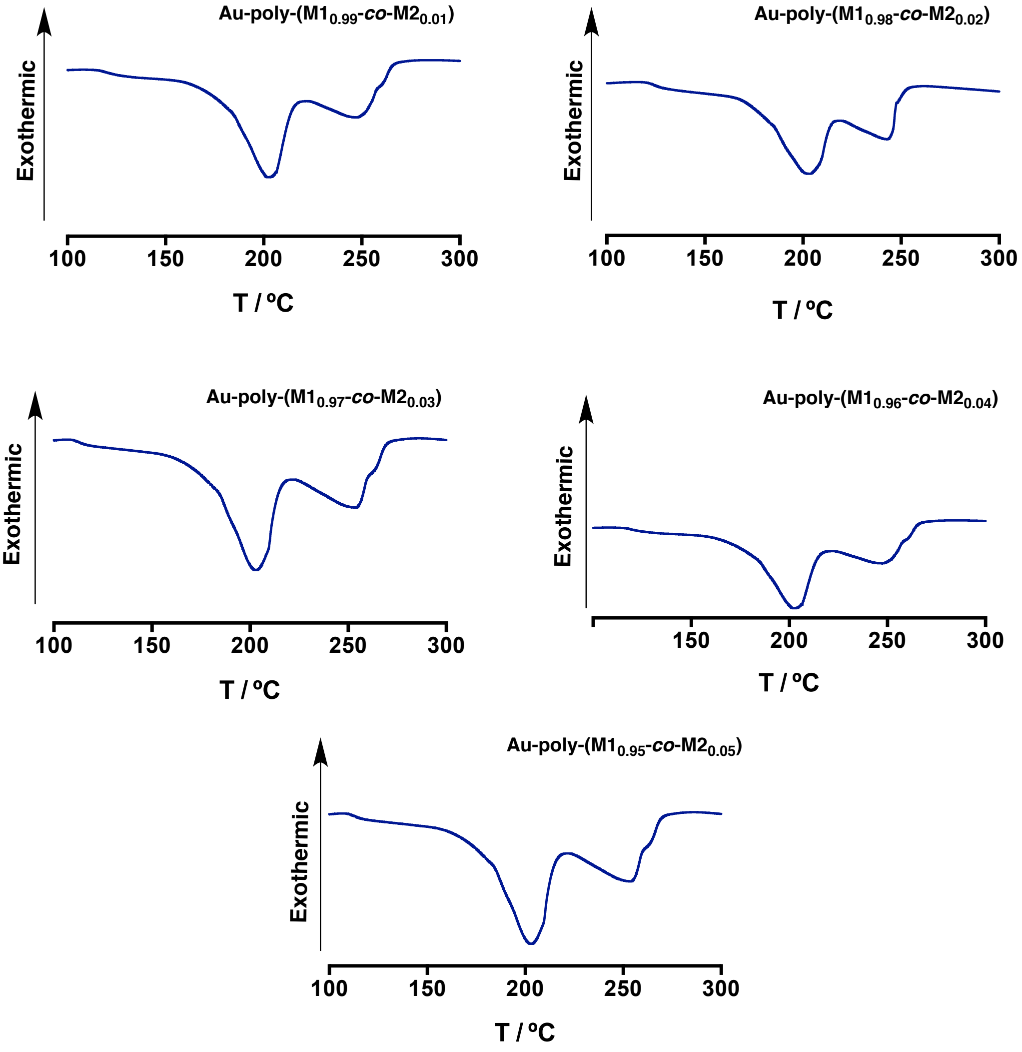

Figure S38: DSC thermograms for Au-poly-(M**1**$_r$-*co*-M**2**$_{1-r}$) nanocomposites.

14.2 TGA studies for Au-poly-(M1$_r$-*co*-M2$_{1-r}$) nanocomposites

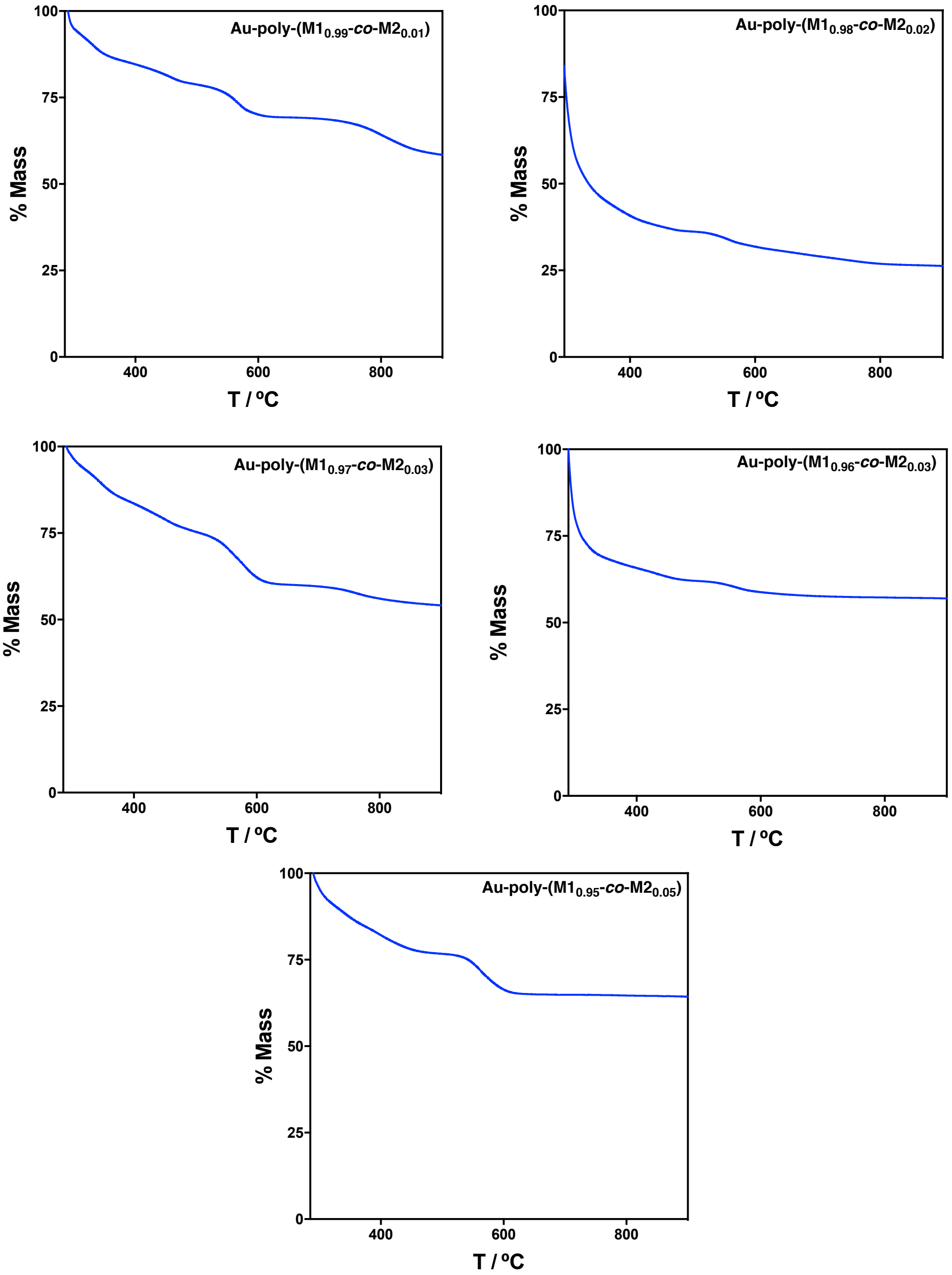

Figure S39: TGA thermograms for Au-poly-(M**1**$_r$-*co*-M**2**$_{1-r}$) nanocomposites.

15. CD and UV-Vis experiments for Au-poly-(M1$_r$-*co*-M2$_{1-r}$) nanocomposites in high polar and low polar solvents

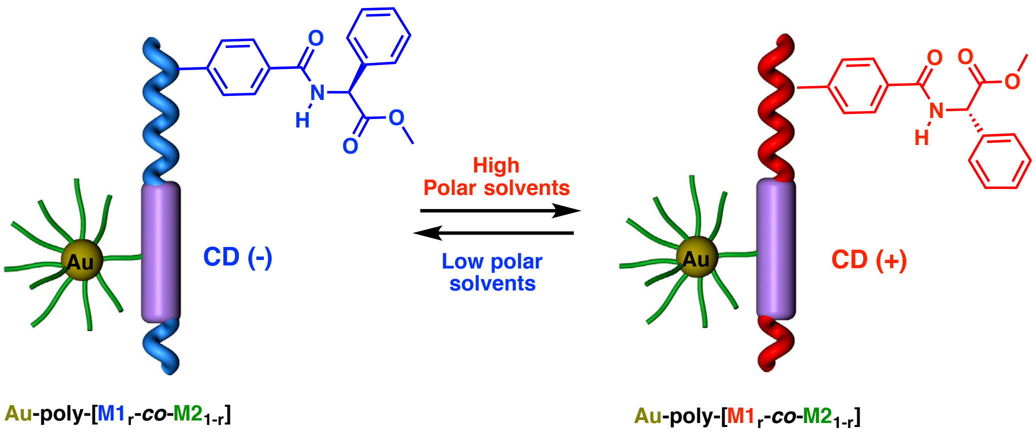

CD and UV-Vis studies were performed with a solution of Au-poly-(M**1**$_r$-*co*-M**2**$_{1-r}$) in high polar (DMSO, DMF) and low polar ($CHCl_3$, THF) solvents.

Au-Poly-(M**1**$_r$-*co*-M**2**$_{1-r}$) dissolved in low polar solvents (0.3 mg mL^{-1}, $CHCl_3$ and THF) presents a negative Cotton effect (*M* helices) in the vinylic region corresponding to a *anti* conformation between carbonyl groups in the pendant group. Differently, Au-poly-(M**1**$_r$-*co*-M**2**$_{1-r}$) dissolved in high polar solvents (0.3 mg mL^{-1}, DMF and DMSO) presents a positive Cotton effect (*P* helices) corresponding to a *syn* conformation between carbonyl groups

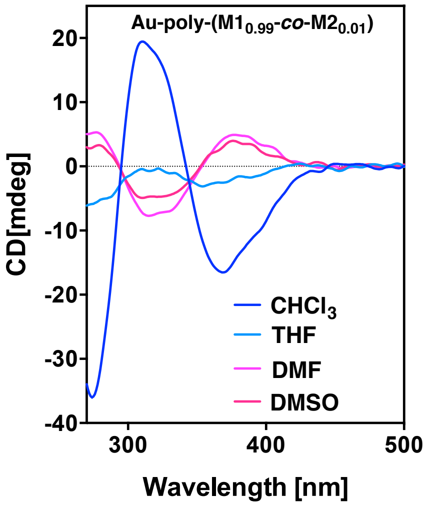

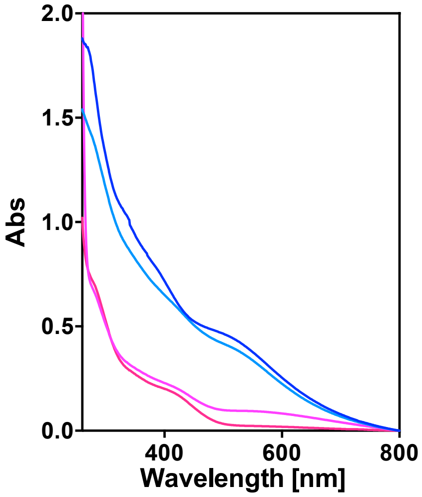

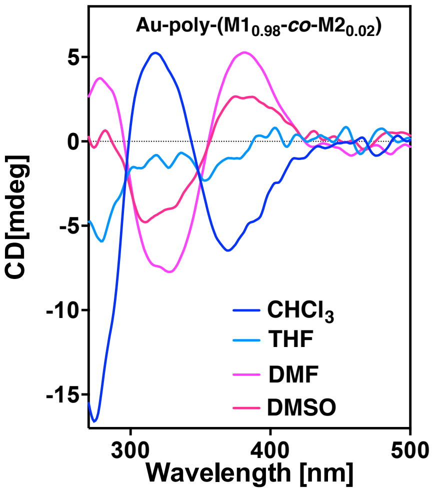
Au-poly-(M1$_{0.98}$-co-M2$_{0.02}$)
CD[mdeg]
5
0
-5
-10
-15
300
400
500
Wavelength [nm]
CHCl$_3$
THF
DMF
DMSO

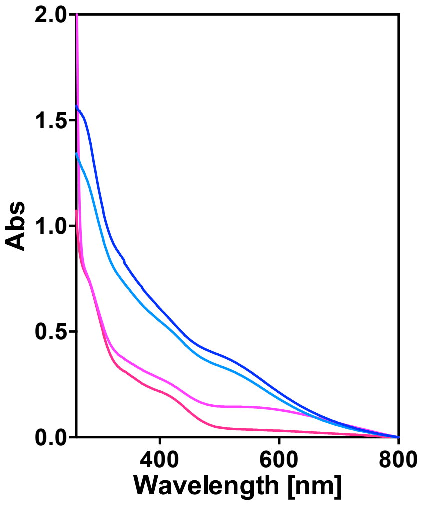
Abs
2.0
1.5
1.0
0.5
0.0
400
600
800
Wavelength [nm]

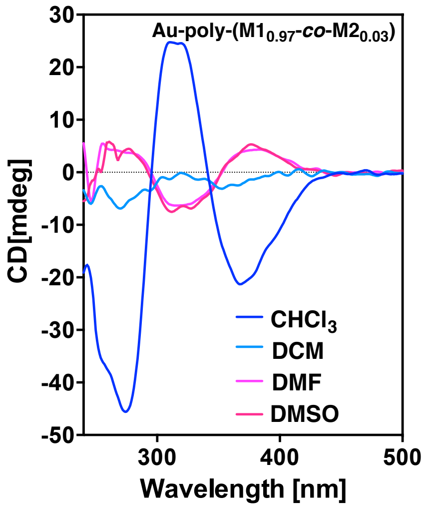
Au-poly-(M1$_{0.97}$-co-M2$_{0.03}$)
CD[mdeg]
30
20
10
0
-10
-20
-30
-40
-50
300
400
500
Wavelength [nm]
CHCl$_3$
DCM
DMF
DMSO

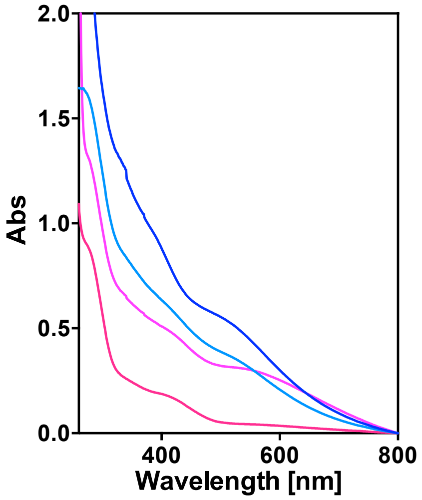
Abs
2.0
1.5
1.0
0.5
0.0
400
600
800
Wavelength [nm]

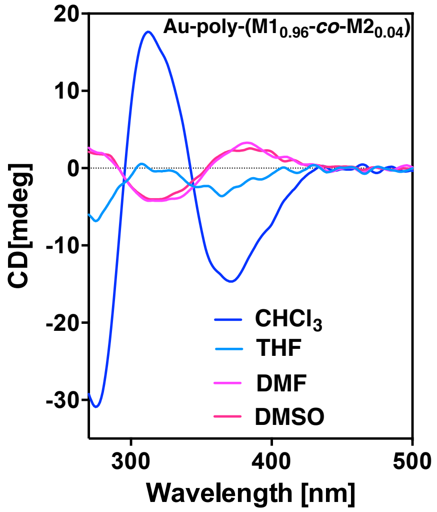
Au-poly-(M1$_{0.96}$-co-M2$_{0.04}$)
CD[mdeg]
20
10
0
-10
-20
-30
300
400
500
Wavelength [nm]
CHCl$_3$
THF
DMF
DMSO

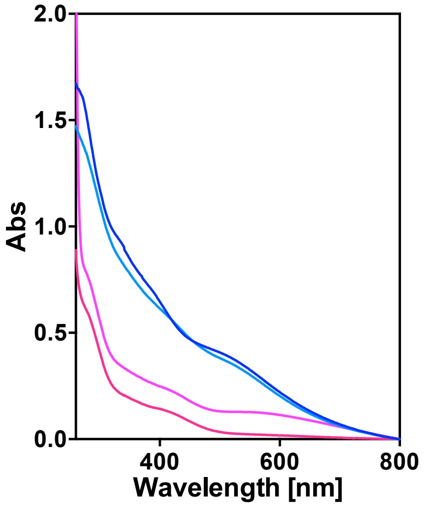
Abs
2.0
1.5
1.0
0.5
0.0
400
600
800
Wavelength [nm]

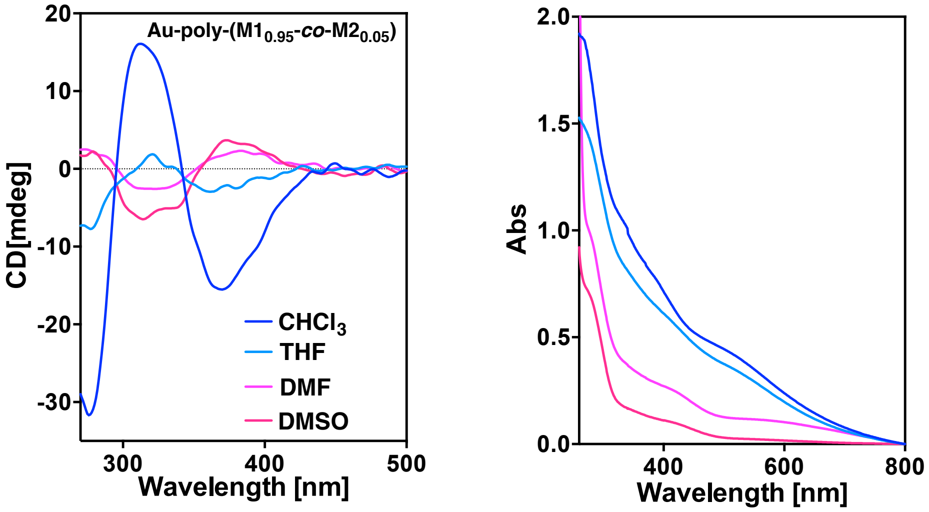

Figure S40: CD and UV-Vis experiments for copolymers Au-poly-(M**1**$_r$-*co*-M**2**$_{1-r}$) in high polar and low polar solvents.

16. CD and UV-Vis experiments for Au-poly-(M1$_r$-co-M2$_{1-r}$) nanocomposites in presence of LiClO$_4$

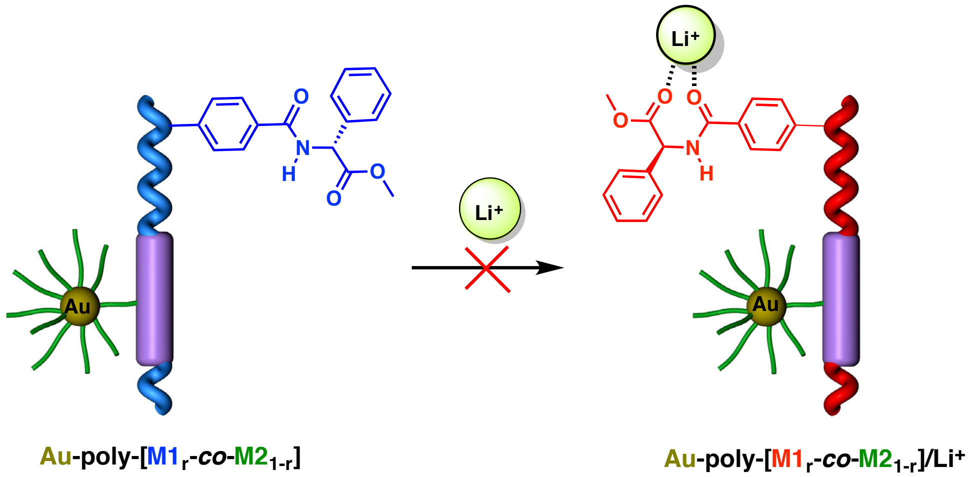

CD and UV-Vis studies were performed with a solution of poly-(M**1**$_r$-*co*-M**2**$_{1-r}$)-AuNPs in CHCl$_3$ (0.3 mg mL^{-1}) using LiClO$_4$ dissolved in MeOH which concentration was 10.0 mg mL^{-1}.

Thus, Au-poly-(M**1**$_r$-*co*-M**2**$_{1-r}$) dissolved in CHCl$_3$ shows a negative Cotton effect (*M* helices) in the vinylic region corresponding to an *anti* conformation between carbonyl groups in the pendant group. The addition of Li$^+$ ions to Au-poly-(M**1**$_r$-*co*-M**2**$_{1-r}$) cannot promote a helical inversion preserving the same helical sense (*M* helices).

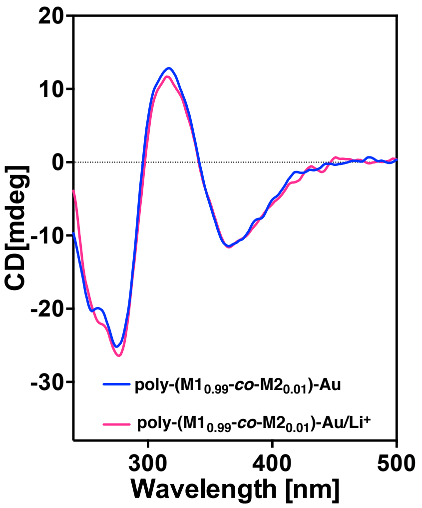

20
10
0
-10
-20
-30
CD[mdeg]
300
400
500
Wavelength [nm]
poly-($M1_{0.99}$-*co*-$M2_{0.01}$)-Au
poly-($M1_{0.99}$-*co*-$M2_{0.01}$)-Au/Li$^+$

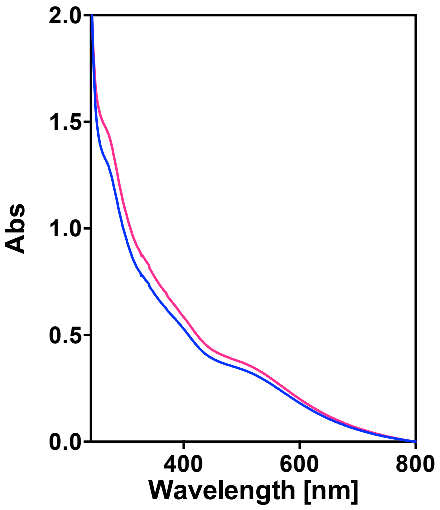

2.0
1.5
1.0
0.5
0.0
Abs
400
600
800
Wavelength [nm]

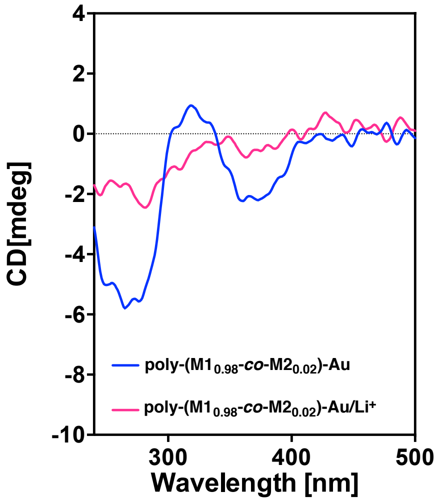

4
2
0
-2
-4
-6
-8
-10
CD[mdeg]
300
400
500
Wavelength [nm]
poly-($M1_{0.98}$-*co*-$M2_{0.02}$)-Au
poly-($M1_{0.98}$-*co*-$M2_{0.02}$)-Au/Li$^+$

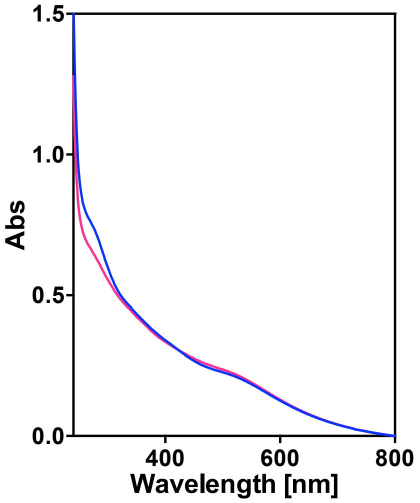

1.5
1.0
0.5
0.0
Abs
400
600
800
Wavelength [nm]

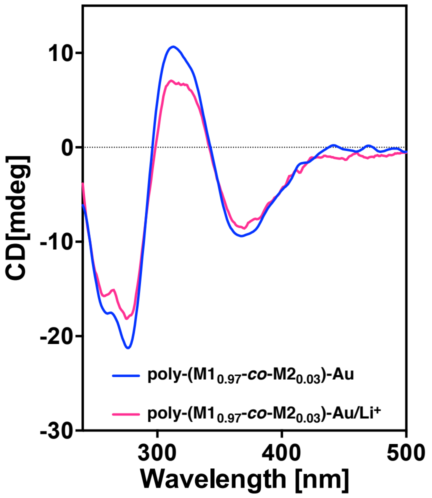

10
0
-10
-20
-30
CD[mdeg]
300
400
500
Wavelength [nm]
poly-($M1_{0.97}$-*co*-$M2_{0.03}$)-Au
poly-($M1_{0.97}$-*co*-$M2_{0.03}$)-Au/Li$^+$

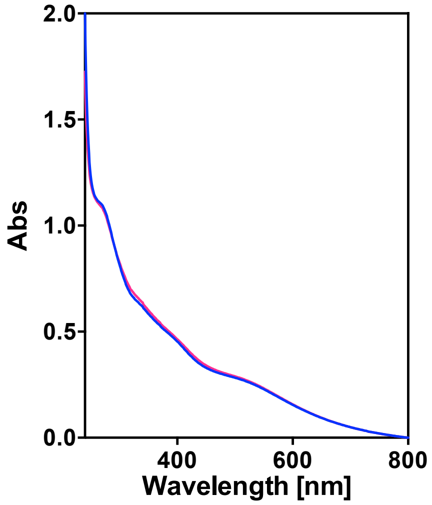

2.0
1.5
1.0
0.5
0.0
Abs
400
600
800
Wavelength [nm]

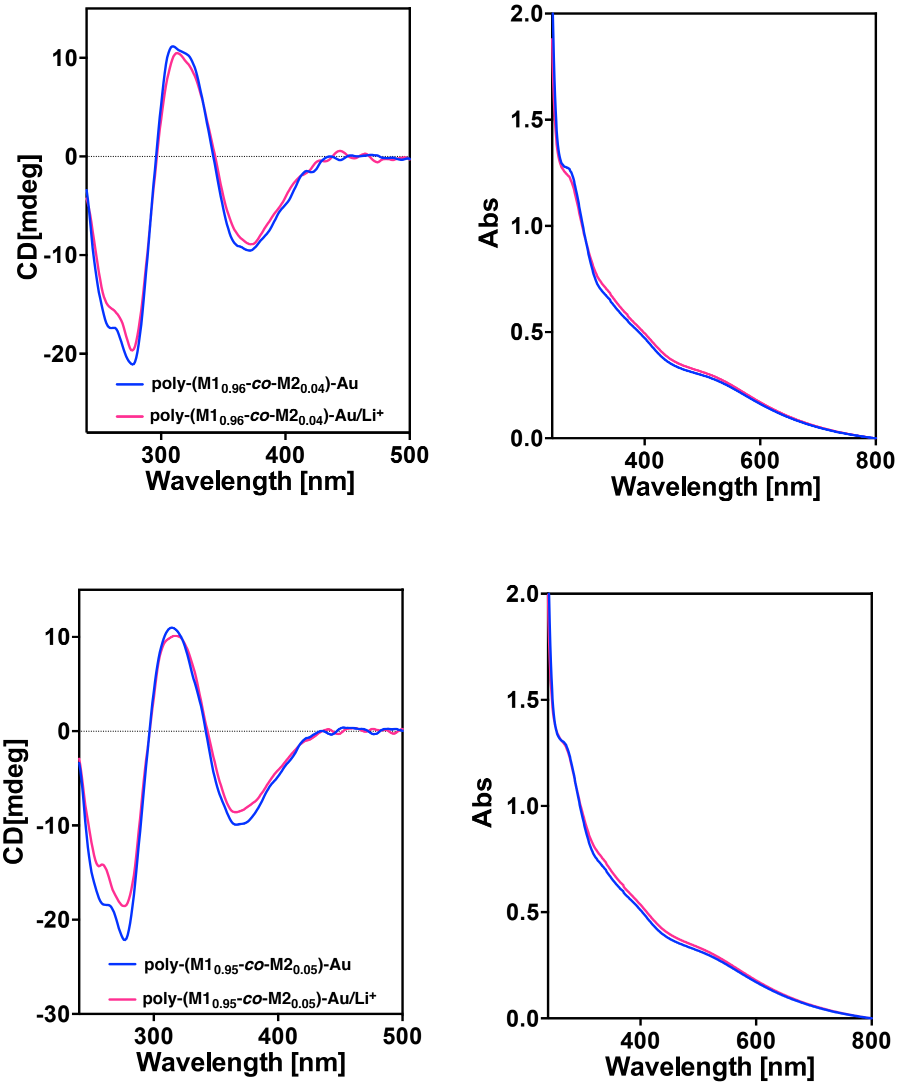

Figure S41: CD and UV-Vis studies for copolymers Au-poly-(M**1**$_r$-*co*-M**2**$_{1-r}$) dissolved in $CHCl_3$ (0.5 mg mL^{-1}) in presence of $LiClO_4$ dissolved in MeOH (10.0 mg mL^{-1}).

17. % Maximum CD signal for poly-M1, poly-($M1_r$-*co*-$M2(STrt)_{1-r}$), poly-($M1_r$-*co*-$M2_{1-r}$) and Au-poly-($M1_r$-*co*-$M2_{1-r}$) nanocomposites

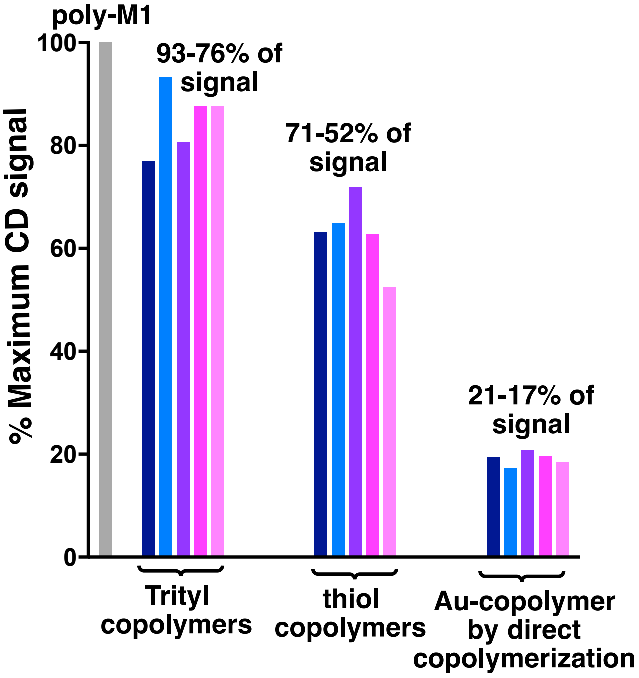

Figure S42: % Maximum CD signal for poly-M**1**, copolymers poly-(M**1**$_r$-*co*-M**2**(Trt)$_{1-r}$), copolymers poly-(M**1**$_r$-*co*-M**2**$_{1-r}$) and Au-poly-(M**1**$_r$-*co*-M**2**$_{1-r}$) nanocomposites.

18. CD and UV-Vis experiments for copolymers Au-poly-(M1$_r$-*co*-M2$_{1-r}$) nanocomposites in solid state

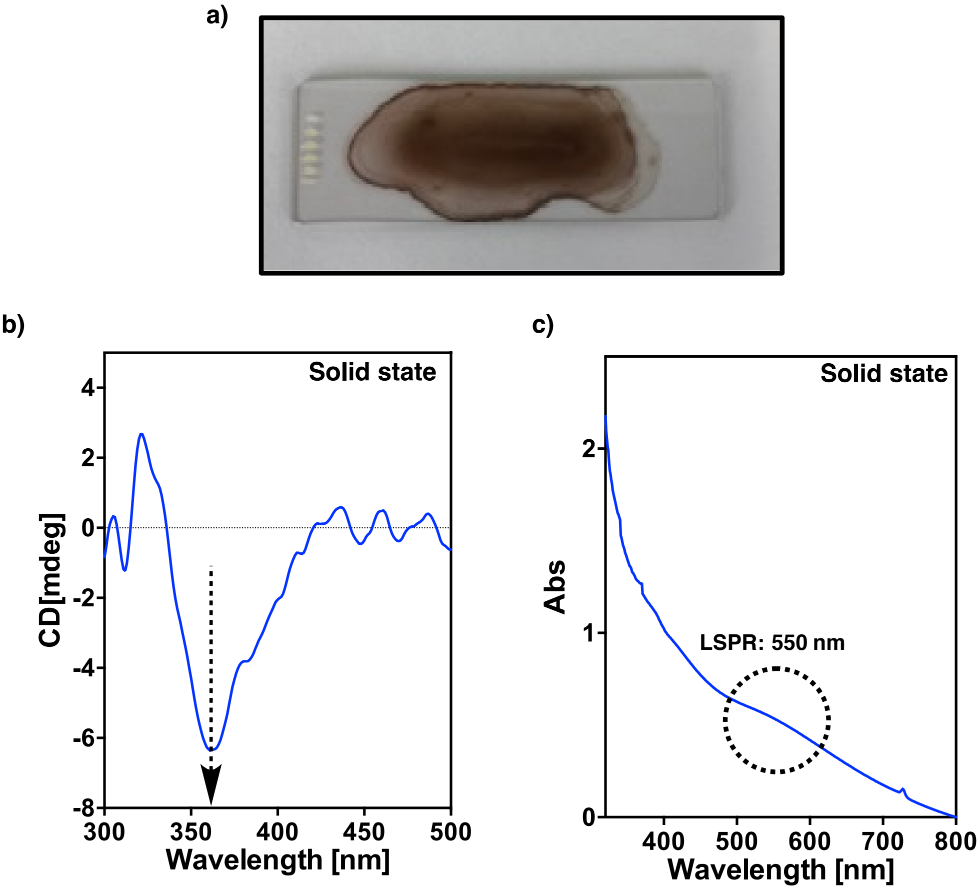

Figure S43: a) Film for Au-Poly-(M**1**$_{0.96}$-*co*-M**2**$_{0.04}$) in solid state. b) CD and c) UV-Vis measurements for Au-poly-(M**1**$_{0.95}$-*co*-M**2**$_{0.05}$) nanocomposites in solid state.

19. Microscopy (SEM and TEM) studies for Au-poly-(M1_r-*co*-M2_{1-r}) nanocomposites

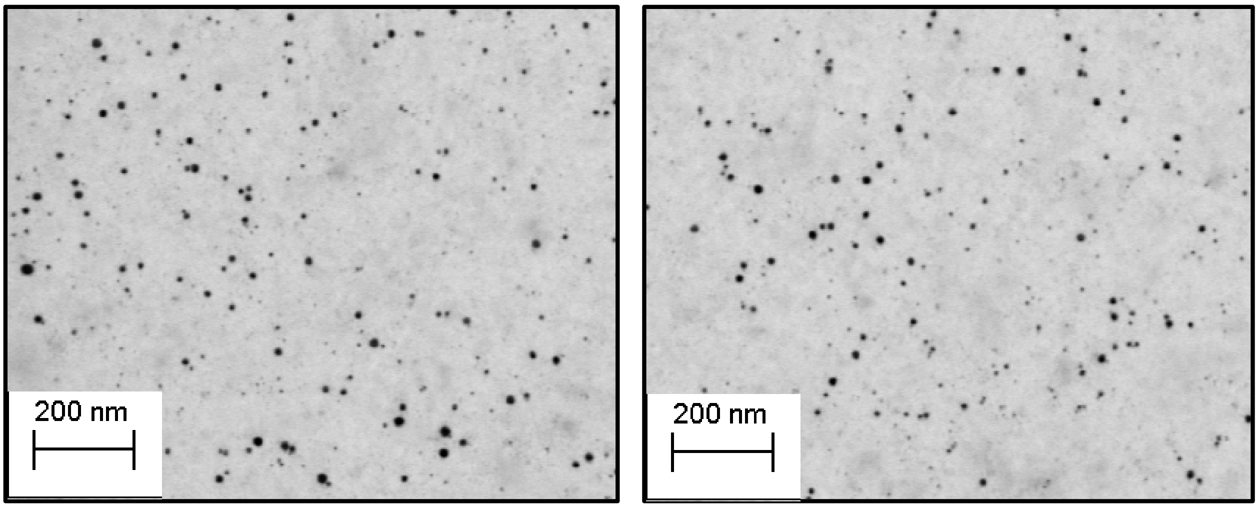

Figure S44: TEM images for Au-poly-(M$\mathbf{1}_{0.99}$-*co*-M$\mathbf{2}_{0.01}$) nanocomposites (size: 12 nm, SD: 3 nm, 101 nanoparticles, scale bar: 200 nm).

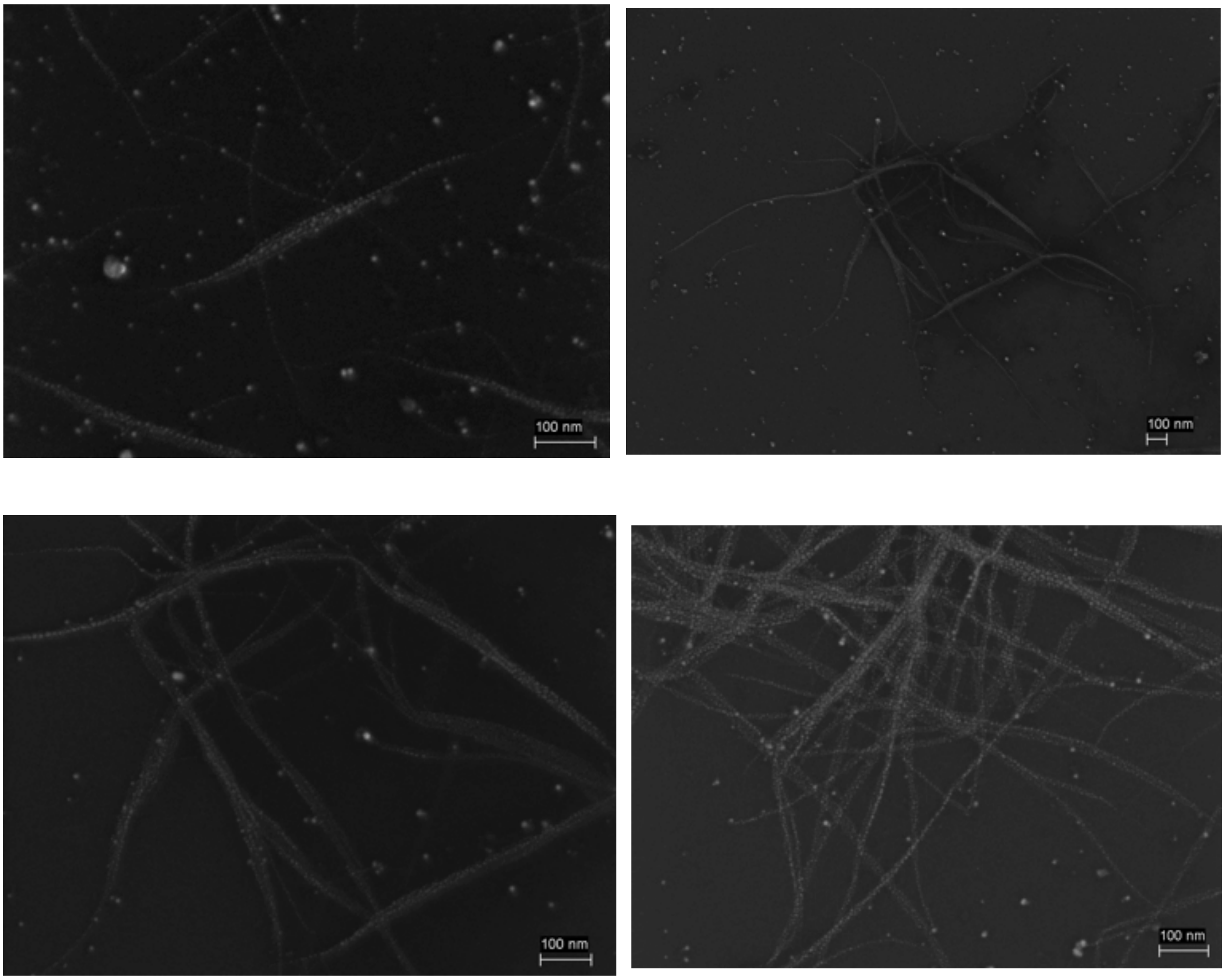

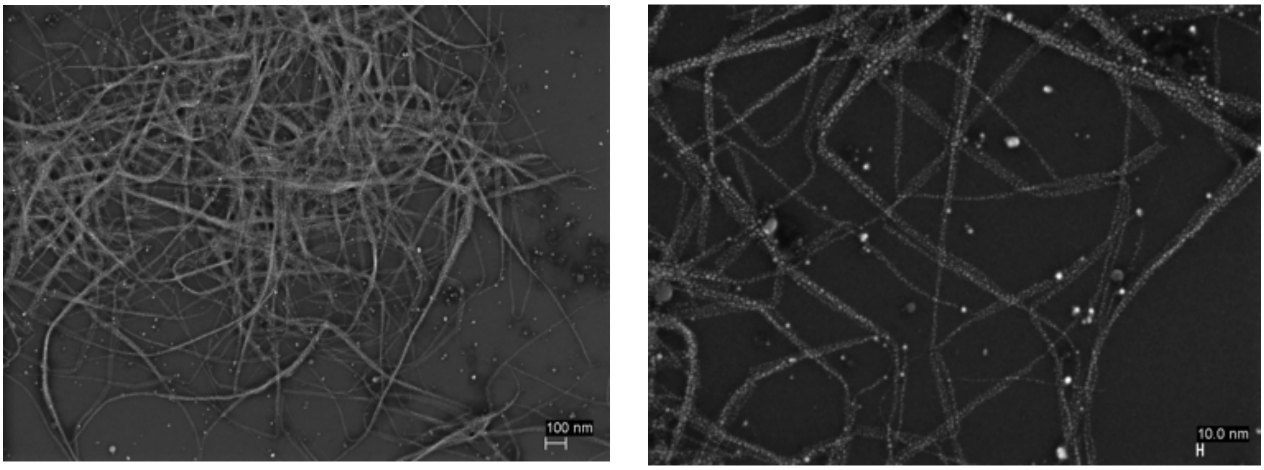

Figure S45: SEM microscopy images for Au-poly-(M$\mathbf{1}_r$-*co*-M$\mathbf{2}_{1-r}$) (r = 0.97-0.95) nanocomposites.

20. Nanostructuration studies for Au-poly-(M1_r-*co*-M2_{1-r}) nanocomposites in presence of $Ba(ClO_4)_2$

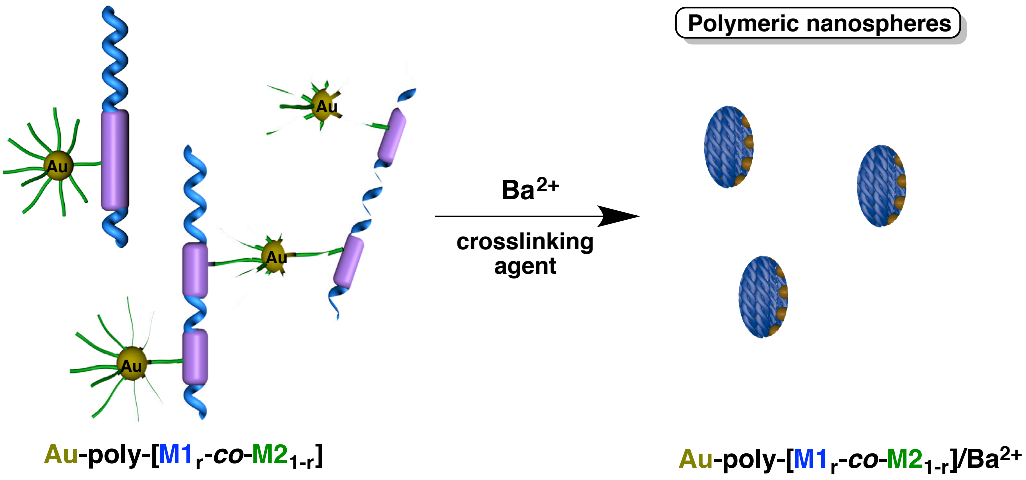

The addition of barium perchlorate (10.0 mg mL^{-1}) in MeOH to a solution of Au-poly-(M$\mathbf{1}_r$-M$\mathbf{2}_{1-r}$) (r = 0.99-0.95) nanocomposites (0.3 mg mL^{-1}, $CHCl_3$) produce the formation of chiral polymeric nanospheres due to the ability of Ba^{2+} to act as a crosslinking agent between polymer chains.

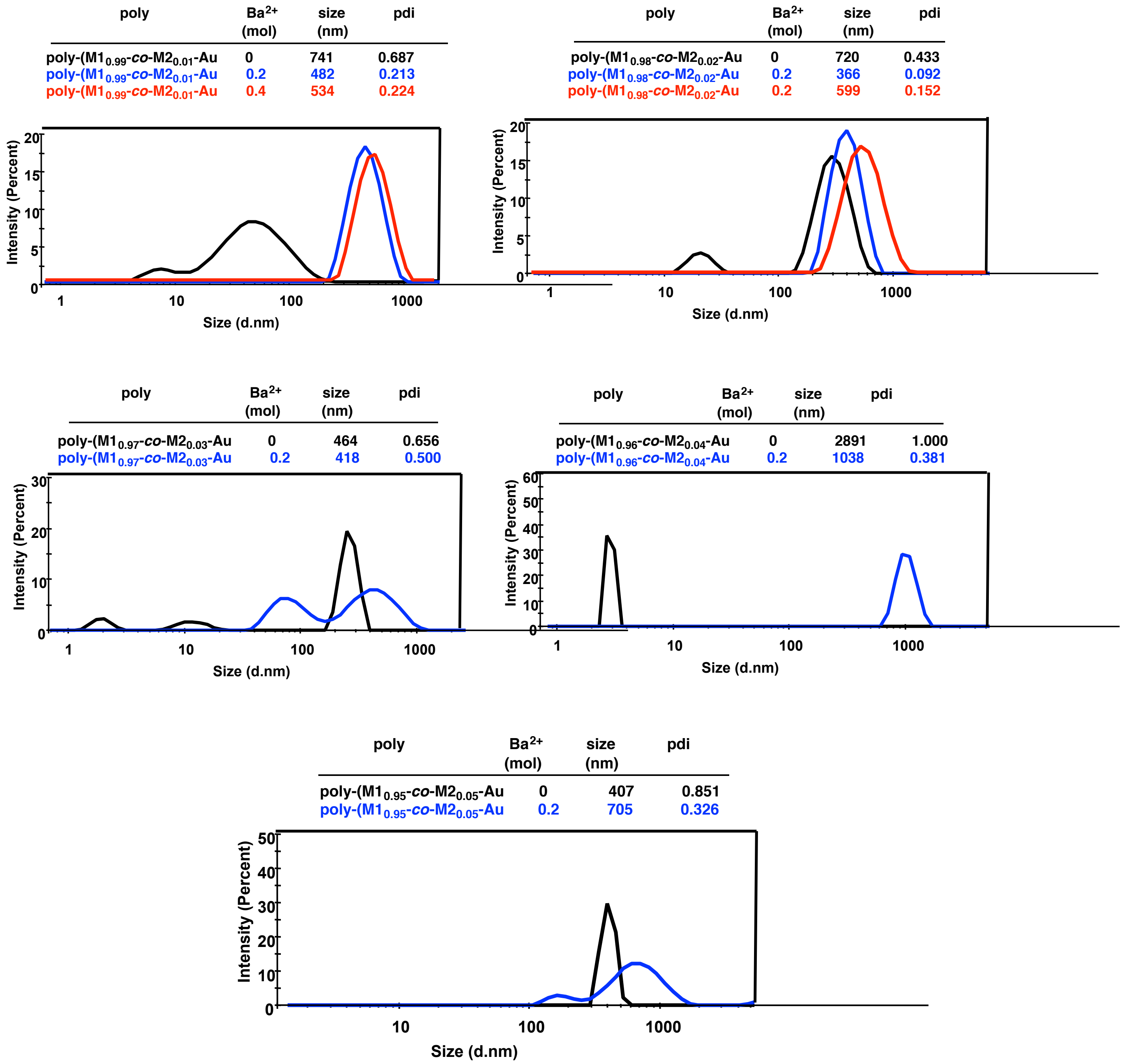

poly	Ba^{2+} (mol)	size (nm)	pdi
poly-(M1$_{0.99}$-*co*-M2$_{0.01}$-Au	0	741	0.687
poly-(M1$_{0.99}$-*co*-M2$_{0.01}$-Au	0.2	482	0.213
poly-(M1$_{0.99}$-*co*-M2$_{0.01}$-Au	0.4	534	0.224

poly	Ba^{2+} (mol)	size (nm)	pdi
poly-(M1$_{0.98}$-*co*-M2$_{0.02}$-Au	0	720	0.433
poly-(M1$_{0.98}$-*co*-M2$_{0.02}$-Au	0.2	366	0.092
poly-(M1$_{0.98}$-*co*-M2$_{0.02}$-Au	0.2	599	0.152

poly	Ba^{2+} (mol)	size (nm)	pdi
poly-(M1$_{0.97}$-*co*-M2$_{0.03}$-Au	0	464	0.656
poly-(M1$_{0.97}$-*co*-M2$_{0.03}$-Au	0.2	418	0.500

poly	Ba^{2+} (mol)	size (nm)	pdi
poly-(M1$_{0.96}$-*co*-M2$_{0.04}$-Au	0	2891	1.000
poly-(M1$_{0.96}$-*co*-M2$_{0.04}$-Au	0.2	1038	0.381

poly	Ba^{2+} (mol)	size (nm)	pdi
poly-(M1$_{0.95}$-*co*-M2$_{0.05}$-Au	0	407	0.851
poly-(M1$_{0.95}$-*co*-M2$_{0.05}$-Au	0.2	705	0.326

Figure S46: DLS measurements for Au-poly-(M**1**$_r$-*co*-M**2**$_{1-r}$) nanocomposites (0.3 mg mL^{-1} in $CHCl_3$) in presence of $Ba(ClO_4)_2$ (10.0 mg mL^{-1} in MeOH).

21. SEM images for Au-poly-(M1$_r$-*co*-M2$_{1-r}$) nanocomposites in presence of Ba(ClO$_4$)$_2$

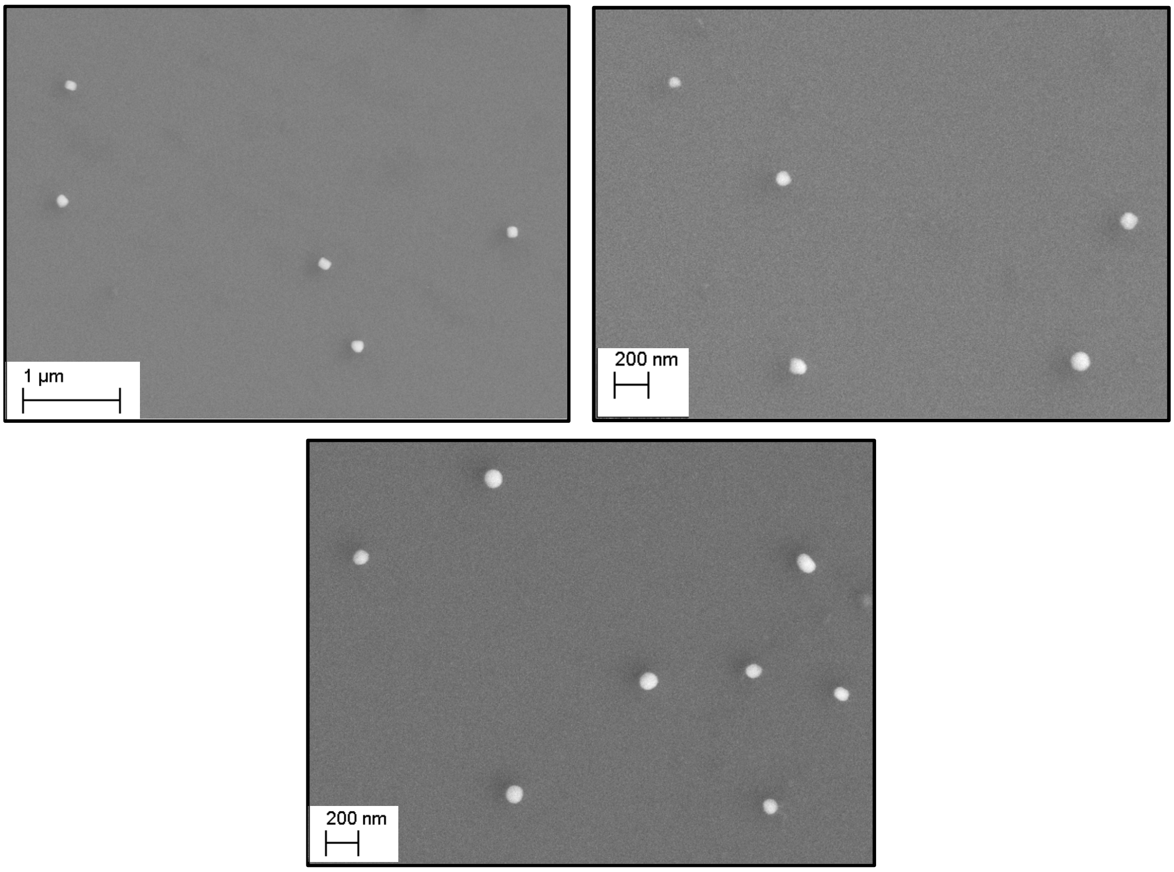

Figure S47: SEM images in solid state prepared from Au-poly-(M**1**$_r$-*co*-M**2**$_{1-r}$) (0.3 mg mL^{-1}, CHCl$_3$) in presence of Ba(ClO$_4$)$_2$ (10.0 mg mL^{-1} in MeOH).

22. Control studies

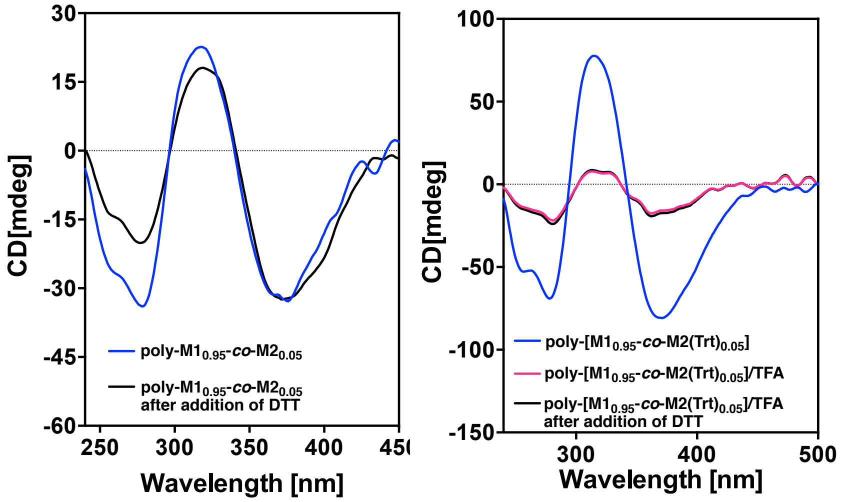

Figure S48: Control studies after addition of DTT for poly-[M**1**$_{0.95}$-*co*-M**2**$_{0.05}$] and poly-[M**1**$_{0.95}$-*co*-M2(Trt)$_{0.05}$].

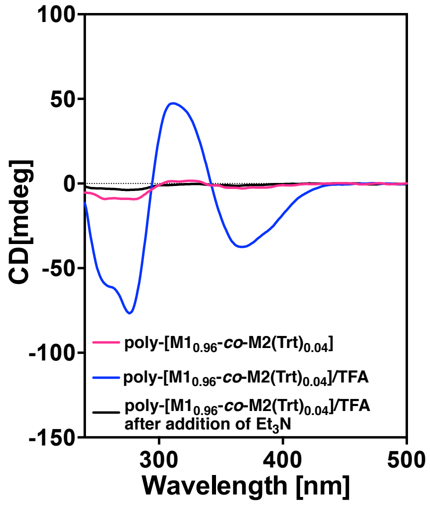

Figure S49: Control studies after addition of Et_3N for poly-[M**1**$_{0.96}$-*co*-M**2**$_{0.04}$]/TFA.

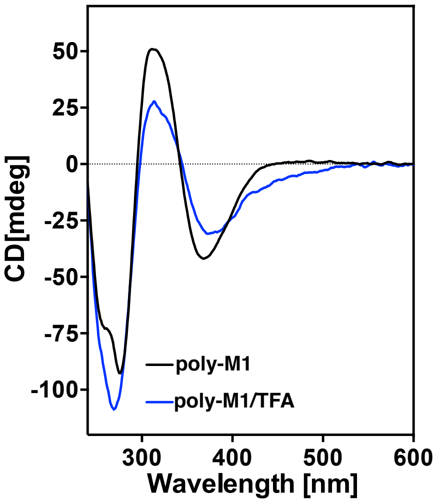

Figure S50: Control studies for poly-M**1** (0.3 mg mL^{-1} , CHCl$_3$) in presence of TFA (1 % v/v).

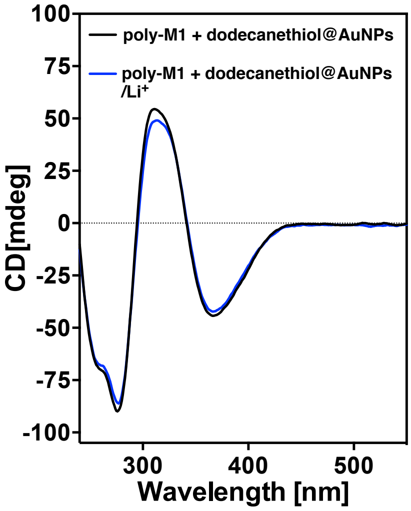

Figure S51: CD studies for a mixture (1:1) of poly-M**1**/dodecanethiol@AuNPs in CHCl$_3$ and poly-M**1**/dodecanethiol@AuNPs (CHCl$_3$) in presence of Li$^+$ ions (10 mg mL^{-1}, MeOH).

23. Supporting references

S1) M. Alzubi, S. Arias, I. Louzao, E. Quiñoá, R. Riguera, F. Freire, *Chem. Commun.* 2017, **53**, 8573.

S2) S. Arias, R. Rodríguez, E. Quiñoá, R. Riguera, F. Freire, *J. Am. Chem. Soc.,* 2018, **140***,* 667.

S3) F. Freire, J. M. Seco, J. E. Quiñoá, R. Riguera, *J. Am. Chem. Soc.*, 2012, **134**, 19374.

S4) G. Yesilbag, T. Mizuhara, K. Saha, Z. Jiang, S. Hou, R. Das, V. Rotello, *Tetrahedron Letters*, 2015, **56**, 3653.

S5) M. Brust, M. Walker, D. Bethell, D. J. Schiffrin, R. Whyman, *J. Chem. Soc. Chem. Commun.,* 1994, 801.